

8-1-2015

# Changes in properties of coal as a result of continued bioconversion

Rohit Pandey

*Southern Illinois University Carbondale*, rohit.mining1990@gmail.com

Follow this and additional works at: <http://opensiuc.lib.siu.edu/theses>

---

## Recommended Citation

Pandey, Rohit, "Changes in properties of coal as a result of continued bioconversion" (2015). *Theses*. Paper 1745.

This Open Access Thesis is brought to you for free and open access by the Theses and Dissertations at OpenSIUC. It has been accepted for inclusion in Theses by an authorized administrator of OpenSIUC. For more information, please contact [opensiuc@lib.siu.edu](mailto:opensiuc@lib.siu.edu).

CHANGES IN PROPERTIES OF COAL AS A RESULT OF CONTINUED  
BIOCONVERSION

by

Rohit Pandey

B.E., Bengal Engineering and Science University, Shibpur, 2012

A Thesis

Submitted in Partial Fulfillment of the Requirements for the  
Master of Science

Department of Mining and Mineral Resources Engineering  
in the Graduate School  
Southern Illinois University Carbondale  
August 2014

THESIS APPROVAL

CHANGES IN PROPERTIES OF COAL AS A RESULT OF CONTINUED  
BIOCONVERSION

By

Rohit Pandey

A Thesis Submitted in Partial  
Fulfillment of the Requirements  
for the Degree of  
Master of Science  
in the field of Mining Engineering

Approved by:

Dr. Satya Harpalani, Chair

Dr. Anthony J. S. Spearing

Dr. Yanna Liang

Graduate School  
Southern Illinois University Carbondale  
June 23, 2015

## AN ABSTRACT OF THE THESIS OF

Rohit Pandey, for the Master of Science degree in Mining Engineering, presented on June 23, 2015, at Southern Illinois University Carbondale.

**TITLE: CHANGES IN PROPERTIES OF COAL AS A RESULT OF CONTINUED BIOCONVERSION.**

**MAJOR PROFESSOR: Dr. Satya Harpalani**

Microbial actions on coal have long been identified as a source of methane in coalbeds. Andrew Scott (1995) was the first to propose imitating the natural process of biogenic gasification, possibly leading to recharging coalbed methane (CBM) reservoirs, or setting up natural gas reservoirs in non-producing coalbeds. This study was aimed at identifying the changes in coal properties that affect gas deliverability in coal-gas reservoirs, when treated with microbial consortia to generate/enhance gas production. The experimental work tested the sorption and diffusion properties for the coal treated and, more importantly, the variation in the relevant parameters with continued bio-conversion since these are the first two phenomena in CBM production.

During the first phase, single component sorption-diffusion experiments were carried out using pure methane and CO<sub>2</sub> on virgin/baseline coals, retrieved from the Illinois basin. Coals were then treated with nutrient amended microbial consortia for different periods. Gas production was monitored at the end of thirty and sixty days of treatment, after which, sorption-diffusion experiments were repeated on treated coals, thus establishing a trend over the sixty-day period. The sorption data was characterized using Langmuir pressure and volume constants, obtained by fitting it over the Langmuir isotherm. The diffusion coefficient,  $D$ , was estimated by establishing

the variation trend as a function of pore pressure. The pressure parameter was considered critical since, with continued production of methane, the produced gas diffuses into the coal matrix, where it gets adsorbed with increasing pressure. During production, the pressure decreases and the process is reversed, gas diffusing out of the coal matrix and arriving at the cleat system.

The results indicated an increase in the sorption capacity of coal as a result of bioconversion. This was attributed to increased pore surface areas as a result of microbial actions. However, significant hysteresis was observed during desorption of methane and was attributed to preferential desorption from sorption sites in the pathways leading to pore cavities. This is corroborated by the increased rates of diffusion, especially for methane, which exhibited rates higher than that for CO<sub>2</sub>. This contradicted the results for untreated/baseline coal, which were in agreement with previous studies. Effort was made to explain this anomaly by the non-monotonic dependence of effective diffusion coefficient on the size of the diffusing particles, where in coalbed environments, CO<sub>2</sub> has smaller kinetic diameter than methane.

## ACKNOWLEDGMENTS

I would like to express my sincere appreciation and gratitude to my academic advisor and Thesis Chair, Dr. Satya Harpalani, for his guidance, encouragement, constructive criticism and patience throughout my study. Without his help and advice, this study would not have been possible. I would also like to thank him for giving me the opportunity to come to Southern Illinois University and work under his supervision.

I would like to express my sincere thanks to Dr. Anthony J. S. Spearing and Dr. Yanna Liang for being a part on my thesis committee and for the stimulating discussions and helpful suggestions on the topic pertinent to the thesis. I appreciate their participation and enthusiasm to be a part of the committee.

I would like to thank Mr. Greg Moroz for his technical assistance and support for the laboratory work conducted as a part of this study. I am also grateful to Dr. Feng, Ji, Sudipta, Vivek and Xinbo for their support and guidance with different experimental procedures. Over the past two years, my friends, Akshat, Bhaskar, Charan, Eshani, Neel, Petar, Sagnik, and Subhankar have stood by me in times of success and setbacks, and motivated me to work continuously towards my goal. My sincere thanks to all of them. Special gratitude is extended to my parents and family members for their constant encouragement and support.

Lastly, the research funding provided by the Illinois Department of Commerce and Economic Opportunity over the course of my Master of Science is greatly acknowledged.

## TABLE OF CONTENTS

<u>CHAPTER</u>	<u>PAGE</u>
ABSTRACT.....	i
ACKNOWLEDGMENTS .....	iii
LIST OF TABLES .....	vii
LIST OF FIGURES.....	viii
CHAPTER 1 – INTRODUCTION .....	1
1.1 – Introductory Statement.....	1
1.2 – Problem Statement .....	2
1.3 – Structure of Thesis .....	3
CHAPTER 2 – BACKGROUND AND LITERATURE REVIEW.....	4
2.1 – Formation of Coal and its Basic Characteristics .....	4
2.2 – Coalbed Methane .....	6
2.3 – Origin of Coalbed Gases .....	8
2.4 – Biogenic Methane .....	9
2.5 – Microbially Enhanced Coalbed Methane.....	11
2.5.1 – Methanogenic Pathways.....	12
2.6 – Physical Structure of Coal.....	15
2.7 – Storage of Gases in Coal.....	18
2.8 – Gas Transport on Coalbed Reservoirs .....	19
2.8.1 – Desorption.....	20
2.8.2 – Diffusion .....	20
2.8.3 – Permeability .....	22

2.9 – Techniques to Determine Gas Storage Characteristics .....	22
2.9.1 – The Langmuir Approach .....	23
2.9.2 – Polanyi’s Potential Theory .....	28
2.9.3 – Theory of Volume Filling Micropores .....	29
2.9.4 – Estimation of Surface Area .....	32
2.10 – Techniques to Determine Diffusion Characteristics .....	32
2.10.1 – Particle Method .....	33
2.11 – Summary .....	38
CHAPTER 3 – EXPERIMENTAL STUDY .....	40
3.1 – Experimental Design.....	40
3.1.1 – High Pressure Vessel Assembly.....	41
3.1.2 – Temperature Control System .....	41
3.1.3 – Data Acquisition System.....	44
3.2 – Sample Procurement and Preparation .....	44
3.3 – Calibration and Testing of Entire Setup.....	45
3.4 – Experimental Procedure.....	45
3.5 – Sorption Isotherms .....	47
3.6 – Estimation of Diffusion Coefficient.....	47
CHAPTER 4 – RESULTS AND DISCUSSION .....	49
4.1 – Production of Gases .....	49
4.2 – Sorbed Gas Calculation.....	50
4.3 – Estimation of Diffusion Coefficient.....	57
4.3.1 – Diffusion Results .....	58



4.4 – Discussion .....	61
4.4.1 – Sorption.....	61
4.4.2 – Surface Area.....	64
4.4.3 – Extended Langmuir Isotherm.....	66
4.5 – Diffusion .....	68
4.5.1 – Possible Explanation Using Non-monotonic Size Dependence of Effective Diffusion Constant .....	73
4.6 – Potential Impacts of the Observed Trends .....	78
4.7 – Summary .....	82
CHAPTER 5 – CONCLUSIONS AND RECOMMENDATIONS .....	83
REFERENCES .....	86
VITA .....	96

## LIST OF TABLES

<u>TABLE</u>	<u>PAGE</u>
Table 2.1: Most important methanogenic reactions ordered from the most to least thermodynamically favored as defined by free energy change. ....	14
Table 4.1: Produced gases during methanogenesis.....	50
Table 4.2: Results obtained from Langmuir isotherms.....	53
Table 4.3: Results of the basic coal characteristics .....	57
Table 4.4: Estimated changes in surface areas.....	65

## LIST OF FIGURES

<u>FIGURE</u>	<u>PAGE</u>
Figure 2.1: The geochemical-biochemical transformation of plant substances as occurring over coalification stages .....	5
Figure 2.2: Molecular structure of bituminous coal.....	7
Figure 2.3: Isotopic analysis of CBM from different basins in US and Australia .....	10
Figure 2.4: Anaerobic degradation of organic matter and the formation of biogenic methane .....	12
Figure 2.5: Scanning electron photomicrograph of coal matrix with visible pore openings .....	15
Figure 2.6: Plan view of coal core with highlighted (visible) cleat structure .....	16
Figure 2.7: Cubic model of coal.....	17
Figure 2.8: Bundle of matchsticks geometry showing flow through vertical fractures .....	18
Figure 2.9: Process of migration of gas in dual porosity coal.....	19
Figure 2.10: Different types of adsorption isotherms .....	23
Figure 2.11: Micropore filling mechanism used in TVFM.....	31
Figure 2.12: A typical diffusion diagnostic graph.....	35
Figure 2.13: Conceptual model of the bidisperse pore structure .....	36
Figure 3.1: Schematic of the sorption/diffusion experimental setup .....	42
Figure 3.2: Pictorial representation of the experimental setup .....	42
Figure 3.3: High pressure vessel assembly .....	43
Figure 4.1: Ad/de-sorption isotherms of methane-baseline coal .....	54
Figure 4.2: CO <sub>2</sub> adsorption isotherm-baseline coal .....	54
Figure 4.3: Ad/de-sorption isotherms of methane- thirty-day treated coal .....	55
Figure 4.4: CO <sub>2</sub> adsorption isotherm for coal – thirty-day treated coal .....	55

Figure 4.5: Ad/de-sorption isotherms of methane – sixty-day treated coal .....	56
Figure 4.6: CO <sub>2</sub> adsorption isotherm for coal – sixty-day treated coal .....	56
Figure 4.7(a): Variation in the value of D with changes in methane pressure – baseline coal .....	58
Figure 4.7(b): Variation in the value of D with increasing CO <sub>2</sub> pressure – baseline coal .....	59
Figure 4.8(a): Variation in the value of D with changes in methane pressure – thirty-day treated coal .....	59
Figure 4.8(b): Variation in the value of D with increasing CO <sub>2</sub> pressure –thirty-day treated coal.	60
Figure 4.9(a): Variation in the value of D with changes in methane pressure – sixty-day treated coal .....	60
Figure 4.9(b): Variation in the value of D with increasing CO <sub>2</sub> pressure –sixty-day treated coal.	61
Figure 4.10: Langmuir isotherms for adsorption of methane and CO <sub>2</sub> on different coals .....	63
Figure 4.11: Extended Langmuir isotherm for coal treated for sixty days.....	67
Figure 4.12: Klinkenberg plot showing D as a function of methane pressure for the three coals tested .....	69
Figure 4.13: Klinkenberg plot showing D as a function of CO <sub>2</sub> pressure for three coals tested ...	70
Figure 4.14(a): Comparison of diffusion coefficient for methane and CO <sub>2</sub> for untreated coal .....	72
Figure 4.14(b): Comparison of diffusion coefficient for methane and CO <sub>2</sub> for coal treated for sixty days .....	72
Figure 4.15: A tube with identical periodic dead ends with entry radius of ‘a’ and a diffusing particle with a radius ‘r’ .....	73
Figure 4.16: Comparison of two cases where, a) normal simulation run for 800 days, and b) where diffusion coefficient variability is taken into account .....	81

## CHAPTER 1

### INTRODUCTION

#### 1.1 Introductory Statement

Underground coal mining in the United States utilizes two methods of operation, longwall and room and pillar. Recovery by the former method is typically ~70% and a mere 50% by the latter (Spearing, 2014). According to EIA (2012), the two mining methods together accounted for over 430 million short tons of coal mined in the US in 2012. As cited by Ruppert et al. (2002), there are over 60 coalbeds and zones in major coal producing regions in the United States, holding more than 1.6 trillion short tons of coal, with only one-tenth of it recoverable economically. Hence, the coal left behind in the mines and unmineable coal present an opportunity for application of unconventional technologies to economically extract and utilize the energy from this resource. Furthermore, as cited by EIA (2012), 1.6 trillion cubic feet (TCF) of natural gas was produced from virgin coal in the US in 2012. From two of the US coal basins, coalbed methane (CBM) has been ongoing for more than three decades, with large areas nearing complete depletion and abandonment. These areas present yet another potential source for extraction of energy from coal, but only if appropriate technologies were to become available.

The role of microbes in producing methane in coal seams from coal as the carbon source has long been identified. Taking cue from the widespread application of microbes in the oil industry to increase the overall recovery, and the impact that naturally occurring microbes have had in producing methane in coal, Scott (1995) introduced the concept of microbially enhanced coalbed methane (MECoM). It aimed at replicating the natural process of secondary biogenic gasification by treating coal with microbes along with suitable nutrient amendments and trace elements. Studies conducted by Strapoć (2007) and Opara (2012) provided substantial evidence

of the potential of generating methane by treating coal fines with bacterial solutions. Jones et al. (2010) showed that coal samples from Zavala County in Texas, which had no biogenic methane generation *in situ*, when treated with bacterial solutions, resulted in substantial methane generation, rates in excess of 95  $\mu\text{moles}$  per gram of coal.

The storage and transport of methane in coal are different from typical natural gas reservoirs. Methane in coal is primarily stored as adsorbed gas on to the coal micropores, and the amount stored depends on coal properties like rank, maceral content, moisture, ash content, temperature and pressure of the reservoir. Basically, migration of methane in a CBM reservoir starts in the matrix of coal (micropores) by diffusion, controlled by the diffusion coefficient and gas concentration gradient. After diffusing through the matrix, gas reaches the naturally occurring fractures (cleats) present in coal, where the flow becomes viscous in nature, and is controlled by the permeability of coal. Production of gas from CBM reservoirs is therefore, determined by two properties of coal, diffusion and permeability. The permeability, in turn, is characterized by the cleats present in coal. The rate of gas diffusion in coal, on the other hand, depends on the physical properties of coal matrix structure and cleat spacing since gas migrates by diffusion in the coal matrix prior to reaching the cleat system.

## **1.2 Problem Statement**

Since Andrew Scott's paper conceptualizing MECoM, there have been a number of studies characterizing local microbial communities across different coal types, and studying the underlying methanogenic pathways that results in the production of methane. Given that the source of this natural gas is coal, there have been no documented studies characterizing the change in the properties of coal as a result of continued bio-conversion although consumption of coal in the process is believed to impact these properties. This study focuses on the changes in

sorption-diffusion characteristics due to bioconversion, which in CBM environments, along with permeability, characterize the viability of the process in terms of techno-economic feasibility.

### **1.3 Structure of Thesis**

The overall objective of this thesis was to study the changes in the sorption/diffusion properties of coal as a result of methanogenesis. The concepts involving transport mechanism and reservoir properties have been discussed in detail in Chapter 2, including the basic theories involved. Chapter 2 also details the previous studies and relevant literature to provide the appropriate background and rationale for the experimental work conducted in this study.

Chapter 3 presents the experimental design and work carried out to determine the sorption capacity of coal, and changes in the gas content during fast and slow diffusion periods for various reservoir pressures representative of the actual pressure changes during CBM production. The experimental principles, design, and procedure are discussed in this Chapter in detail.

Chapter 4 presents a detailed analysis of experimental results of the study. This chapter also lays out different scientific theories validating the observed results. Some correlation with past work has also been carried out, proving the applicability of the Klinkenberg diffusion model under certain conditions. Finally, conclusions based on the experimental results and simulation, along with several recommendations for future work, are presented in Chapter 5.

## CHAPTER 2

### BACKGROUND AND LITERATURE REVIEW

#### 2.1 Formation of Coal and its Basic Characteristics

The precursor of coal is peat, formed from the burial of swampy plants over millions of years. Over time, due to the action of high temperatures and pressures, peat undergoes progressive coalification to form different types of coal, classified in order of increasing ranks as lignite, sub-bituminous, bituminous, anthracite and graphite, higher rank representing greater degree of coalification. The carbon content of coal increases with rank. Peat has a carbon content of ~ 55 % by weight, whereas anthracite presents itself with more than 91.5 % carbon. A negative correlation exists for percentages of hydrogen and oxygen with increasing ranks. Hydrogen decreases from 10 % to 3.75 % and oxygen from 35 to less than 2.5 % between peat and anthracite respectively (Ward, 1984). Figure 2.1 presents a pictorial representation of the gradual process of coalification, and the associated bio-geochemical changes that occur.

The constituents of coal are divided into two primary fractions: the macerals, which are the organic, fossilized plant remains; and the mineral matter, which is the inorganic fraction made up of a variety of minerals. In addition to the organic and inorganic fraction, the third part, accounting for the remaining fraction of coal is the moisture content.

The macerals are further classified into three distinct groups, namely the vitrinite, exinite and inertinite (Thomas, 2002). Vitrinite, due to its origin in the woody plant materials, mainly lignin, is also termed as huminite. It is the most prevalent group, accounting for ~80% of the macerals in coal. Exinite is derived from lipids and waxy plant substances, and is alternatively



termed as liptinite. Intertinite originates from the oxidized plant materials, like char, attributed to wood fires that occurred during dry periods, during the formation of peat (Lin, 2010).

#### Peatification

- a) Plant materials in peat are humified and macerated;
- b) Compaction of material begins;
- c) Primary biogenic methane develops in along with accumulation of peat.

#### Dehydration

- a) Significant loss of water with orders of magnitude loss of porosity;
- b) Organic material enters lignite through sub-bituminous rank range;
- c) Holding capacity of methane increases allowing storage of secondary biogenic gas;
- d) Continued development of biogenic gas provided conditions are right.

#### Bituminization

- a) Mobilization of hydrocarbons;
- b) Initiation of generation of thermogenic methane, occurring any time and throughout the subbituminous A to high volatile A bituminous stages;
- c) Maximum gas holding capacity increases substantially, although mobilization of bitumens may clog pores, decreasing capacity.

#### Debituminisation

- a) Maximum generation of thermogenic methane and other oil substances;
- b) Exits the oil window;
- c) Moisture value reach the minimum.

#### Graphitization

- a) The organic material is composed entirely of Carbon;
- b) Capacity to hold gas continues to increase;
- c) Methane production can continue into the anthracite rank range, but by the time organic matter is graphitized methane is virtually zero and remnants of gas have been driven off;
- d) Moisture increases slightly as a result of increase in porosity.

*Figure 2.1: The geochemical-biochemical transformation of plant substances as occurring over coalification stages, re-constructed after Moore (2012).*

The incombustible fraction of coal constitutes the inorganic minerals. The major minerals in coal include clay, carbonates, iron disulphides, oxides, hydroxides, sulphides, etc (Thomas, 2002). The origin of these minerals are either detrital, i.e., rock particles originating from pre-existing rock through process of weathering and erosion, and being transported through

sedimentary processes into depositional systems (Marshak, 2012); or authigenic, i.e., the rock particles are found at the place of its formation or origin. The minerals are formed during sedimentation by precipitation or recrystallization, and were induced into coal either during the deposition of peat or during later coalification process (Simmons, 1897).

The third component of coal is its moisture content. *In situ* coal is typically saturated with water to different extents. Apart from groundwater, there is moisture held within coal itself, known as the inherent moisture. The moisture in coal occurs in four different forms: surface moisture, which is held on the surface of the coal particles or macerals; hygroscopic moisture, that is held by the capillary force within the microfractures of coal; decompositional moisture, which is incorporated in the decomposed organic compounds of coal; and mineral moisture comprised part of the crystal structure of hydrous silicates, such as clays (Ward, 1984).

In essence, coal is an aggregate of heterogeneous substances, composed of organic and inorganic materials. The complexity of the mixture of the organic molecules in coal is well represented in figure 2.2, which represents the chemical structure of bituminous coal. The molecular formula for the same is  $C_{661}H_{561}N_4O_{74}S_6$  and the molecular weight is 10,023 grams per mole (Lin, 2010).

## **2.2 Coalbed Methane**

Gas that is retained in deep coals is termed as coalbed methane. As the name suggests, coalbed gas predominantly contains methane, along with carbon dioxide, carbon monoxide, nitrogen and ethane. The gases are by-products of the physical and chemical reactions that occur during the process of coalification from peat to anthracite (Van Krevelen, 1993). Different from conventional natural gas in sandstone reservoirs, where gas is stored mainly as free gas in the

pore spaces, gas in coalbed exists primarily in adsorbed phase on the internal surface area of the coal (Gray, 1987). Gas in coal is kept in place by the pressure of water that the coal is saturated

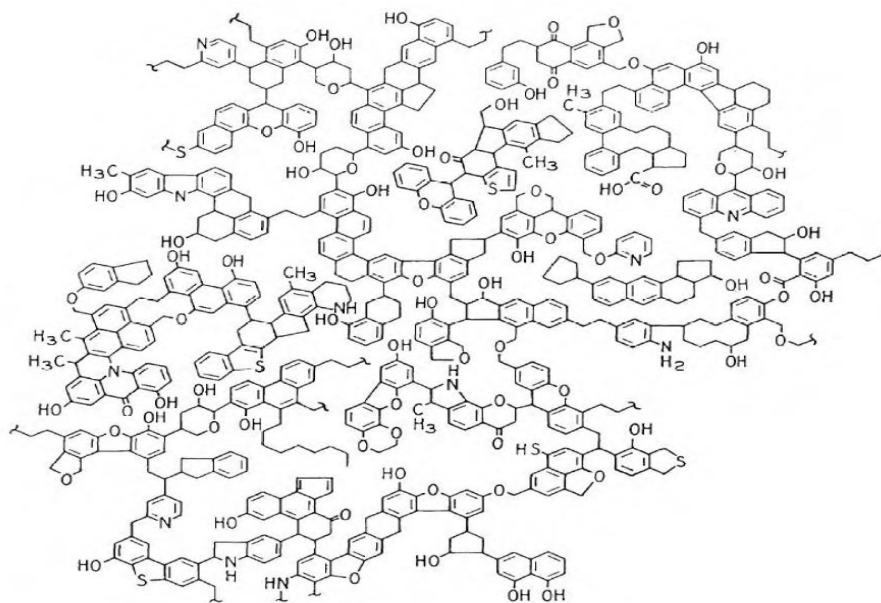


*Figure 2.2: Molecular structure of bituminous coal, Shinn 1984.*

with. Gas production from coal via wells is facilitated by gradual reduction of water pressure by pumping out of formation water, resulting in desorption of methane from the coal surface, its migration towards the wellbore and flow to the surface. All coals have methane, and the amount of methane generated over time exceeds the storage capacity of coalbed reservoirs (Tissot and Welte, 1984). The gas generated in addition to the storage capacity of the coalbed is lost to the surface through fractures, fissures, or charged to the adjacent carbonate/sandstone formations through permeable connections (Rogers, 1994). Thus, it is important to provide the pertinent background about the mechanisms of formation and storage of gas, and its flow in coal reservoirs. This includes not only the formation of coalbed gases, but the structure of coal, storage of gases in coal, sorption isotherms and diffusion of gas in coal, the last two phenomena being the primary thrust areas of this study.

## 2.3 Origin of Coalbed Gases

Presence of methane in coal has come a long way from initially being a hazardous nuance in mining operations to a commercially viable source of natural gas. The origin of methane in coal seams can be distinctly related to two processes: thermogenic and biogenic. Thermocatalytic conversion of coal is initiated at a temperature greater than 70°C. At such temperatures, when coal attains a rank of ~0.6% vitrinite reflectance (high volatile bituminous), and with continued application of heat and overlying pressure over time, thermogenic gases like carbon dioxide (CO<sub>2</sub>), water (H<sub>2</sub>O), methane (CH<sub>4</sub>), ethane (C<sub>2</sub>H<sub>6</sub>), hydrogen sulphide (H<sub>2</sub>S) and other higher hydrocarbons devolatilize (Stach et al., 1982; Faiz and Hendry, 2006; Moore, 2012). Carbon dioxide is generated in large quantities by the thermal decarboxylation or devolatilization of coal prior to the main stage of the thermogenic methane production (Karweil, 1969; Hunt, 1979; Tissot and Welte, 1984). However, carbon dioxide is highly soluble in water and very reactive. There are also other sources of carbon dioxide, such as, (1) thermal destruction of carbonates (Hunt, 1979), (2) carbonate dissolution linked to silicate hydrolysis (Smith and Ehrenberg, 1989), (3) migration from magma chambers or crust (Smith et al., 1985; Kotarba, 1988), and (4) bacterial degradation of organic matter.

Biogenic methane, as the name suggests, has its origin in the biosphere of the subsurface, specifically consisting of various forms of microbes. Primary biogenic methane and CO<sub>2</sub> are formed microbially during the initial stages of peat formation at shallow depths. Biogenic action from microbes is believed to have generated in excess of 6% CO<sub>2</sub> in the northwest San Juan basin (Ayers, 1991). Due to the large porosity and lower burial rates, primary biogenic methane is volatilized over time, or dissolved in water and expelled during compaction (Rice, 1993). Late stage biogenic methane, also known as secondary biogenic methane, is formed post-compaction

in all ranks of coal due to combination of active groundwater flow recharging the underground systems with suitable microbes, along with uplift of the basin helping in the meteoric recharge (Rice, 1993; Faiz et al., 2006).

## 2.4 Biogenic Methane

The final product of degradation of organic material under anoxic conditions in the absence of inorganic oxidants, such as, sulphate, nitrate and ferric ions is biogenic methane (Conrad, 2005). During formation of coal, *primary* biogenic gas is microbially produced during the early coalification process at shallow depths. However, due to low burial rates, the primary biogenic gas is expelled out of the system (Faiz and Hendry, 2006). Although the produced biogenic gases are lost in due course, isotopic analysis of coalbed methane invariably points towards a biogenic origin of methane in a number of different settings. The isotopic signature of Carbon (C), typically used to identify the source of methane, is indicated by the  $\delta$  notation, relative to a Pee Dee Belemnite (PDB) standard (Craig, 1953). Biogenic methane generation occurs at low temperatures, and is thus associated with lower energies than for thermogenic gas generation. The microbes, with lower energy available to them, preferentially breaks down the lighter isotopes of C, i.e., the  $^{12}\text{C}$  having lower bond energies. Thus, biogenically derived methane is isotopically light. The  $\delta^{13}\text{C}$  value for biogenic methane ranges between -40 to -110‰ PDB, depending on the isotopic composition of the original substrate, partial pressure of hydrogen in the system, methanogenic pathways, and the species of microbes involved (Games and Hayes, 1978; Jenden and Kaplan, 1986; Valentine et al., 2004; Conrad, 2005). Some studies have suggested inaccurate estimation of the origin of methane for  $\delta^{13}\text{C}$  values between -40 and -55‰. In such cases, the  $\delta^{13}\text{C}$  values are analyzed in conjunction with Deuterium (isotope of

Hydrogen) value,  $\delta D$  for methane and gas dryness index (Whiticar, 1996). Figure 2.3 presents the isotopic analysis of methane from four basins in US and Australia.

Presence of biogenic methane in a number of bituminous coal basins in Australia, Germany, Poland and US indicates a second source, in addition to the primary biogenic methane. Methane from this source is called the *secondary* biogenic methane. Methane present in high rank coals is formed in association with meteoric water flow into permeable coals after burial, coalification and subsequent uplift and erosion along basin margins (Scott, 1994). This mineral water influx is believed to recharge the native microbial community in the coal seams which, in turn, produce gases.

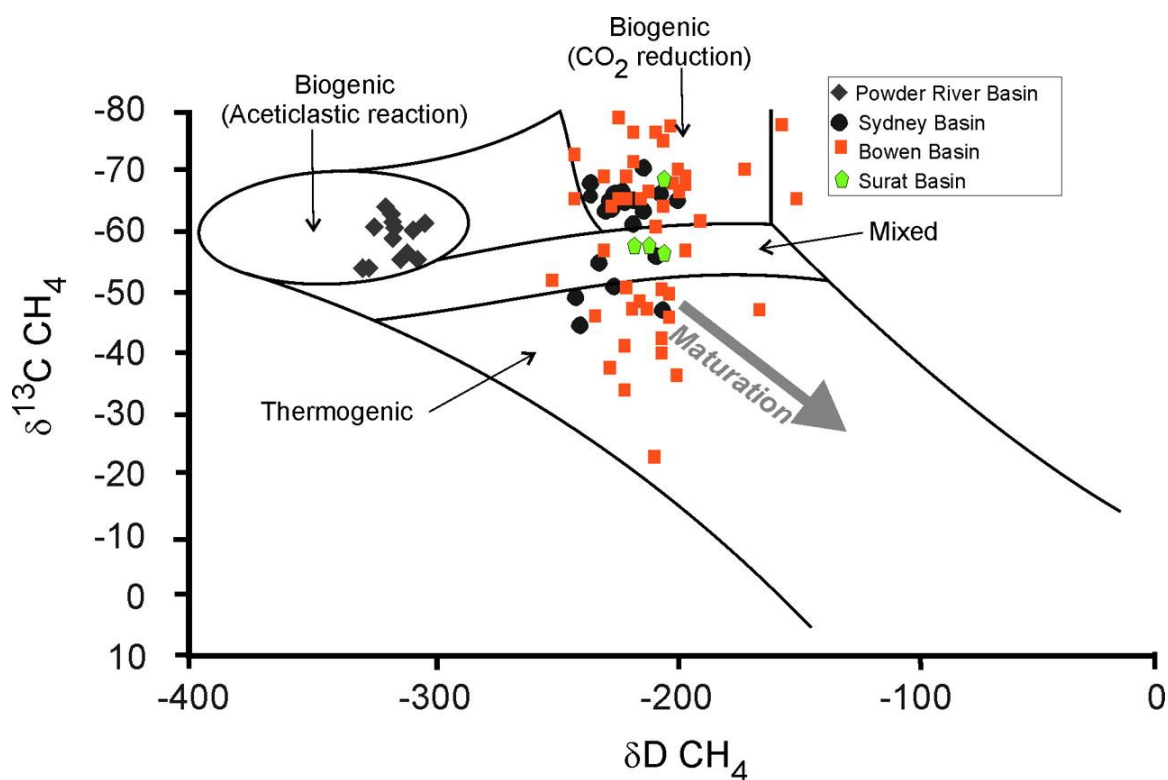


Figure 2.3: Isotopic analysis of CBM from different basins in US and Australia, Faiz and Hendry, 2006.

## 2.5 Microbially Enhanced Coalbed Methane

Microbially enhanced coalbed methane, or MECoM, as it is known, imitates the natural process of the formation of secondary biogenic gas (Scott, 1994). Scott suggested introduction of nutrients, trace elements and/or anaerobic bacterial consortia into coalbed methane wells to stimulate CBM production. Anaerobic bacterial consortia could be collected from produced formation waters or whole core samples. Once collected, these bacteria can be grown in laboratory cultures to evaluate and determine factors enhancing, and/or limiting their ability to convert coal to methane.

There have been a number of studies since 1994, aimed at producing methane from bio-treated coal. It was identified that a group of hydrolytic bacteria initially acts on substrates, i.e., coal, and the products of hydrolysis result in the formation of smaller aliphatic and aromatic compounds. These products of hydrolysis are further broken down into simpler compounds by fermentative bacteria or, different forms of syntrophic acetogens, bacteria that generates acetate as a product of anaerobic respiration, depending on localized chemical environment. The products of these syntrophic acetogens and fermentative bacteria provide the substrate for the anaerobic archaea, called methanogens, which produce methane. Figure 2.4 illustrates the process of conversion of coal to methane. The different methanogenic pathways are discussed in Section 2.5.1. More recent studies were aimed at producing methane from coal. Strapoc et al. (2007) and Jones et al. (2010) reported methane generation rates between 10 to 8000 standard cubic feet (scf) per ton of coal per year. Jones et al used coal from Zavala County in Texas. The coal was endemic and had no biogenic gas *in situ*. Some studies also used patented methods in which the nutrient amendments and other materials added to the test system were themselves a significant source of methane. Studies by Opara et al. (2012) had methane generation rates

similar to the studies by Strapoc and Jones, with nearly zero to a small percentage (1-3%) of the gases generated from direct conversion of different nutrients.

### 2.5.1 Methanogenic Pathways:

There are two main methanogenic pathways: the conversion of  $\text{CO}_2$  and  $\text{H}_2$ , formate or alcohols; and conversion of methylated compounds or acetate to methane (Worm et al, 2010). The first methanogenic pathway accounts for ~one third of the methane. The methane produced from freshwaters and bioreactors uses the hydrogen or formate as the substrate. The substrate also acts as the electron donor. The  $\text{CO}_2$  here acts as the carbon source and the electron acceptor. Most methanogens can use hydrogen as the electron donor. The second methanogenic pathway

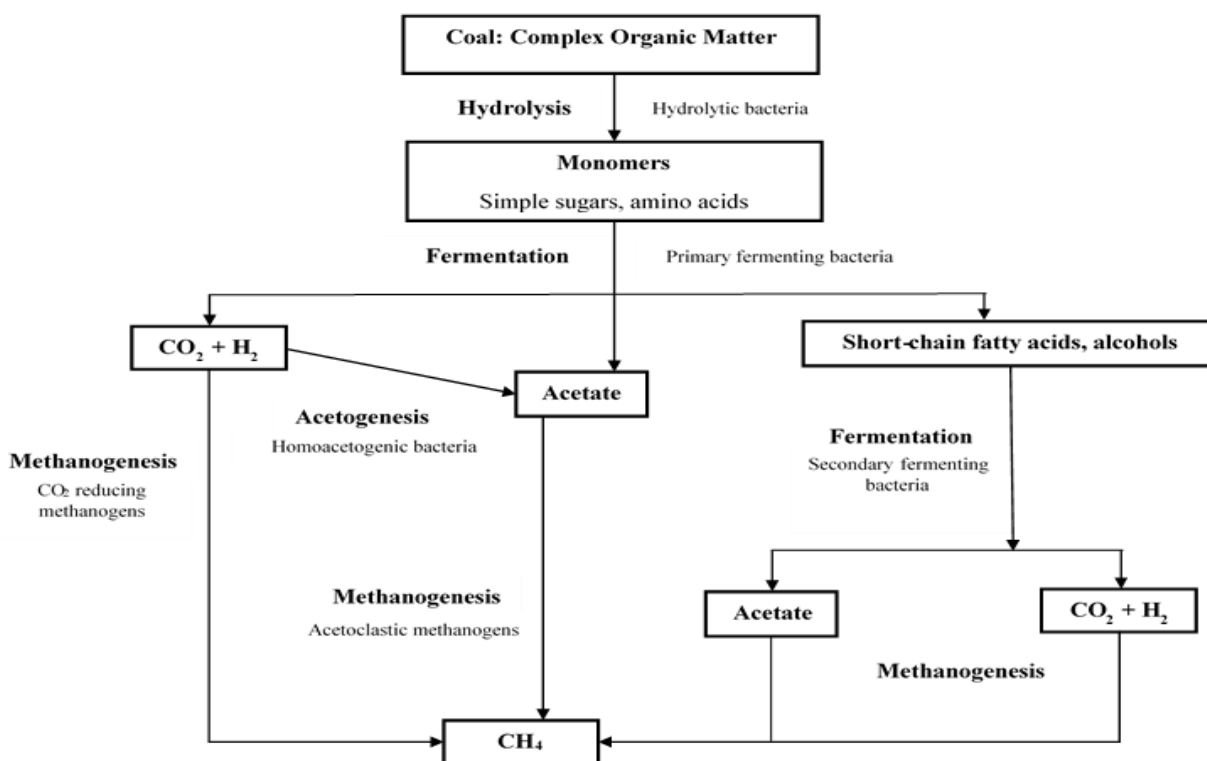
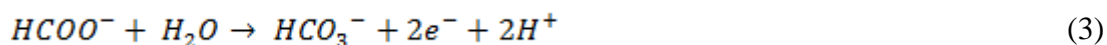
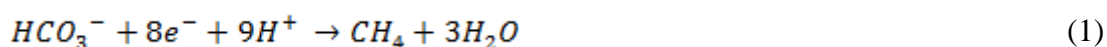


Figure 2.4: Anaerobic degradation of organic matter and the formation of biogenic methane, reconstructed from Formolo (2010).



uses the acetate or methylated compounds as both the electron donor and the carbon source (Vandecasteele, 2008).

Conversion of CO<sub>2</sub> is the only methanogenic pathway having a net negative electron flow. Moreover, only a handful of electron donors, including hydrogen, formate and alcohols, have been identified as suitable for this pathway.



The lack of electrons and availability of electron donors may be the reason for limited production of methane via this pathway. Methylated compounds, on the other hand, can be simultaneously oxidized to CO<sub>2</sub>, releasing six electrons, and reduced to methane through the reaction with coenzyme B, accepting two electrons. Lack of electron acceptors could be the limiting factor in this case. Finally, during the acetoclastic pathway, two electrons are donated through the conversion of the carboxylic group into CO<sub>2</sub>, while a series of reactions between the methyl group with coenzymes B, M and tetrahydrosarcinapterin accepts two electrons, resulting in net zero free electrons (Ferry, 2011). Various methanogenic reactions are shown in Table 2.1, indicating the importance of electron donors and acceptors in the process.

*Table 2.1: Most important methanogenic reactions ordered from the most to least thermodynamically favored as defined by free energy change (Zinder 1993, Thauer, 1998).*

<b>Electron Donor</b>	<b>Carbon Source</b>	<b>Reaction</b>	<b><math>\Delta G</math> (kJ/mol CH<sub>4</sub>)</b>
Formate	CO <sub>2</sub>	$4 \text{ HCO}_2^- + \text{H}_2 + \text{H}_2\text{O} \rightarrow 3\text{HCO}_3^-$	-145
Hydrogen	CO <sub>2</sub>	$4\text{H}_2 + \text{HCO}_3^- + \text{H}^+ \rightarrow \text{CH}_4 + \text{H}_2\text{O}$	-135
Alcohol	CO <sub>2</sub>	$2\text{CH}_3\text{CH}_2\text{OH} + \text{HCO}_3^- \rightarrow 2\text{CH}_3\text{COO}^- + \text{H}^+ + \text{CH}_4 + \text{H}_2\text{O}$	-116
Methanol	Methanol	$4\text{CH}_3\text{OH} \rightarrow 3\text{CH}_4 + \text{HCO}_3^- + \text{H}_2\text{O} + \text{H}^+$	-105
Methylamine	Methylamine	$4(\text{CH}_3)_3\text{NH}^+ + 9\text{H}_2\text{O} \rightarrow 9\text{CH}_4 + 3\text{HCO}_3^- + 4\text{NH}_4^- + 3\text{H}^+$	-76
Acetate	Acetate	$\text{CH}_3\text{COO}^- + \text{H}_2\text{O} \rightarrow \text{CH}_4 + \text{HCO}_3^-$	-31

## 2.6 Physical Structure of Coal

Although coal is visibly heterogeneous with varied properties, as discussed in section 2.1, there are several regular and repeating features which have definable physical structure. One such feature is the pores within the organic matrix. These pores are of varying sizes and shapes, 1- 10000 nm in size, and affect the electrical, strength, density and molecular transport properties of coal (Meyers, 1982). The porosity of coal is generally characterized as a dual-porosity structure: micropore and macropore systems, as suggested by Warren and Root (1963). Micropores are defined as pores less than 2 nm in size. These occur in coal as a part of the coal matrix. Figure 2.5 presents a scanning electron micrograph representing the pores in coal matrix. More than 95% of the gas in coalbeds is stored in adsorbed form on the surface of these pores (Gray, 1987). The average micropore diameter has been estimated to be in the range of 1 nanometer. The development of micropores is greatly influenced by the geochemical changes that occur in coal. The complex chemistry of coal can be divided into the aliphatic and aromatic

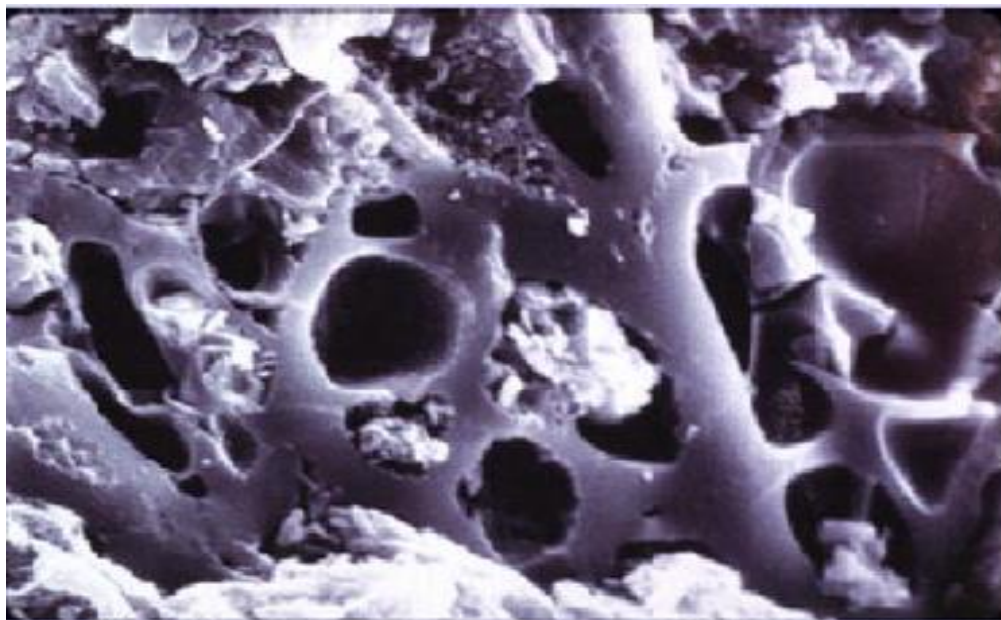


*Figure 2.5: Microscopic coal pore structure (Harpalani, 2002).*

components. There is increase in aromaticity with increasing coal rank. Coal attains a more aromatic chemical makeup from about 40% to over 90% in course of transformation from subbituminous to anthracite. The aromatic clusters and their realignment are instrumental in establishing the micropore network, and in releasing volatiles (Whitehurst, 1978).

The macropore system consists of naturally occurring network of closely spaced fractures, greater than 50 nm in width, surrounding the matrix. This is called the cleat system and provides the flow path for gas and water in coal. The spacing of cleats ranges from a fraction of an inch to several inches (Rogers, 1994). A fully fractured coal may have the following cleats: face cleats, butt cleats, tertiary third order cleats, fourth order cleats, and joints (Close and Mavor, 1991). The face cleats are considered the primary cleat structure. They are relatively longer and have wider aperture openings compared to the secondary butt cleats, which are

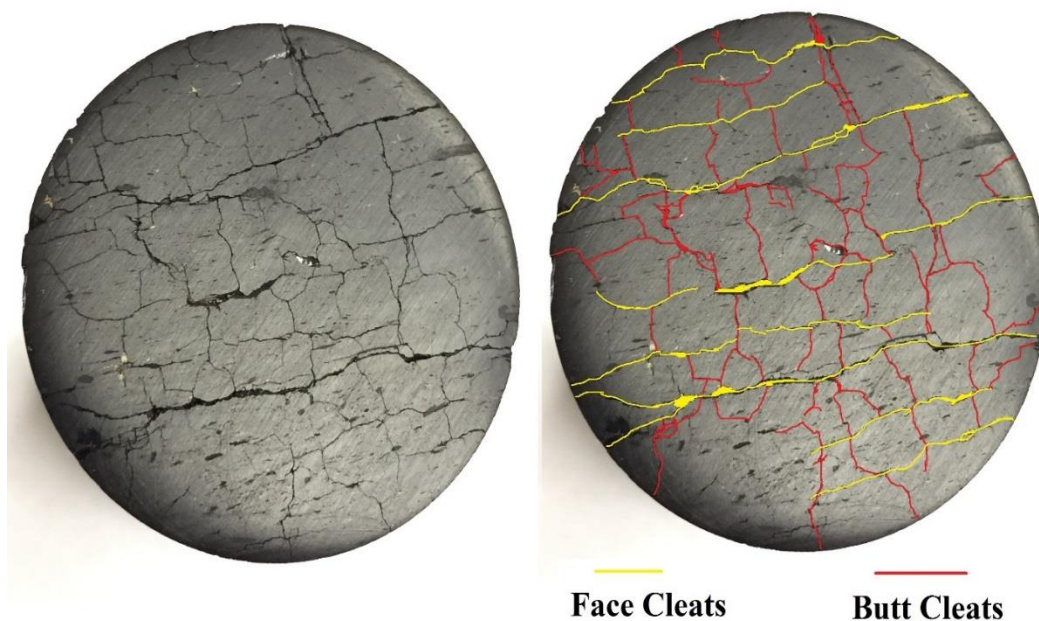


*Figure 2.6: Plan view of a coal core with highlighted (visible) cleat structure.*

perpendicular to them. The third and fourth order cleats, if present, develop after the face and butt cleats, and terminate at the face and butt cleats. These higher order cleats may be characterized as being  $45^\circ$  to their primary and secondary cleats.

Joints are the natural fractures that generally run parallel to the face cleats. The joint faces show no slippage relative to each other. The joints generally traverse the coal vertically, crossing interbedded inorganic layers and crossing the interface of the bounding rock (Ting, 1977).

Figure 2.6 shows the plan view of a core of coal cut perpendicular to the direction of the bedding plane with face and butt cleats highlighted. A simplified structure of coal can be represented by a cubic model, as shown in figure 2.7. However, since the horizontal fractures do not transmit any fluids, the ‘bundle of matchsticks’ model, as illustrated in figure 2.8, is considered to be a more appropriate model when studying flow in coal.

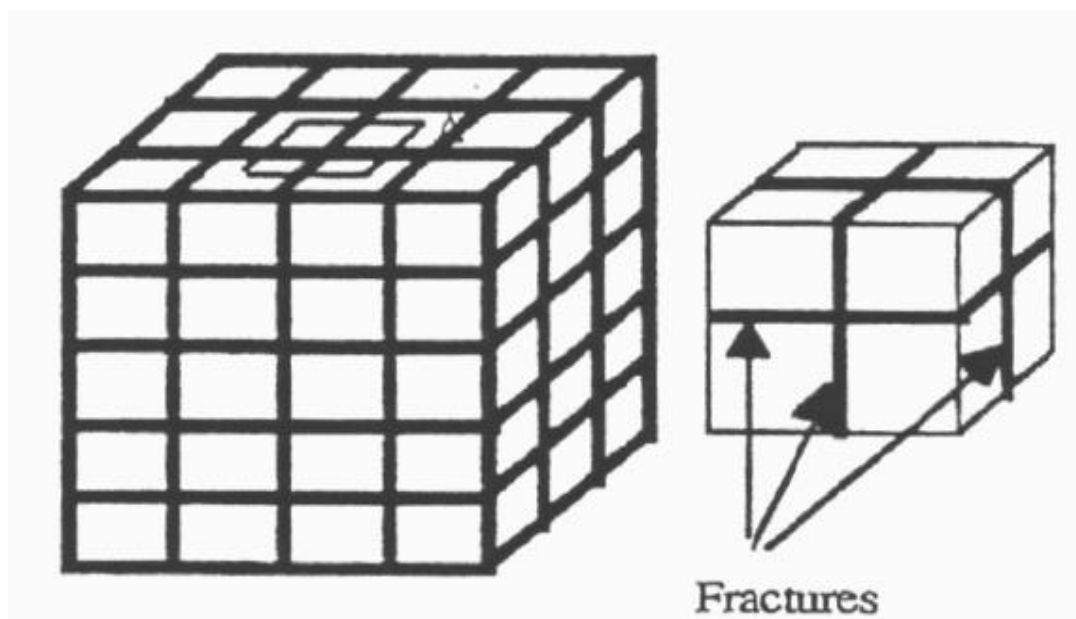


*Figure 2.7: Cubic model of coal, (Kumar, 2007)*

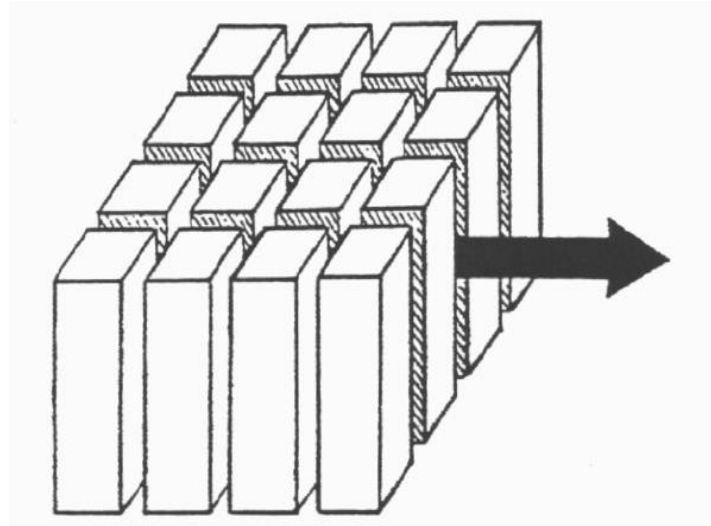


*Figure 2.8: Bundle of matchsticks geometry showing flow through vertical fractures, (Kumar, 2007).*

## **2.7 Storage of Gases in Coal**

Coalbed gases are primarily stored in the coals: (a) as gas dissolved in water within the reservoir, (b) as free gas within the pores or fractures, (c) as adsorbed molecules within the molecular structure of coal, and (d) as adsorbed molecules on the surface of the micropores (Rightmire et al., 1984). Gases dissolved in water follow the Henry's law, which describes the solubility of gas in water under pressure. Free gas within pores and fractures are the gas molecules which can easily move in the cleat system. This component of gas can be evaluated in the same way as traditional natural gas reservoir engineering, by applying the gas equation-of-state. Gases trapped within the molecular structure, are generally adsorbed to the surface of the coal. These gases are generated during the early coalification process, before the capacity of coal to retain gases threshold is reached.

In spite of the different storage sites of coalbed gases, as discussed above, ~95 % of gases stored in the coal seams is adsorbed to the internal pore surface area of the coal. These gases

exist as a monomolecular layer on the internal surface area of coal (Harpalani and McPherson, 1986). The quantity of gases that can be stored can be very large since the internal surface area of coal can be very large, and the gas molecules are packed tightly in the sorbed layer.

The sorptive capacity of coal for methane and  $\text{CO}_2$  is directly proportional to the pore pressure and rank, and is inversely proportional to temperature. The relationship between pressure and volume of methane adsorbed on the solid surface at a specific temperature, and moisture content is best described by an isotherm, and is unique for every specific coal type. The various techniques to determine gas storage (sorption) characteristics is discussed in detail in a later section.

## 2.8 Gas Transport in Coalbed Reservoirs

Gas transport in coal is commonly understood as three hydrodynamic mechanisms, taking the dual porosity nature of coal into account (King, 1985): (1) desorption of gas from the internal coal surface, (2) diffusion through the coal matrix bounded by the cleat (Fick's law) (King et al., 1986), and (3) laminar flow through macroscopic cleat (Darcy's law). The migration process of methane in the coal seam is shown in the following figure 2.9.

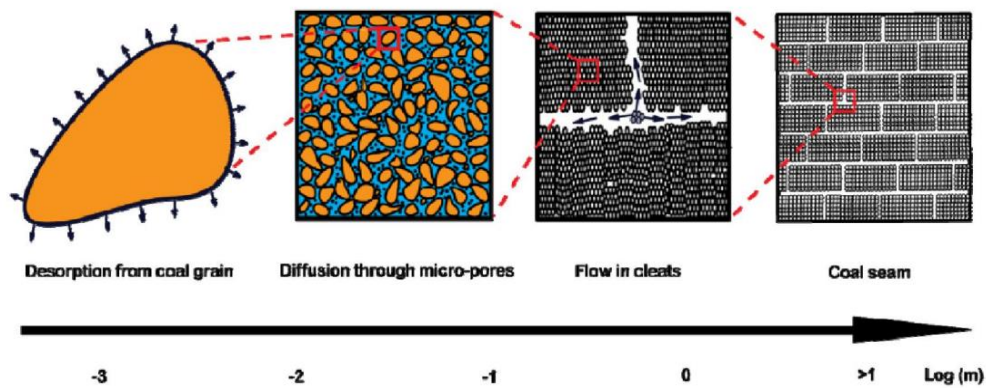


*Figure 2.9: Process of migration of gas in dual porosity coal.  
(Kumar, 2007)*

### **2.8.1 Desorption**

Desorption is the process by which methane molecules detach from the micropore surfaces of the coal matrix, which is followed by its diffusion through the pore structure and entry into the cleat system, where they exist and flow as free gas. When the reservoir pressure is reduced, either by dewatering or by gas production, the gas retaining capacity of coal for methane decreases and the process of desorption is initiated. Under ideal conditions, sorption of methane is considered reversible, that is, desorption follows the adsorption plot, as described by the Langmuir isotherm. Hence, the process of desorption can be explained by adsorption characteristics for a type of coal (Kumar, 2007).

### **2.8.2 Diffusion**

Diffusion is the process where flow occurs as a result of random molecular motion from a location of high concentration to a location of lower concentration (Kolesar et al., 1990a, 1990b; Smith and Williams, 1984; and Crank, 1975). Diffusion in coal is a combination of Knudsen, bulk, and surface diffusions, depending on the coal structure and pressure (Smith and Williams, 1984).

When the mean free path of gas molecules is greater than the molecular diameter, or when the pressures are very low, Knudsen diffusion takes place, and gas molecules flow from higher to lower gas concentration (Collins 1991; Zhao, 1991). In this transport phenomenon, the gas molecules collide more with the walls of the flow paths than with other molecules, and it is believed that the gas molecules never see each other (Thorstenson, 1989). Broadly, the resistance to flow is not due to molecules colliding with pore walls.



Surface diffusion of gas occurs when adsorbed gas molecules move along the micropore surface like a liquid (Collin, 1991). The exchange rate between the gaseous and adsorbed molecules is much higher than the rate of surface migration when equilibrium is achieved between gaseous and adsorbed phases. For this reason, at room temperature, the surface diffusion is much smaller than Knudsen diffusion. Typically, this is ignored in CBM production.

Bulk diffusion is the opposite of Knudsen diffusion, because (a) it occurs at higher pressures (Collins, 1991), (b) pore diameter is larger than the mean free path of the gas molecule, and (c) the resistance to diffusion comes primarily from collision between different gas molecules. Bulk diffusion involves momentum transfer between gas molecules themselves, as well as momentum transfer between molecules and pore walls. However, the wall effect is considered to be negligible compared to the momentum transfer between gas molecules.

The entire process of diffusion in coalbed reservoirs is described by Fick's Law and the driving force is a gas concentration gradient established between the coal matrix and cleat system. The law states that the rate of flow of gas per unit area is directly proportional to the concentration gradient normal to the direction of flow, and is given as:

$$m = -D \nabla C \quad (4)$$

where,  $m$  is the mass flow rate,  $D$  is the diffusion coefficient, and  $\nabla C$  is the concentration gradient. The diffusion effects in CBM operations are typically quantified by determining the sorption time,  $\tau$ , defined as the time required for lump(s) of coal to desorb 63% of the gas content. This is related to the cleat spacing and diffusion coefficient. It is also typically a known parameter for CBM reservoirs. The diffusion coefficient for methane in coal is a function of

temperature, pressure, pore length, pore diameter, and water content (Rogers, 1994). A detailed description of the diffusion process is presented in a later section.

### 2.8.3 Permeability

Once methane reaches the cleat or fracture network, flow becomes viscous and follows the Darcy's Law, given by:

$$m = -\rho \frac{k}{\mu} \nabla P \quad (5)$$

where,  $m$  is the mass flow rate per unit area,  $\nabla P$  is the pressure gradient,  $\mu$  is the viscosity of the gas,  $\rho$  is the density of the gas and,  $k$  is the apparent permeability of coal. Gas production in coalbed reservoir is initiated by pumping water through the wellbore to lower the pressure and initiate desorption. As water is produced, a two phase (water-gas) flow regime is initiated, which continues further as a result of the pressure drop in the reservoir, as discussed by Sawyer et al. (1987). Finally, a flow regime is reached where the gas moves through the cleat network accompanied by only small amounts of water.

## 2.9 Techniques to Determine Gas storage Characteristics

Temperature and pressure dictate the amount that a specific adsorbate will get adsorbed by a specific adsorbent at adsorption equilibrium (Yang, 1987). For constant temperature, the amount of adsorption is a function of pressure. Adsorption of different gases on coal is usually described by isotherms. A sorption isotherm relates the amount of adsorption of a specific adsorbate on a unit of a specific adsorbent and pressure at a constant temperature. Isotherms are generally categorized into five types, as shown in figure 2.10. Typical adsorption on microporous solids is represented by type 1 isotherms, which is also known as the Langmuir's isotherm. Type

1 isotherm has a monolayer coverage constraint during adsorption, while type 2, 3, 4 and 5 isotherms do not have this constraint. The last two types have a constraint in terms of the maximum amount of adsorption due to finite pore volume of the porous media (Do, 2008). These isotherms have been numerically modeled using three different approaches. They are the Langmuir approach, potential theory approach, and volume filling micropore approach (Yang, 1987).

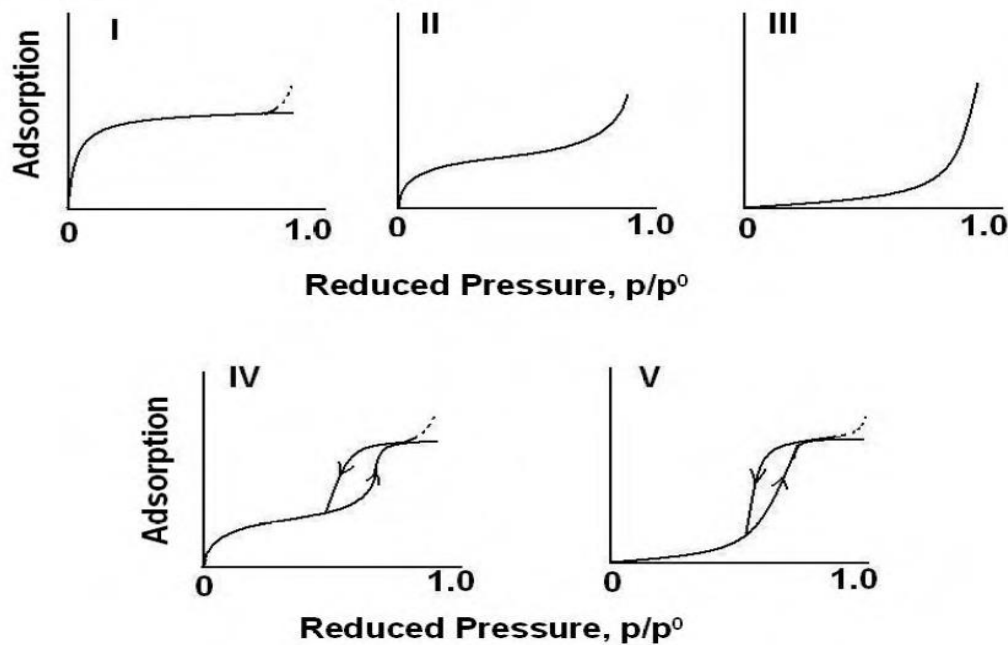


Figure 2.10: Different types of adsorption isotherms,  $p^0$  is the saturation vapor pressure (Yang 1987).

### 2.9.1 The Langmuir Approach

#### a. Langmuir Equation

For this approach, it is assumed that the adsorption reaches dynamic equilibrium when the rate of adsorption equals the rate of desorption, and each site of adsorption can accommodate only one adsorbate molecule/atom. Thus, the maximum amount of adsorption

is reached when all adsorptive sites are occupied by a monolayer of adsorbate molecules/atoms. The Langmuir adsorption falls into type 1 of the adsorption isotherms.

The rate of adsorption per unit area of adsorbent is  $\propto v(1 - \theta)$ , where  $\propto$  is the sticking probability,  $v$  is the collision frequency of adsorbate molecules/atoms striking the adsorbent surface, and  $\theta$  is the percentage of the available adsorbent surface which has already been occupied by adsorbate molecules/atoms. The collision frequency of gas molecules striking a solid surface according to the kinetic theory of gases is given by:

$$v = \frac{p}{(2\pi M \kappa T)^{1/2}} \quad (6)$$

where,  $M$  is the mass of one gas molecule/atom,  $T$  is the temperature, and  $\kappa$  is the Boltzmann constant.

The rate of desorption is given by  $\beta \theta e^{-E_d/RT}$ , where  $\beta$  is the rate constant of desorption,  $E_d$  is the activation energy of desorption,  $R$  is the universal gas constant. At adsorption equilibrium, the rate of desorption equals the rate of adsorption. This is mathematically represented as:

$$\beta \theta e^{-E_d/RT} = \propto \frac{p}{(2\pi M \kappa T)^{1/2}} (1 - \theta) \quad (7)$$

where,  $\beta$  is the rate constant for desorption,  $\theta$  is the fractional coverage of adsorption,  $E_d$  is the activation energy of desorption,  $R$  is the universal gas constant and  $\propto$  is the sticking probability. Hence,

$$\theta = \frac{Bp}{1 + Bp} \quad (8)$$

where,

$$B = \frac{\propto}{\beta(2\pi M \kappa T)^{1/2}} e^{-E_d/RT} \quad (9)$$

is called the Langmuir constant.

The fractional coverage of adsorption,  $\theta$  is defined as:

$$\theta \equiv \frac{n}{m} = \frac{V}{V_{max}} \quad (10)$$

where,  $n$  is the amount of adsorption (moles) on one unit of adsorbent at pressure  $p$ , and  $m$  is the maximum amount of monolayer adsorption in moles on one mass unit of adsorbent at infinite pressure. The expression can also be expressed in volume of sorption instead of moles.  $V$ , similar to  $n$ , is the gas volume adsorbed per unit mass of solid at pressure  $p$ , and  $V_{max}$  is the maximum monolayer volumetric capacity per unit mass of solid. Thus, the Langmuir equation (eq. 8), can be rewritten as:

$$V = \frac{p V_L}{p + P_L} \quad (11)$$

where, the Langmuir volume,  $V_L$  is  $V_{max}$ ; and the Langmuir pressure,  $P_L = \frac{1}{B}$ . These are the two Langmuir constants analogous to the parameters  $m$  and  $B$  respectively. These define the characteristic isotherm, where  $V_L$  points the asymptotic value of the isotherm and  $P_L$  is the pore pressure at which the sorbed volume is one half of the Langmuir volume.

In addition to the Langmuir equation, the modified spiral equations also represent type 1 sorption isotherm. Mathematically, this is given as:

$$p = \frac{n}{H} \left[ \frac{m}{m-n} \right] \exp(C_1 n + C_2 n^2 + C_3 n^3 + C_4 n^4) \quad (12)$$

where,  $n$  is the adsorption amount in moles;  $C_1, C_2, C_3, C_4$  are constants; and  $H$  is the Henry's constant defined as (Talu et al., 1995):

$$H \equiv \lim_{p \rightarrow 0} \frac{n}{p} \quad (13)$$

In the modified spiral equation, the term  $\left[ \frac{m}{m-n} \right]$  enforces Langmuir behavior at high pressure, whereas the viral expansion terms modify the low-pressure adsorption.

### Extended Langmuir Equation

The Extended Langmuir (EL) equation is the simplest and most commonly used model for prediction of mixed gas adsorption on coal (Clarkson and Bustin, 2000). In order to predict the binary adsorption equilibria, it requires pure component isotherm data only, and no binary sorption constants are necessary. The EL equation is given as:

$$V_i = \frac{(V_L)_i b_i P_i}{1 + \sum_j b_j P_j} \quad (14)$$

where,  $V_L$  and  $b$  are the pure gas isotherm Langmuir constants, and  $P_i$  and  $P_j$  are the partial pressures of individual gas in free-gas phase. The partial pressure is related to the total pressure by the relation:

$$P_i = P y_i \quad (15)$$

where,  $y_i$  is the gas phase mole fraction of the component  $i$ , and  $P$  is the total pressure. The relative adsorption of the two components is calculated by estimating the separation factor, or the selectivity ratio. The selectivity ratio of a binary gas adsorption system is defined as:

$$\alpha_{ij} = \frac{(x/y)_i}{(x/y)_j} \quad (16)$$

where,  $x$  and  $y$  are the molar fraction of a component gas in the adsorbed and free phase respectively. For the EL model, the separation factor is simply the ratio of the adsorption equilibrium constants (Arri et al., 1992; Ruthven, 2984), given as:

$$\alpha_{ij} = \frac{(V_L b)_i}{(V_L b)_j} \quad (17)$$

The simple nature of the EL model makes it easy to use for most adsorption applications although it does not have a strong theoretical foundation. In order to have a theoretical backing for the EL equation, the Langmuir volumes for all individual components must be equal (Ruthven, 1984). However, for adsorption of molecules of widely different sizes, such an assumption is unrealistic and is usually not true. The Extended Langmuir isotherm is, therefore, viewed more as a correlation rather than an accurate physical model with firm theoretical basis. Extrapolations outside the range of experimental data should be made with caution.

#### **b. The BET Model (Brunauer et al., 1938)**

For gases like CO<sub>2</sub>, which are rather strongly adsorbed onto coal surfaces, monolayer adsorption is not an accurate estimate of the sorption capacity. The BET model provides a quantitative description of sorption that is not limited to one adsorption layer on the adsorbent surface. The model is mathematically given as:

$$n = \frac{mCp}{(p^0 - p)[1 + (C - 1)(p/p^0)]} \quad (18)$$

where,  $p^0$  is the saturation pressure of the adsorbate at the temperature of adsorption,  $p/p^0$  is the relative pressure or the reduced pressure. Eq. 18 is called the Brunauer-Emmett-Teller (BET) equation. The fitting parameters for this equation are:  $m$ , which is the maximum

monolayer adsorption in moles; and  $C$ , which is the shape parameter at low pressure range.

The value of  $C$  is usually greater than unity, indicating that the heat of adsorption of the first adsorption layer is greater than the heat of liquefaction.

According to the BET equation (eq. 18), when  $p = p^0, n \rightarrow \infty$ . Thus, the BET model does not have a limit on the maximum amount of adsorption, indicating that there can be infinite layers of molecules built up on the surface. When the adsorption space is finite, the maximum number of layers that can be built on top of the surface is limited, which results in the  $n$ -layer BET equation, expressed as:

$$\frac{n}{m} = \frac{C p_R}{1 - p_R} \frac{1 - (N+1)p_R^N + N p_R^{N+1}}{1 + (C-1)p_R + C p_R^{N+1}} \quad (19)$$

where,  $p_R = p/p^0$  is relative pressure, and  $N$  is the allowed number of adsorption layers. For  $N = 1$ , the equation reduces to Langmuir equation. The maximum amount of adsorption is reached when the pressure approaches the vapor pressure, which depends on the number of adsorption layers allowed on the adsorbent surface. For pure gas adsorption, the BET equation works well by adjusting the fitting parameters. It falls short in modeling multi-component adsorption, where the adsorbed phase composition is not readily predicted by fitting the parameters. For this, thermodynamics has to be taken into account. The Gibbs approach is the most developed approach to model multi-component adsorption, but it is beyond the scope of this study.

### 2.9.2 Polanyi's Potential Theory

Analogous to gravitational potential around a planet, Polanyi assumed the existence of a potential field around the surface of the solid into which the adsorbed gas molecules falls. The



surface force field can be represented by equipotential contours, where the space between each set of equipotential surfaces corresponds to a definite adsorbed volume. The adsorption potential is defined as the work done per mole of adsorbate in transferring molecules from the gaseous to adsorbed state. The adsorption potential represents the work done by temperature independent dispersion forces. The potential curve is, therefore, not dependent on temperature, and is characteristics of the particular gas solid system alone. It is a function of only the volume enclosed by an equipotential surface surrounding the adsorbent surface. Thus, the sorbed volume becomes a function of adsorption potential  $A$ , that is:

$$V = f(A) \quad (20)$$

The above relation is characteristic of a gas-solid system, and is known as the characteristic curve (Yang, 1987). The characteristic curve generated from one experimental isotherm thus permits prediction of isotherms at different temperatures (Mehta, 1982). Assuming that the adsorbate behaves as an ideal gas, the adsorption potential is given as:

$$A = RT * \ln\left(\frac{P_o}{P}\right) \quad (21)$$

where,  $A$  is the adsorption potential,  $R$  is the Universal Gas Constant,  $T$  is the adsorption temperature in absolute units,  $P$  is the adsorption pressure and  $P_o$  is the saturation vapor pressure of the adsorbate at temperature  $T$ . The Potential Theory has been substantiated by the work of several researchers. Although the concept of the original theory has not changed, its mathematical functional relations have changed significantly to utilize its predictive capability (Mehta, 1982). Dubinin (1967) used this to describe adsorption on microporous adsorbents and proposed a new theory, which is known as the theory of volume filling of micropore (TVFM).

### 2.9.3 Theory of Volume Filling Micropore (TVFM)

Microporous adsorbents (pore size less than 20 nanometer) have an enhanced adsorption potential in the pores owing to the superposition of the adsorption energy fields of the opposite walls (Amankwah and Schwarz, 1995). Coal is, therefore, a microporous adsorbent since most of its pores fall in this size range. Borrowing the well-known concept of colloid chemistry, Dubinin (1967) argued that the macroscopic notion of the surface of a solid body loses its physical significance when the pore size is less than  $20 \text{ \AA}$ , and this is true for coal. The concept of adsorption on surfaces by the layering mechanism can, therefore, not be accurate. The basic geometrical parameter for microporous adsorbent is the volume of the micropores rather than their surface area. Based on Polanyi's Potential Theory, Dubinin (1975) developed a new theory for adsorption of gases on microporous solids, and named it as the Theory of Volume Filling of Micropore. It was postulated that, in micropores, the adsorbate occupies the pore volume by the mechanism of volume filling, as shown in figure 2.11, and hence, does not form discrete layers in the pores.

Dubinin (1967) showed that, for several vapors, the ratio of limiting adsorption values on two varieties of zeolite crystals was essentially constant and equal to the ratio of void volumes calculated from X-ray data. The ratio was, however, not equal to the geometric surface area of the zeolites. This observation provided proof for the volume filling mechanism of the micropores. Based on this, Dubinin and Astakhov proposed an equation representing the isotherms that obeyed the TVFM (Amankwah and Schwarz, 1995). Known as the Dubinin-Astakhov (D-A) equation, it is expressed as follows:

$$V = V_0 * \exp \left[ - \left\{ D * \ln \left( \frac{p_0}{p} \right) \right\}^n \right] \quad (22)$$

where,  $V$  is the amount adsorbed,  $V_0$  is the volume of micropores,  $n$  is the structural heterogeneity parameter and is a small number varying between 1 and 4,  $D = \left(\frac{RT}{\beta E}\right)^n$  is a constant, where  $E$  is the characteristic energy of the adsorption system,  $T$  is the absolute temperature,  $R$  is the universal gas constant, and  $\beta$  is the adsorbate affinity coefficient.  $D$  is a constant for a particular adsorbent adsorbate system, and is determined experimentally.  $P_0$  is the saturation vapor pressure of the adsorbate at temperature  $T$ , and  $P$  is the equilibrium free gas pressure. Dubinin and Radushkevich suggested that  $n = 2$  may be appropriate for some cases, and the equation can be modified as follows:

$$V = V_0 * \exp \left[ - \left\{ D * \ln \left( \frac{P_0}{P} \right) \right\}^2 \right] \quad (23)$$

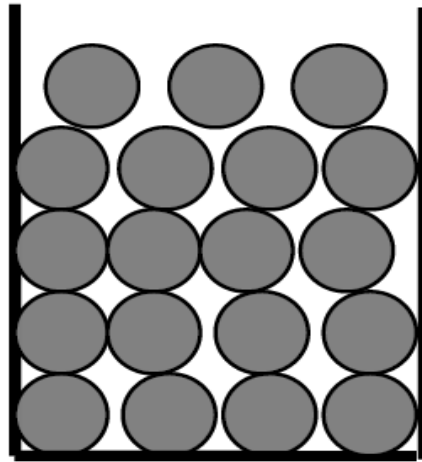


Figure 2.11: Micropore filling mechanism used in TVFM (Do, 1998).

The above equation is known as the Dubinin-Radushkevich (D-R) equation. The D-A and D-R equations are also known as the Dubinin-Polanyi (D-P) equation. One unique advantage of the D-P isotherm equations is that, if one isotherm at a particular temperature is available, then

the characteristic curve can be derived from that single isotherm and used to obtain another isotherm for the same solid-gas system at any other temperature. This unique advantage is really useful where isotherm data at multiple temperatures cannot be obtained readily.

#### 2.9.4 Estimation of Surface Area

Specific surface area is defined as the accessible area of solid surface per unit mass of material, coal in our case. Use of the techniques discussed in sections 2.9.1 through 2.9.3 enables the estimation of the surface area available to sorption in a number of cases. We make use of the Langmuir equation to estimate the specific surface area of coverage of a particular sorbent, coal in our case, for a sorbate, which is methane or CO<sub>2</sub>. Itodo et al., (2010) used the following equation to estimate the specific surface area:

$$S_{MB} = (q_m \times a_{MB} \times N_A \times 10^{-20})/M \quad (24)$$

where,  $S_{MB}$  is the specific surface area in  $10^{-3} \text{ km}^2\text{kg}^{-1}$ ,  $q_m$  is derived from the Langmuir constant providing an estimate of the number of molecules of the sorbate adsorbed at the monolayer of coal with units of  $\text{mgg}^{-1}$ ,  $a_{MB}$  is the occupied surface area of one molecule of sorbate in  $\text{\AA}^2$ ,  $N_A$  is the Avogadro's number with units of  $\text{mol}^{-1}$  and  $M$  is the molecular weight of the sorbate in  $\text{g mol}^{-1}$ .

#### 2.10 Techniques to Determine Diffusion Characteristics

The three primary laboratory techniques used to estimate the diffusion coefficient,  $D$ , of coal are the Particle Method, Steady-state Flow Method and Counter Diffusion Method. This study makes use of the particle method since it is the most commonly used in CBM industry, the primary reason being that the sorption isotherms are established as well, using pulverized coal. The different methods are discussed in the following sections:

### 2.10.1 Particle Method

The particle method involves grinding of coal to eliminate the cracks and micropores completely, ensuring that the movement of gas is purely diffusive in nature. It is reported that the crushing of coal increases sorption of gases due to increase of surface area for gas adsorption. Jones et al., (1988) reported the increase to be between 0.1 and 0.3% for 40-60 mesh coal size, thus representing near *in situ* conditions in terms of accuracy of the experiment. The experimental procedure is discussed in detail in chapter 3.

There are two diffusion models that have been used successfully based on the particle method. They are the “unipore” and “bidisperse” models.

#### a. Unipore Diffusion Model

The unipore model assumes that all pores in the coal matrix are of the same radius.

The model is based on Fick’s second law for spherically symmetric flow, given as:

$$\frac{D}{r^2} \frac{\partial}{\partial r} \left( r^2 \frac{\partial C}{\partial r} \right) = \frac{\partial C}{\partial t} \quad (25)$$

where,  $r$  is the radius of the micropore,  $C$  is the adsorbate concentration,  $D$  is the diffusion coefficient, and  $t$  is the time between two measurements. This form of equation assumes that the diffusion coefficient is independent of the concentration and location within the solid coal.

The solution to the above equation for a constant surface concentration of the diffusing adsorbate can be expressed as (Crank, 1975):

$$\frac{M_t}{M_\infty} = 1 - \frac{6}{\pi^2} \sum_{n=1}^{\infty} \frac{1}{n^2} \exp\left(-\frac{D n^2 \pi^2 t}{r_p^2}\right) \quad (26)$$

where,  $M_t$  is the total mass of the diffusing gas that has desorbed in time  $t$ ,  $M_\infty$  is the total desorbed mass, and  $r_p$ , the diffusion path length. Following a step change in surface concentration, this relationship for sorbed gas can be written as (Clarkson and Bustin, 1999):

$$\frac{V_t}{V_\infty} = 1 - \frac{6}{\pi^2} \sum_{n=1}^{\infty} \frac{1}{n^2} \exp\left(-\frac{Dn^2\pi^2 t}{r_p^2}\right) \quad (27)$$

where,  $V_t$  is the total volume of gas desorbed in time  $t$ , and  $V_\infty$  is the total sorbed volume.

This equation is commonly referred to as the unipore model equation. The value of  $D$  is determined using the data collected from experimental work. The experimentally determined fraction of gas sorbed is plotted versus the square root of time and the unipore equation is curve fitted to the experimental data to obtain an estimate of  $\frac{D}{r_p^2}$ .

For  $\frac{V_t}{V_\infty} < 0.5$ , the unipore equation can be approximated as:

$$\frac{V_t}{V_\infty} = 6 \left(\frac{D_s t}{\pi}\right)^{1/2} \quad (28)$$

Mavor et al., in 1990 used the above equation to calculate the diffusion coefficient using an averaged value for particle size. In order to obtain the diffusion coefficient during a pressure step, a diagnostic plot of the gas content change during the pressure step with elapsed time is required. The monitored pressure variation enables the calculation of the quantity leaving or entering the sample, or change in the capacity of the sample to store gas with time. Figure 2.12 is a typical example of the diagnostic plot required for one of the pressure steps. The purpose of the plot is to verify that the measured data satisfies the condition for short time diffusion for spherical geometry. The slope of the log-log plot should be  $\sim 0.5$ . The model during the half slope period is given as:

$$g - g_{I-1} = 3.3851 (g_I - g_{I-1}) \left[ \frac{D}{r_s^2} \Delta t \right]^{0.5} \quad (29)$$

where,  $g$  is the gas storage capacity in scft,  $g_I$  is the gas content at the end of step I in scft,  $g_{I-1}$  is the gas content at the end of step  $I - 1$  in scft,  $D$  is the diffusion coefficient in  $\text{cm}^2/\text{sec}$ ,  $r_s$  is the spherical particle radius in cm, and  $\Delta t$  is the time elapsed between measurements of  $g_I$  and  $g_{I-1}$ , in seconds.

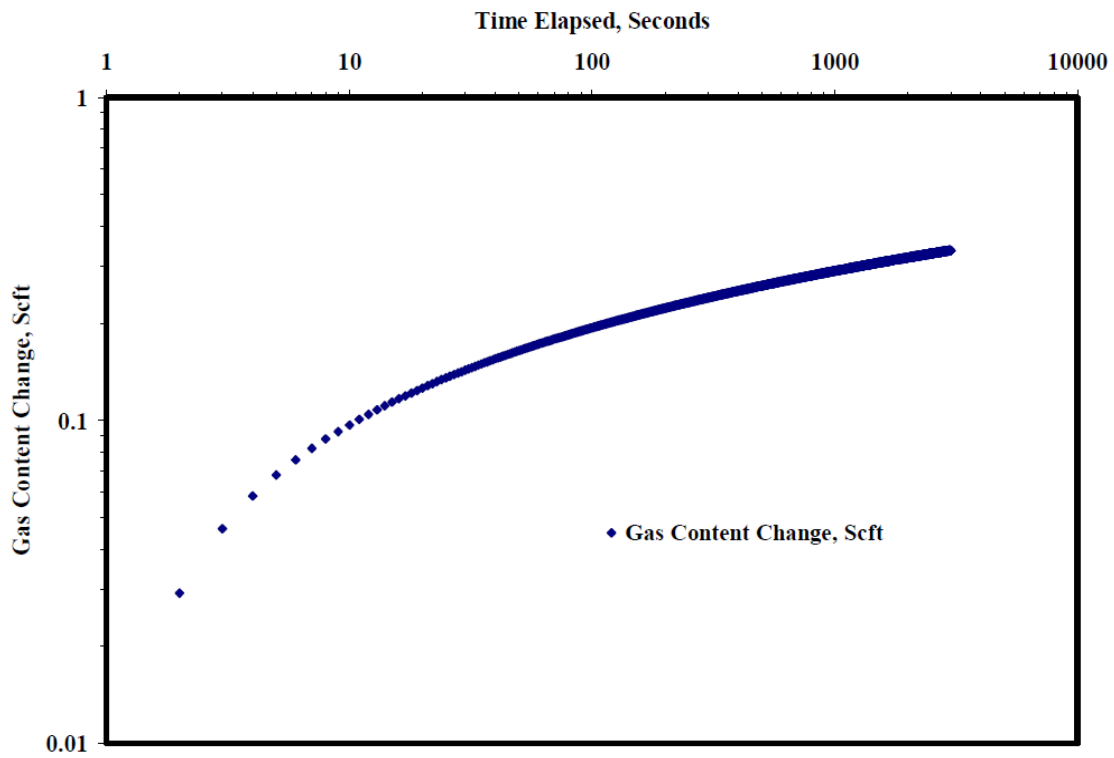


Figure 2.12: A typical diffusion diagnostic graph.

Mavor et al. (1990) stated that the unipore diffusion model is more applicable to high pressure steps of the isotherm rather than all steps. However, for a complete analysis, using the bi-disperse model of diffusion may be necessary. The diffusion coefficient is estimated from the slope of the initial graph,  $b$ , based on the following:

$$D = \left\{ \frac{b r_s}{3.3851 (g - g_{1-1})} \right\}^2 \quad (30)$$

### b. Bi-disperse Diffusion Model

Ruckenstein et al. (1971), developed this model assuming that some coals have bi-modal pore size distribution. The model assumes that the adsorbent is a spherical particle, which is a macrosphere, containing microspheres of uniform size, as shown in figure 2.13. Few researchers, like Smith and Williams (1984), used this study to better represent the diffusion behavior of coal and found that the bi-disperse diffusion model describes the entire desorption regime better than the unipore models for some coals, but might be inadequate for application to high pressure volumetric sorption experiments. The model assumes a step

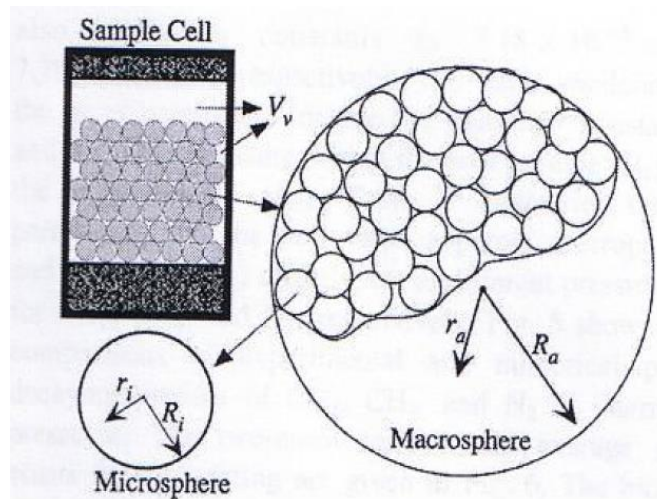


Figure 2.13: Conceptual model of the bidisperse pore structure (Yang, 1997).



change in external concentration in the diffusing gas at time zero, and that this concentration remains unchanged with time (Clarkson and Bustin, 1999). This assumption is not true for constant volume and variable pressure adsorption rate experiments as described by Mavor et al. (1990). Moreover, methane and carbon dioxide adsorption isotherms for bituminous coal are known to be nonlinear, and the application of linear models is truly inadequate for most coals.

In previous research effort at SIU Carbondale, Ajayendra Kumar (2007) showed that, for coal samples taken from the Illinois basin, the estimated values of the diffusion coefficient using the unipore and bi-disperse results produced similar data. Significant difference was not observed in terms of the diffusivity trend with pressure. The current study will, therefore, use the computationally simple unipore approach to study diffusion behavior in coal.

### **c. Steady State Flow Model**

This technique utilizes experimental setups similar to ones typically required for estimation of the permeability, where flow rates are measured through a solid coal sample, typically cylindrical cores. A pressure gradient is applied across the sample to initiate gas flow, limited by the condition that the gas flow is not turbulent. The diffusion coefficient is measured after measuring steady-state flow. The samples used for this experiment is required to be cleat and fracture free to prevent viscous flow of gas due to the applied pressure gradient. This is the major disadvantage of the method, since obtaining a sample of cleat free coal is difficult. Moreover, the experiments take a very long time, compared to the particle method, because the sorption of methane on solid coal is very slow (Thimons and Kissel, 1973).

#### **d. Counter Diffusion Model**

This technique is similar to the steady-state flow method with a major improvement since it avoids a pressure gradient across the sample, thus eliminating any possibility of viscous flow. The method involves passage of an adsorbing gas and a non-adsorbing gas through the opposite faces of a sample, resulting in zero pressure gradient across the two ends. This is the reason for the technique being also known as the constant pressure, counter diffusion method. By measuring the flowrate and outlet concentration of each stream at steady-state, the flux of each component across the sample is determined (Smith, 1982). This is followed by calculation of the diffusion coefficient. The disadvantage with this method is that it has to be performed at much lower pressures than those encountered in CBM operations. The results for higher pressure, therefore, can only be extrapolated for application in CBM applications. Since the variation in the value of diffusion coefficient with pressure might be different at high pressures, use of this method is discouraged.

### **2.11 Summary**

In this chapter, an effort was made to present the basic background about coal as a natural gas reservoir. It is understood that bacterial actions on coal have resulted in the formation of (secondary) biogenic methane that is stored in coal along with methane from thermogenic origin. A number of studies have been successfully conducted to simulate the process of secondary biogenic methane formation in laboratory setup. Given that methane can be generated by microbial consortia, it is critical to study the properties of coal that determine its storage and flow properties. A number of approaches necessary to model single and multi-gas sorption were discussed. The Langmuir approach provides accurate estimation of storage characteristics of coalbed reservoirs with computational ease. Different approaches to model diffusion

characteristics have also been presented. The diffusion characteristics can be studied over pressure ranges using the unipore model, providing acceptable estimates of the diffusion coefficient.

## CHAPTER 3

### EXPERIMENTAL STUDY

The basis of the experimental work is that sorption of a small quantity of methane or CO<sub>2</sub> on/from coal results in a change of pressure in a closed container. Hence, monitoring the pressure enables calculating the volume sorbed. Second, precise monitoring of pressure changes during early stages of sorption enables estimation of the diffusion coefficient. The experimental setup for this study was, therefore, designed to fulfil this requirement of precise and accurate pressure monitoring. Since temperature impacts the sorption capacity significantly, effort was made to maintain the system temperature constant during the entire experiment. This ensured that the changes in pressure were only due to *ad/de* -sorption of methane, and not the result of variation in temperature. This also enabled establishing the sorption characteristics at the desired *in situ* temperature.

#### 3.1 Experimental Design

The experimental setup was designed to measure very small changes in gas pressure over very short periods of time resulting due to *ad/de* -sorption of methane or CO<sub>2</sub> on/from the coal sample. A schematic of the experimental setup is shown in Figure 3.1. The primary components of the setup were a pressure vessel assembly, capable of withstanding very high pressures, a high-precision data acquisition system (DAS), and a computing interface. The setup was designed so that it could be completely immersed in water, maintained at constant temperature using a water bath with fairly precise temperature control. Figure 3.2 shows the setup pictorially.

### 3.1.1 High Pressure Vessel Assembly

A high pressure vessel assembly, as shown in Figure 3.3, was fabricated especially for this experiment. The sample container, made of stainless steel, was designed to withstand a pressure of more than 5000 psi. All other connections and fittings used were capable of withstanding pressures up to 3000 psi. The sample container and fixed volume cylinder were connected with a filter and a control valve in between. The filter was provided to prevent movement of coal particles between the sample container and the fixed volume cylinder when the pressure in the sample container dropped suddenly. The control valve was provided in order to control the flow of gas between the sample container and fixed volume cylinder. A set of two-/three- way valves was used in the setup to achieve the desired flow and storage of gas. A pressure transducer was connected to the fixed volume cylinder.

### 3.1.2 Temperature Control System

Since *ad/de* -sorption of methane or CO<sub>2</sub> on coal is very sensitive to temperature, maintaining a constant temperature throughout the experimental phase is critical. A precision constant temperature water bath, with  $\pm 0.1^\circ\text{C}$  error, was used for this purpose. The pressure vessel assembly was kept in this bath throughout the experiment, which lasted over a period of several weeks.

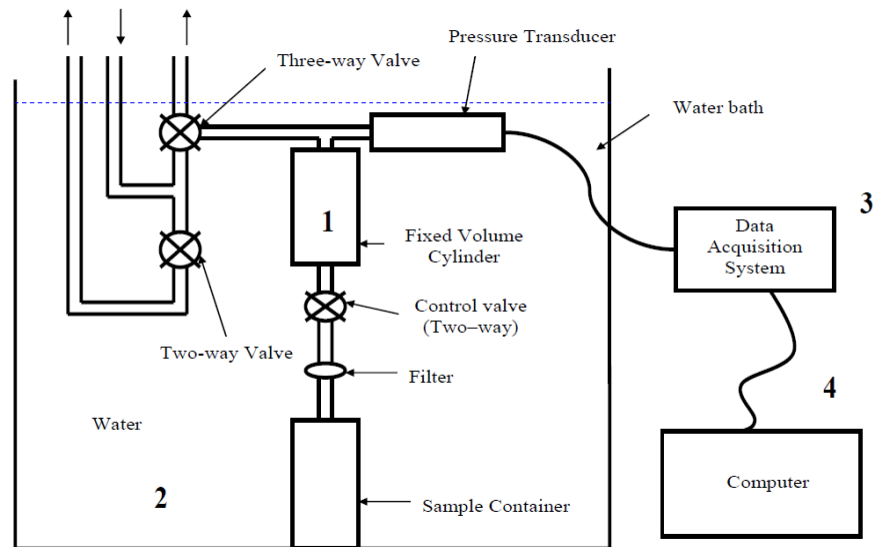


*Figure 3.1: Schematic of the sorption/diffusion experimental setup.*

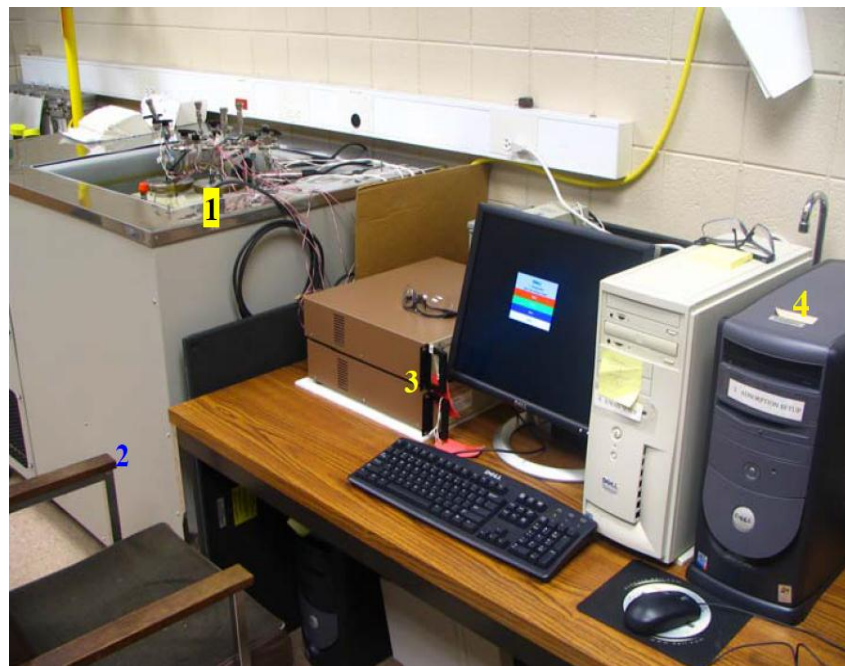


*Figure 3.2: Pictorial representation of the experimental setup.*

(1) Pressure vessel assembly immersed in water bath; (2) constant temperature water bath with the pressure vessel; (3) DAS; and (4) computer for DAS.

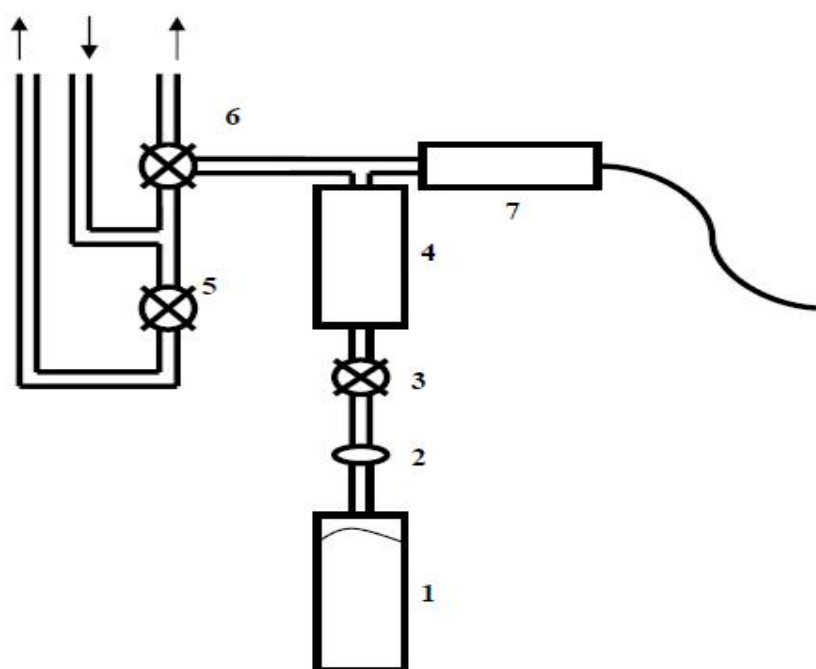


*Figure 3.3: High pressure vessel assembly.*

(1) Sample container; (2) filter; (3) two-way control valve; (4) reference volume cylinder;  
(5) two-way valve; (6) three-way valve; and (7) pressure transducer.

### **3.1.3 Data Acquisition System**

A 16-bit data acquisition system (DAS) was used in order to collect the pressure data. The purpose of using 16-bit high precision DAS was to acquire data at very small time intervals, with the least amount of bit-flip since a minute deviation from the exact pressure during initial diffusion process could easily result in erroneous results. The hardware provided a physical connection to the sensors with high-level voltage outputs through an instrumentation card. This card, incorporating all the necessary power supplies, circuit completion components, signal conditioning amplifiers and analog- to-digital converters, was housed in a scanner, which measured the data in a digital form and transferred them through a high-speed digital interface. The data was collected by the software “StrainSmart” which works on Windows NT platform. The data collection procedure included collection of raw data with the pressure transducer, defining instrumentation and software parameters, calibration and zeroing of the transducer, and reductions of the digital raw data to usable measurements data. The system was set to collect data every 0.5 second interval during the initial period, which was gradually increased to 50 seconds as pressure approached equilibrium.

### **3.2 Sample Procurement and Preparation**

The experimental phase included carrying out tests for three sets of coal samples. Pieces of coal, taken from blocks of coal, were ground and separated using sieve analysis. The size of the test specimens was between 40 and 100 mesh, providing an average particle radius of 0.0143 cm. The first set of samples was virgin, untreated coal. This provided the baseline for comparison with the data for treated coal. The sieved coal was then treated with microbial solutions along with a nutrient profile. Methane and CO<sub>2</sub>



production rates were monitored over a period of thirty and sixty days respectively. The second set of coal tested was for the sample treated for thirty days. The third set of coal tested was for the sample treated for sixty days. The microbial solution producing the most methane was utilized for the experiment. A discussion about the experimental setup for setting up microbial solutions for treating the coal is beyond the scope of the study. However, detailed description of the methods used is included in Zhang et al (2015).

Approximately 60 g of sample was used for each set of sorption-diffusion experiment. Prior to starting the experiment, the samples were kept in an environmental chamber at the desired temperature and 97% humidity for twenty four to thirty six hours for moisture equilibrium. Five grams of sample was used to measure the ash and moisture content while the remainder was used for the sorption/diffusion experiment.

### **3.3 Calibration and Testing of Entire Setup**

The pressure vessel assembly was tested for leakages by injecting helium at a pressure of ~1500 psi and leaving it for 48 hours. This testing was also carried out prior to every experiment to ensure that there was no leakage path generated during opening and closing of sample container when changing samples. The calibration and testing of the entire setup, including the DAS and software, was conducted by performing a trial test using a coal sample from the San Juan basin with known parameters.

### **3.4 Experimental Procedure**

For each experiment, the sample container was blow-dried before placing the sample in it. The water bath was set to the required temperature and the entire pressure vessel assembly was immersed in it. The experiment was first carried out for methane.

The CO<sub>2</sub> cycle was repeated for the same coal type. The following procedure was followed:

- a. The dead space of the sample container was calculated using Boyle's Gas Law using helium at a pressure of ~200 psi. The compressibility of helium was taken into consideration since, at high pressures, helium volume change would eventually result in incorrect calculated dead space. This step was achieved in four steps by gradually increasing the pressure, and the values of calculated dead volume was averaged.
- b. Keeping the control valve closed, the fixed volume cylinder was then subjected to a methane/CO<sub>2</sub> pressure of 100 psi and allowed to equilibrate.
- c. After achieving equilibration, the control valve was opened as quickly as possible. The sample container, initially at atmospheric pressure, quickly equilibrated with the fixed volume cylinder. Thermal equilibrium was attained in 5 to 10 seconds, after which data recording at 0.5 second interval was started, since adsorption rate is extremely fast during the initial period.
- d. Acquiring data at this pace continued until the pressure variation became insignificant, in this case, 0.1 psi per hour. After this, readings were taken at 50 second intervals and continued for approximately 22 hours, at which time, there was almost no further change in the pressure. The sample was believed to have attained complete equilibrium.
- e. At this condition, the coal sample was fully saturated with methane/CO<sub>2</sub> at the equilibrium pressure. This procedure was repeated for a step-wise pressure

- increase of ~150 psi at low pressures and ~200 psi at higher pressures. The final pressure was ~1100 psi for methane and ~900 psi for CO<sub>2</sub>.
- f. Finally, the entire procedure was followed in reverse for decreasing pressure steps of 150 psi. This was believed to be more critical for CBM applications where methane and CO<sub>2</sub> only desorbs during production.
  - g. The procedure described above was the same for all three sets of coal.

### **3.5 Sorption Isotherms**

The change in a pressure step reading of a particular gas, as described in section 3.4, was representative of the volume of gas sorbed during the step. A mass balance analysis allowed calculation of the amount of gas sorbed. The change over all the pressure steps, until the pressure reached equilibrium for the gas, is best described by the Langmuir pressure and volume constants,  $P_L$  and  $V_L$ , respectively. The constants, calculated from the experimental data for methane and CO<sub>2</sub> cycles for each coal type, describes the methane and CO<sub>2</sub> Langmuir isotherm. The isotherm estimates the volume of gas sorbed over varying pore pressures and the maximum sorption capacity of the coal type for a particular gas.

### **3.6 Estimation of Diffusion Coefficient**

Unlike the sorption experiments, where only the final equilibrium pressure is required, estimation of the diffusion coefficient requires precise and continuous change in pressure in the sample cylinder over time in order to calculate the amount of ad/de-sorbed gas as a function of time. This change in pressure over time was measured for every pressure step, that is, every time the pressure in the sample cylinder was changed due to

ad/de-sorption of gas. At the time of calculation of the diffusion coefficient, more weight was given to the initial ad/de-sorption period since the rate of sorption is the highest during this period.

A model derived from Fick's Second Law, as discussed in Chapter 2, was used to calculate the value of diffusion coefficient. In order to simplify the calculation, the value of diffusion coefficient for each pressure step was calculated using the best-fit plot method. First, a value of diffusion coefficient was chosen from the values of diffusion coefficient estimated by previous researchers (Kumar, 2007). A program was written in visual basic to execute equation (48). Using the chosen value of diffusion coefficient and estimated volume of gas ad/de-sorbed, the program was executed for twenty iterations. A plot was generated between the iterated values and time. A second plot between the pressure values and time, recorded during sorption experiment, was then superimposed on the previously generated plot. The value of the diffusion coefficient was determined by obtaining the best-match plot.

## **CHAPTER 4**

### **RESULTS AND DISCUSSION**

As discussed in Chapter 3, three sets of experiments were performed, first using virgin coal to establish the baseline, followed by coal treated for thirty days and, finally, that treated for sixty days respectively. The experiments were completed using step-wise increase/decrease in gas pressure, as typically practiced in ad/de- sorption experiments. During the initial sixty minutes of every step, the increase/decrease in pressure was monitored at a frequency of two readings/ second. This provided the data to determine the diffusion characteristics for the particular pressure step. Results of both sorption and diffusion experiments are discussed in detail in this chapter.

To ascertain proper functioning of the entire system, rigorous testing of the data acquisition system (DAS) was first carried out to ensure the accuracy of the results during the experiments. A trial experiment was then conducted using a sample from San Juan basin. The results were in agreement with past studies, thus increasing the confidence in the experimental setup and testing procedure.

#### **4.1 Production of Gases**

Before discussing the sorption-diffusion properties of the types of coal, it is essential to identify the gases that are produced due to methanogenesis. Details of the methods employed in this study can be found in published literature, and is beyond the scope of the study (Zhang et al., 2015). But once produced, the fate of the gases would be a function of the sorption-diffusion characteristics of a particular coal. Given that all gases do not get sorbed equally by coal, coal

having a higher sorption affinity for CO<sub>2</sub> than methane, identifying the amounts of gases produced is important.

The average volumes of methane and CO<sub>2</sub> produced, as detected by the gas chromatograph after thirty and sixty days of bio-degradation are presented in Table 4.1. Since the reactors were purged by nitrogen prior to initiation of methanogenesis, the undetected gas(es) can either be nitrogen, or a mixture of nitrogen with other (undetected) gases produced during methanogenesis.

**Table 4.1: Produced gases during methanogenesis**

<b>Duration</b>	<b>CH<sub>4</sub> (scft)</b>	<b>CO<sub>2</sub> (scft)</b>	<b>Undetected (scft)</b>
<b>30 Days</b>	92.7	65.4	60.9
<b>60 Day</b>	141.8	72.4	4.7

## 4.2 Sorbed Gas Calculation

The principle of volumetric measurement of gas sorption is based on the phenomenon that adsorption removes the adsorbate gas molecules from free gas phase to adsorbed phase, thus resulting in a decrease in free gas pressure within the experimental system (Krooss et al., 2002). The amount (number of moles) of adsorbed gas ( $n_{sorbed}$ ) during a particular pressure step is the difference between the total amount of gas ( $n_{total}$ ) introduced into the void volume of the sample container (SC) and the amount of free gas occupying the void volume ( $n_{free}$ ) in the sample container.

$$n_{sorbed} = n_{total} - n_{free} \quad (31)$$

The total amount of gas introduced into the SC during a particular pressure step is calculated using the following equation:

$$n_{total} = \left( \frac{V}{RT} \times \left( \frac{P_1}{Z_1} - \frac{P_2}{Z_2} \right) \right)_{FV} \quad (32)$$

where,  $P_1$  and  $P_2$  refer to the pressure in the fixed volume container (FVC) before and after the FVC-SC valve is opened during a partial pressure step,  $V$  is the volume of FVC,  $Z_1$  and  $Z_2$  are the compressibility factors of the adsorbate gas at the two pressures, and other symbols have their usual meaning. The free gas amount calculated using the above equation refers to the incremental or new free gas that appears in the SC during a particular pressure step. In the first adsorption step, all the free gas that appears in the void volume in the SC is new. However, in subsequent steps, free gas that is calculated also includes the free gas already present in the SC from previous steps. It is, therefore, important to calculate the volume of new free gas at a particular step by subtracting the free gas volume of previous adsorption step from the total free gas volume. The incremental free gas volume in the void space is calculated using the following equation:

$$n_{free} = \left( \frac{PV_V}{RTZ} \right)_{current} - \left( \frac{PV_V}{RTZ} \right)_{last} \quad (33)$$

where,  $V_V$  is the void space in the SC. It is important to note that all of the above volume calculations are extremely sensitive to the compressibility factor, and a small change in the  $Z$  value usually has a significant impact on the calculated sorbed volume. For this study, NIST 14 software, which uses the Peng-Robinson equation of state to calculate the properties of single gas, and mixtures, was used to calculate  $Z$  (Friend, 1992).

The amount of gas sorbed at different pressures, expressed in terms of volume at standard pressure (14.7 psi) and temperature (77°F) conditions (STP), was first calculated by conducting the adsorption experiment using a single gas, first methane and then CO<sub>2</sub>. The sorbed gas volume, as measured in the laboratory, is known as the Gibbs excess sorption, or Gibbs sorption. In most of the published literature, Gibbs sorption has been measured and reported. Although it is obvious that sorbed gas occupies a certain amount of space in the pore space of the adsorbent, the concept of Gibbs sorption ignores the volume. At low pressures, the volume occupied by the sorbed gas is not significant, and the actual sorbed volume is not much different from the Gibbs sorption volume calculated. However, at higher pressures, the volume occupied by the sorbed volume can be significant, and cannot be ignored since the actual sorbed gas amount can be significantly larger than the Gibbs sorption values (Mavor, 2004). To accommodate this difference, the concept of absolute sorption is used by researchers, which corrects the Gibbs adsorption by taking into account the volume occupied by the sorbed gas (Sudibandriyo et al., 2003; Arri et al., 1992).

Absolute sorption is calculated using the following equation:

$$n_{abs} = \frac{n_{Gibbs}}{\left(1 - \frac{\rho_{gas}}{\rho_{sorbed}}\right)} \quad (34)$$

where,  $n_{abs}$  and  $n_{Gibbs}$  are absolute and Gibbs sorption in moles,  $\rho_{gas}$  and  $\rho_{sorbed}$  are the densities of gas in gaseous and sorbed phases (g/ml), respectively. The value of the sorbed gas density, or molar volume, must be known to calculate the absolute sorption. Since direct measurement of the sorbed phase density/volume is difficult, empirical approaches are used to calculate the adsorbed phase molar volume/density. The values for methane and CO<sub>2</sub> are 0.421 and 0.871 g/ml respectively.



In this study, experiments were carried out to establish methane absolute ad/de-sorption isotherms for three types of coal: the baseline, and coal treated for thirty and sixty days. The isotherms are presented in figures 4.1, 4.3 and 4.5 respectively. Only absolute adsorption isotherms were established for the CO<sub>2</sub> cycle. Figures 4.2, 4.4 and 4.6 are the CO<sub>2</sub> isotherms for the baseline coal, and coal treated for thirty and sixty days respectively. The isotherms provide the values of the Langmuir constants, as listed in Table 4.2. Additional basic testing included the ultimate and proximate analysis of coal, the results are which are shown in Table 4.3.

**Table 4.2: Results obtained from Langmuir isotherms**

		Baseline Coal		Thirty-day Treated Coal		Sixty-day Treated Coal	
		Adsorption	Desorption	Adsorption	Desorption	Adsorption	Desorption
CH <sub>4</sub>	P <sub>L</sub> (psi)	551	559	1729	219	3715	436
	V <sub>L</sub> (scft)	428	412	683	253	1907	232
CO <sub>2</sub>	P <sub>L</sub> (psi)	247	-	391	-	749	-
	V <sub>L</sub> (scft)	823	-	1164	-	1821	-

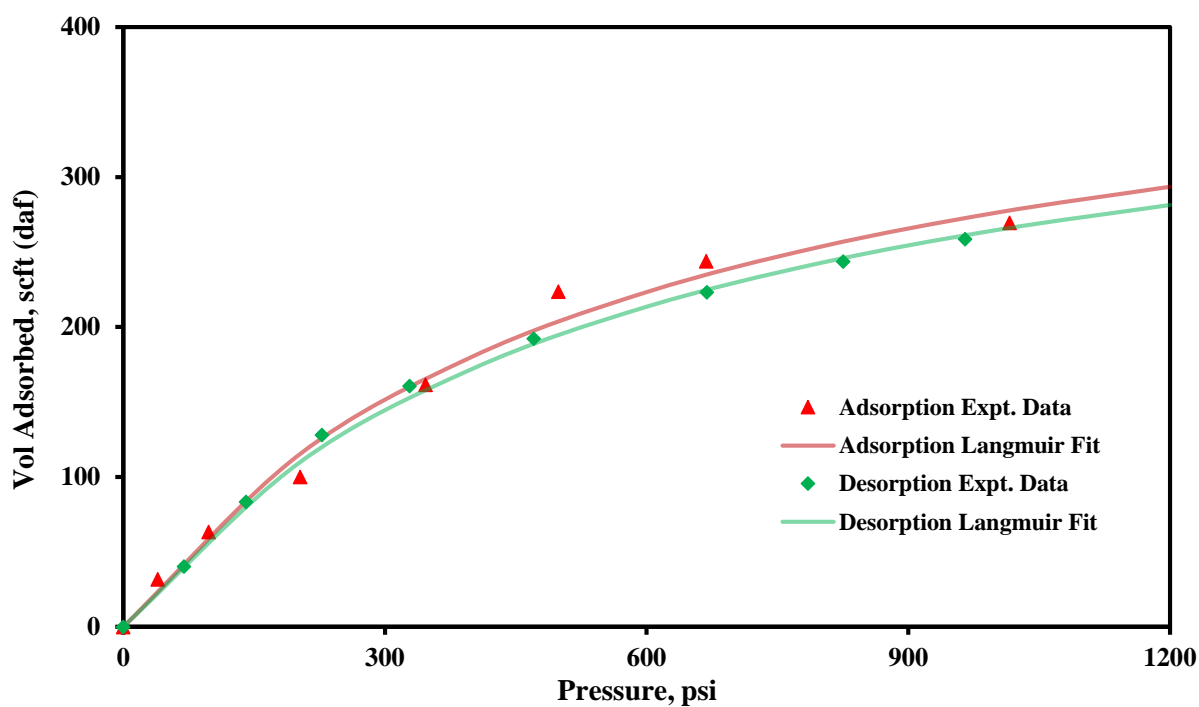


Figure 4.1: Ad/de- sorption isotherms of methane – baseline coal.

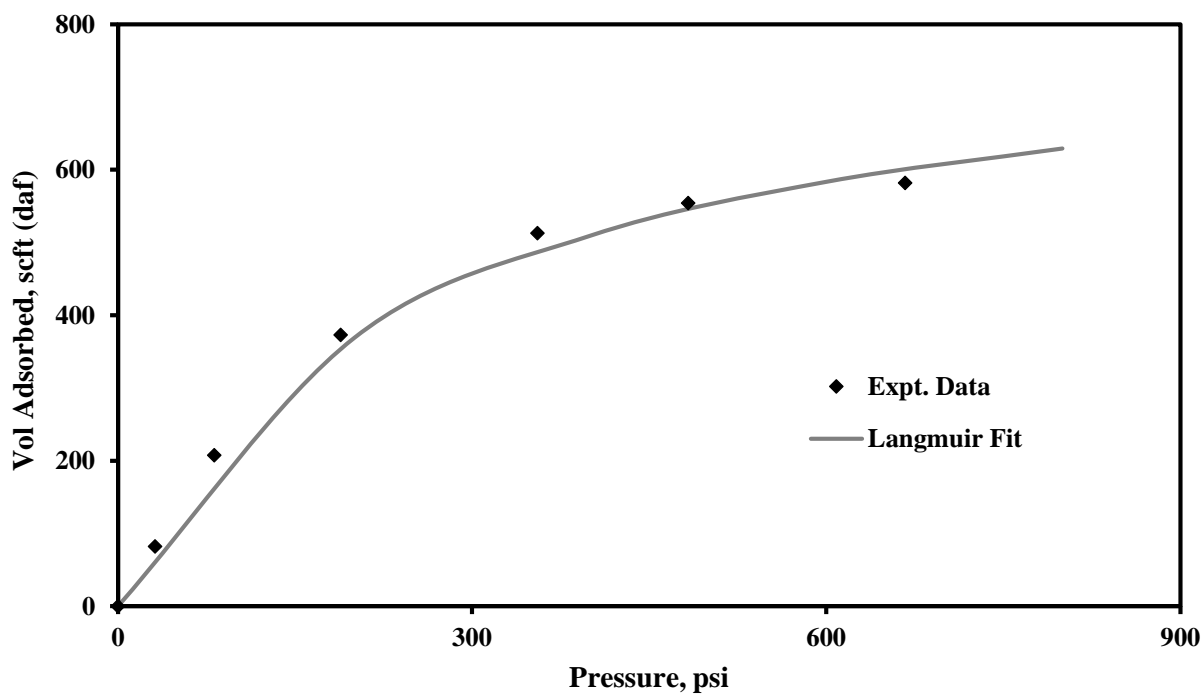


Figure 4.2: CO<sub>2</sub> adsorption isotherm – baseline coal.

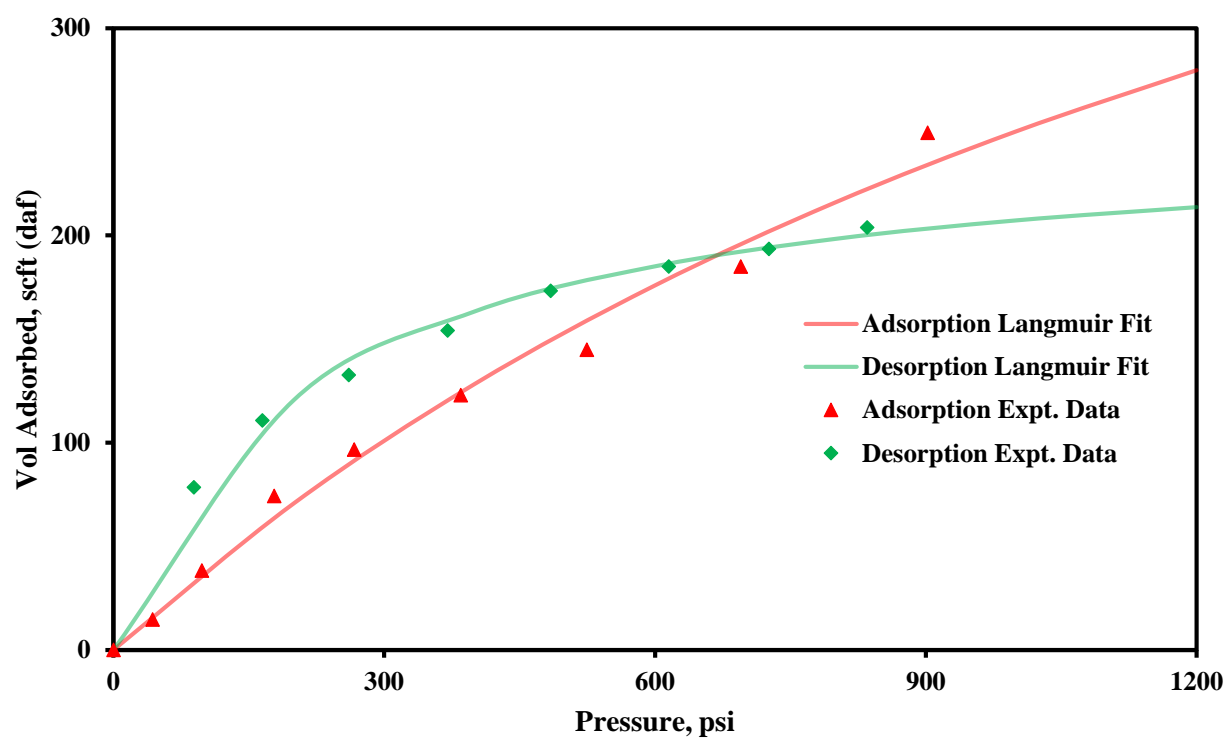


Figure 4.3: Ad/de- sorption isotherms of methane – thirty-day treated coal.

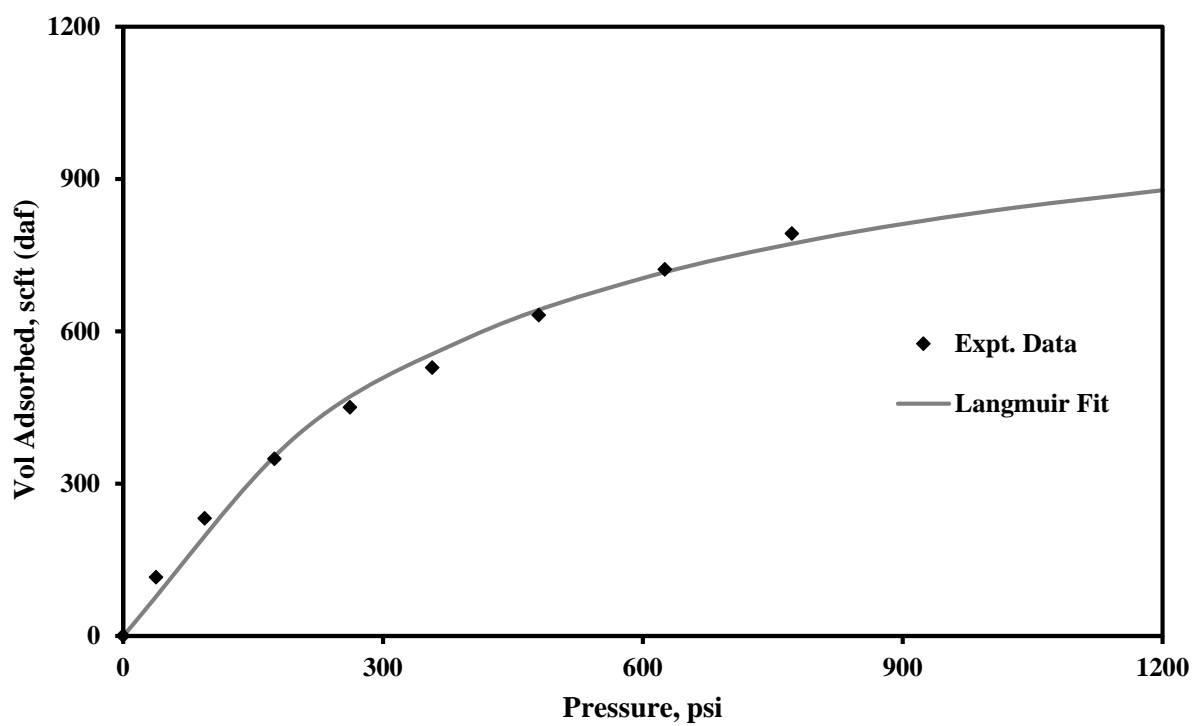


Figure 4.4: CO<sub>2</sub> adsorption isotherm for coal – thirty-day treated coal.

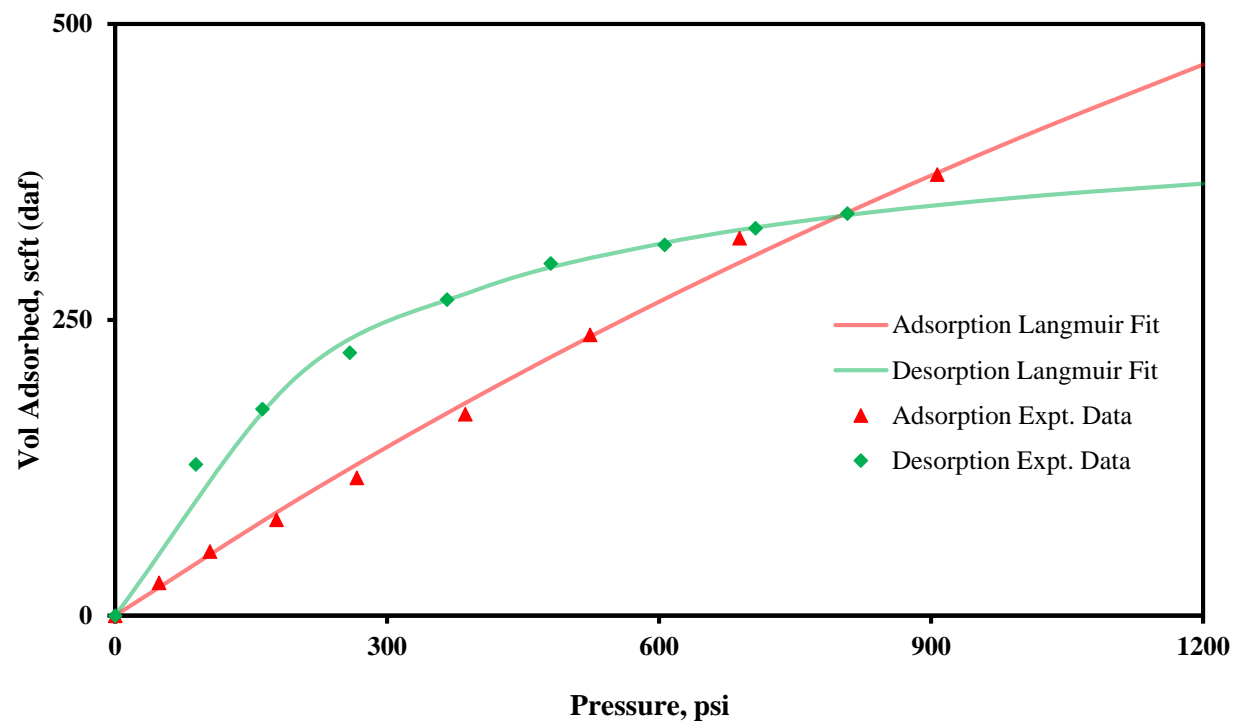


Figure 4.5: Ad/de- sorption isotherms of methane – sixty-day treated coal.

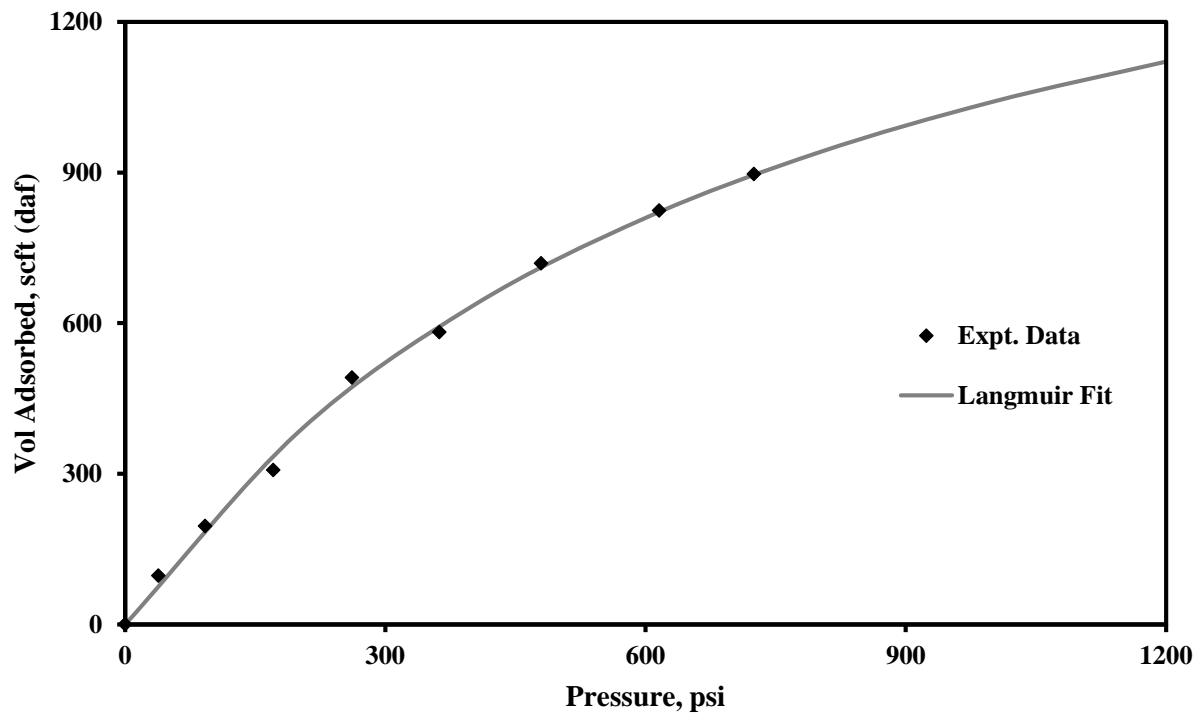


Figure 4.6: CO<sub>2</sub> adsorption isotherm for coal – sixty-day treated coal.

**Table 4.3: Results of the basic coal characteristics**

<b>Sample</b>	<b>Carbon (%)</b>	<b>Nitrogen (%)</b>	<b>Hydrogen (%)</b>	<b>Oxygen (%)</b>	<b>Sulfur (%)</b>	<b>Ash (%)</b>	<b>Moisture (%)</b>
<b>Baseline</b>	70.1	1.4	5.2	15.4	0.6	6.1	11.5
<b>Day 30</b>	59.5	1.2	4.3	16.8	0.7	8.1	17.4
<b>Day 60</b>	57.3	1.2	4.2	16.6	0.7	7.6	16

### 4.3 Estimation of Diffusion Coefficient

The various methods to estimate the diffusion coefficient were discussed in Sections 2.10 and 3.6. As illustrated in figure 14, estimation of diffusion coefficient requires the calculation of slope for the initial period. The exact point where the slope is calculated is subjective. The value of the slope,  $b$ , determines the value of the diffusion coefficient,  $D$  as indicated by equation 30. Hence the coefficient of diffusion presents values within a given range with a standard deviation. Kumar (2007) conducted a sensitivity analysis of the values obtained for  $D$  using the same methods. He reported that, for sorption of methane on Illinois coals, the errors in calculation ranged from -7.9 to 6.7% of the calculated values. The error calculations in this study were

completed for the values of the coefficient of diffusion at every pressure step. The graphs presented are within one standard deviation of the expected results.

### 4.3.1 Diffusion Results

Using equation 30, the value of  $D$  for each pressure step for methane and  $\text{CO}_2$  cycles was calculated. The variation, calculated as a function of pressure, for the three coals tested is shown in figures 4.7, 4.8 and 4.9 respectively. The methane and  $\text{CO}_2$  cycles are represented as plots (a) and (b) respectively. It is apparent from the results that there is a negative correlation between  $D$  and pressure, both for adsorption and desorption steps, and for methane and  $\text{CO}_2$  cycles.

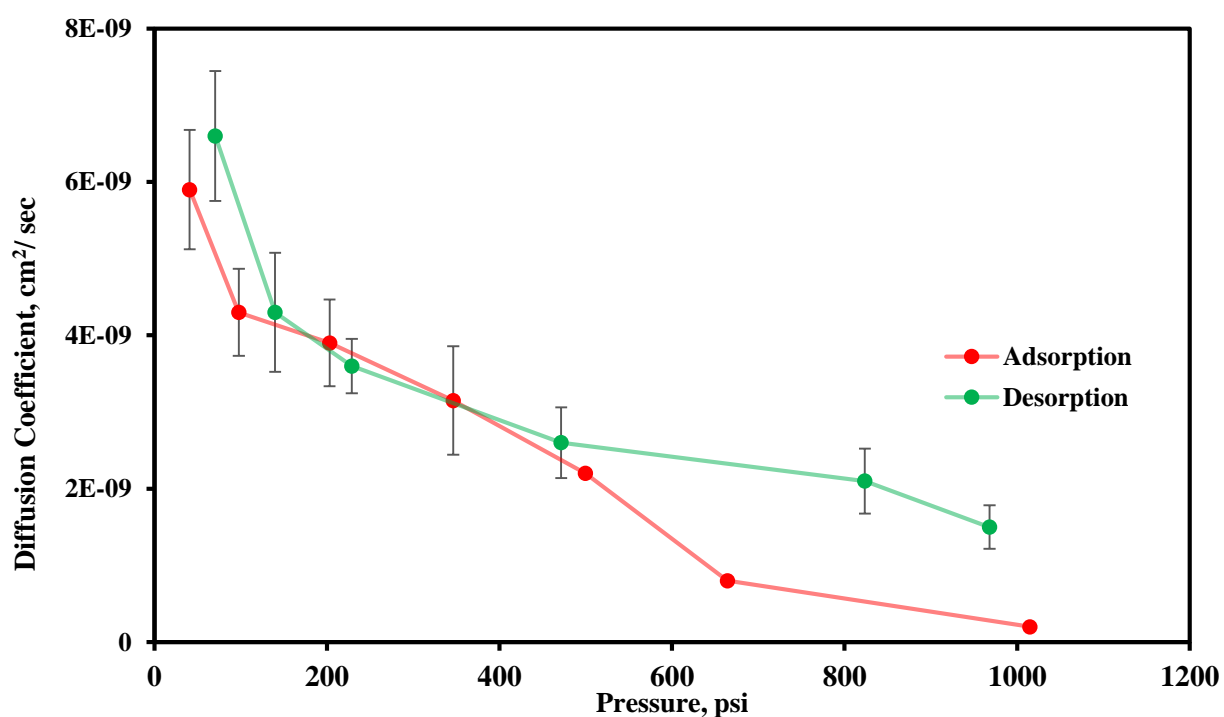


Figure 4.7(a): Variation in the value of  $D$  with changes in methane pressure – baseline coal.

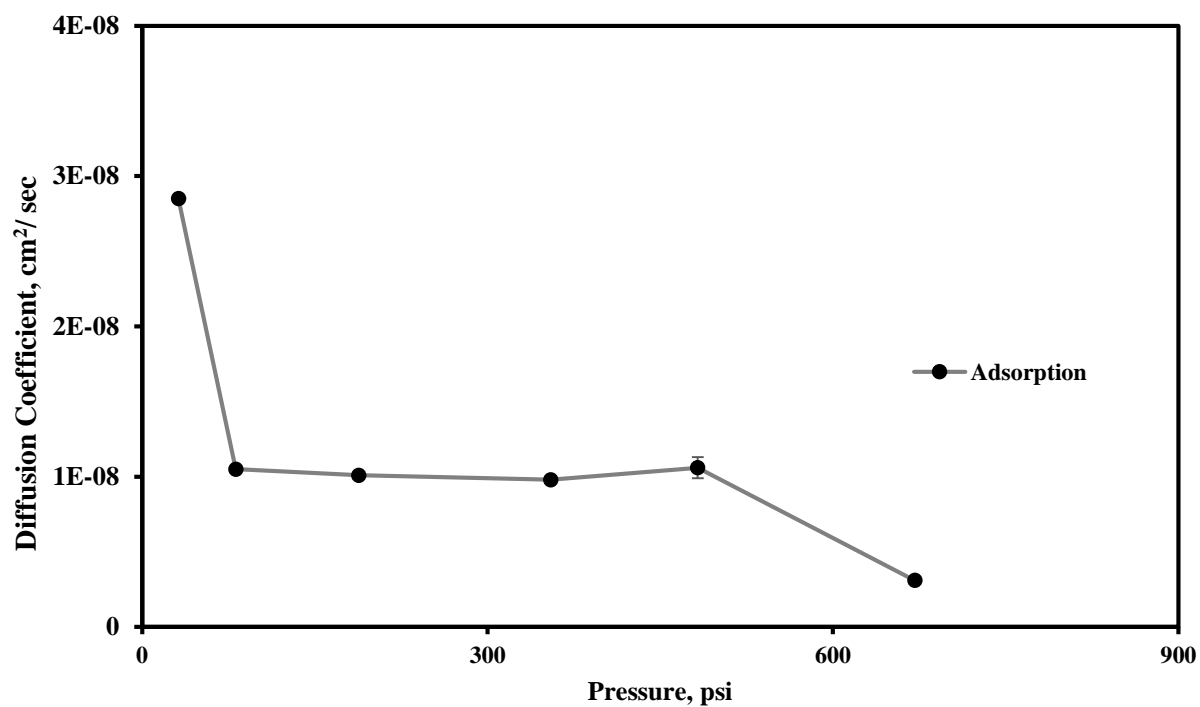


Figure 4.7(b): Variation in the value of  $D$  with increasing  $\text{CO}_2$  pressure – baseline coal.

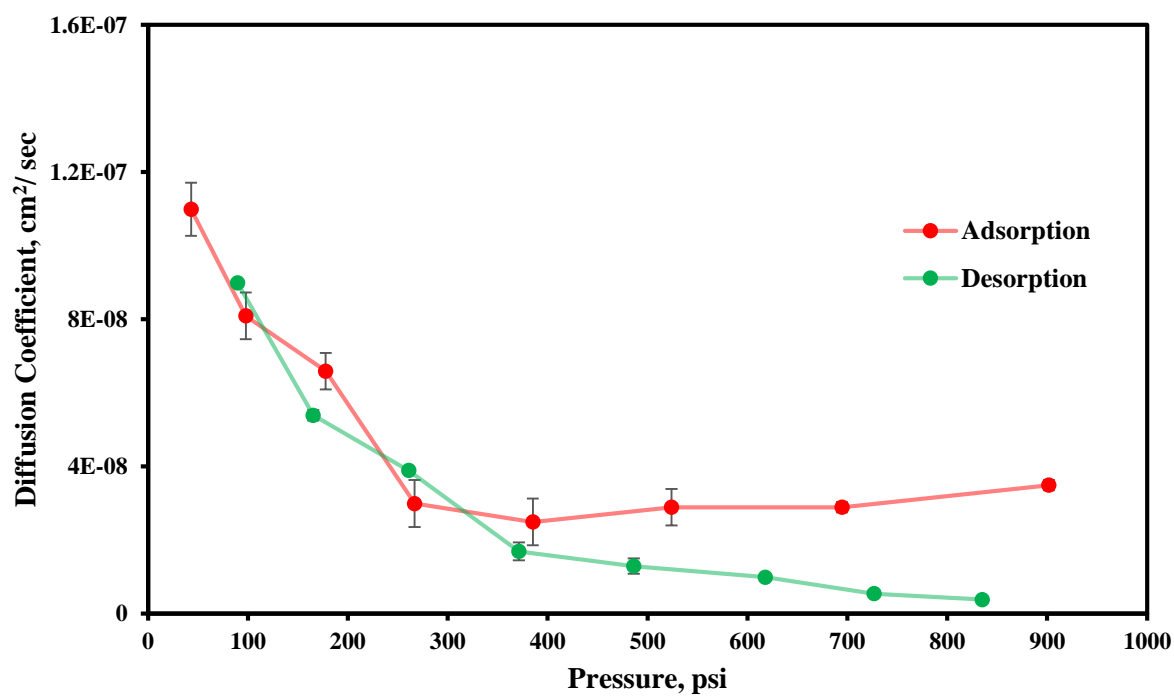


Figure 4.8(a): Variation in the value of  $D$  with changes in methane pressure – thirty-day treated coal.

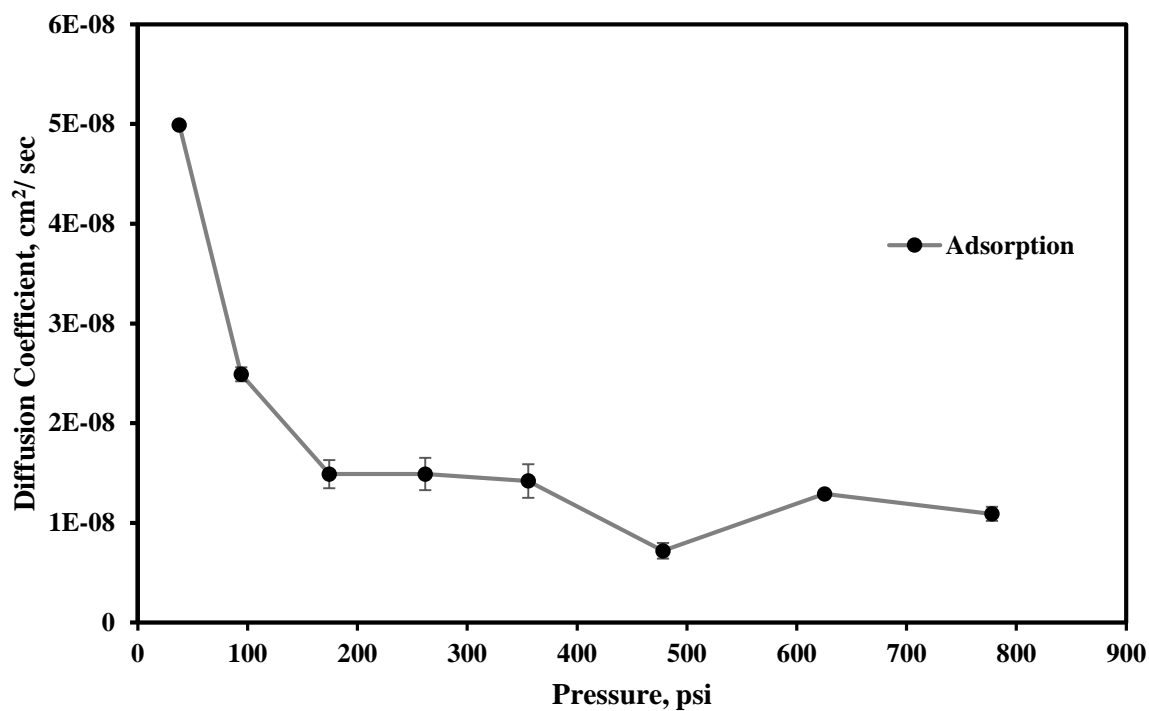


Figure 4.8(b): Variation in the value of  $D$  with increasing  $\text{CO}_2$  pressure – thirty-day treated coal.

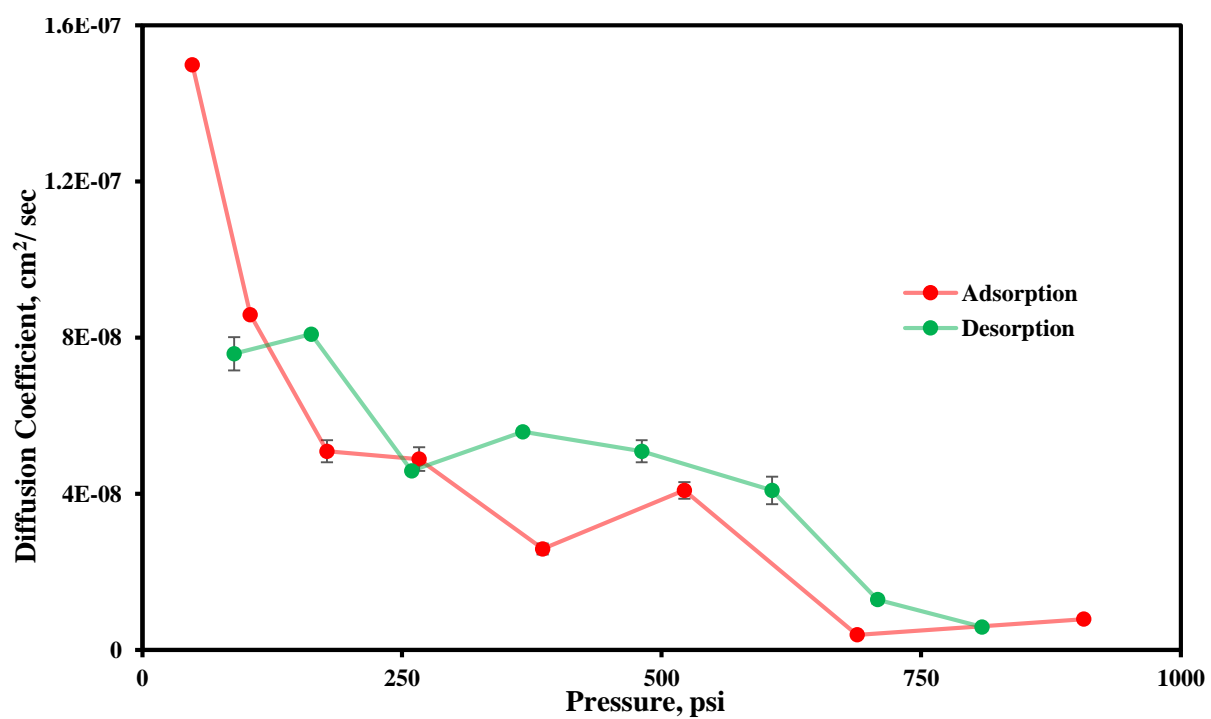


Figure 4.9(a): Variation in the value of  $D$  with changes in methane pressure – sixty-day treated coal.



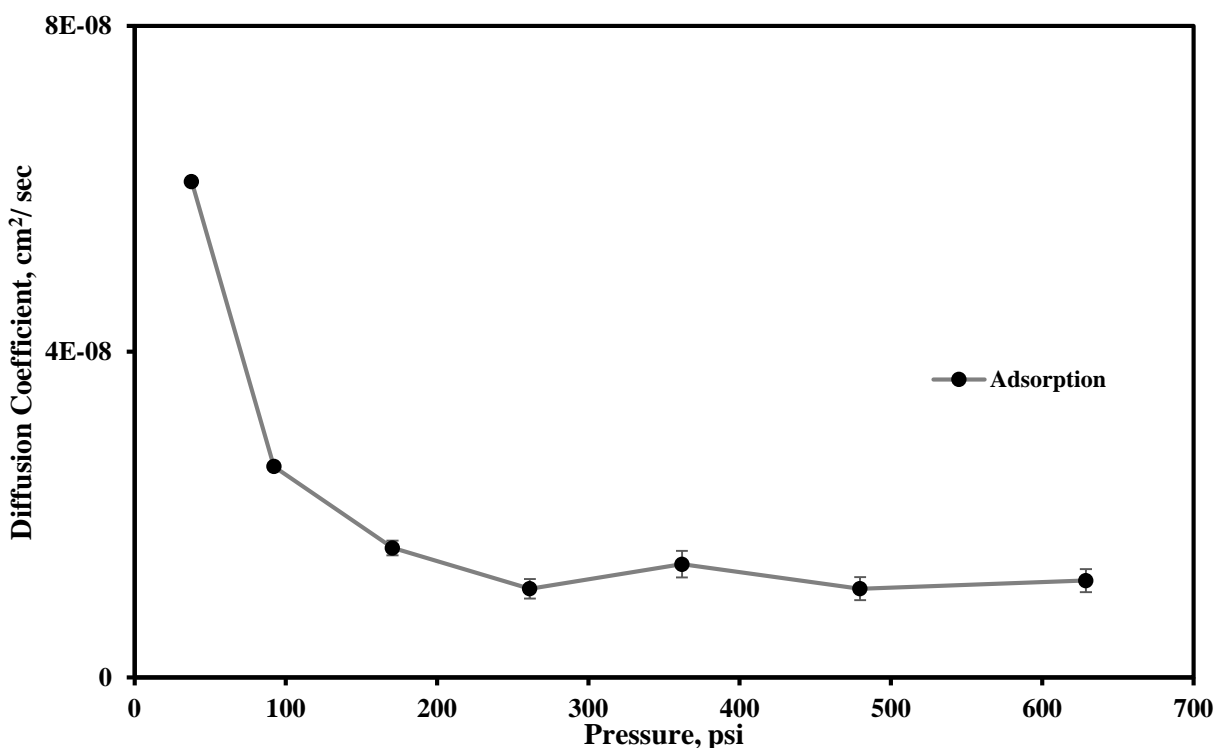


Figure 4.9(b): Variation in the value of  $D$  with increasing  $\text{CO}_2$  pressure – sixty-day treated coal.

## 4.4 Discussion

### 4.4.1 Sorption

The results of ad/de-sorption of methane and adsorption of  $\text{CO}_2$  on untreated (baseline) coal are similar to past studies. The experimental data obtained fits Type 1 Langmuir isotherm, that is, the sorbed volume increases initially with pressure linearly but, at higher pressures, the rate of increase slows down, reaching a stable value. The Langmuir pressure and volume constants for adsorption of methane for untreated coal were estimated to be 551 psi and 428 scft respectively. The values for desorption were 551 psi and 412 scft respectively. For adsorption of  $\text{CO}_2$ , the Langmuir parameters were estimated to be 247 psi and 823 scft. The difference in the experimental values, and that estimated by the Langmuir parameters is 0.05% and ~0.00002% for methane adsorption and desorption cycles respectively. The difference observed for

adsorption of CO<sub>2</sub> was slightly higher, at 0.68%. Such ranges of deviations are within acceptable ranges as per published literature (Dutta et al., 2013).

Langmuir constants for adsorption of methane on coal treated for 30 days were determined to be 1729 psi and 683 scft; whereas, the constants for desorption of methane were 219 psi and 253 scft. For sorption of CO<sub>2</sub> on coal treated for thirty days, the Langmuir constants were estimated to be 391 psi and 1164 scft. The difference in the predicted values by the Langmuir isotherm were 0.01%, 0.31% and 0.35% for methane ad/de-sorption and CO<sub>2</sub> sorption respectively. The Langmuir constants for the adsorption of methane on coal treated for sixty days were determined to be 3715 psi and 1907 scft, and that for desorption of methane 436 psi and 232 scft. The constants for CO<sub>2</sub> were 749 psi and 1821 scft. The difference in the modeled Langmuir sorption values and the ones estimated experimentally was 0.01%, 0.11% and 0.04% for methane ad/de-sorption and CO<sub>2</sub> adsorption respectively.

Given that the Langmuir isotherm assumes a monolayer surface coverage, adsorption of methane and CO<sub>2</sub> on treated coal, compared to that on untreated coal, reveal high values of Langmuir constants.  $V_L$ , which signifies the maximum sorption capacity for coal, for coals treated for thirty and sixty days was ~1.6 and ~4.5 times that of the values for untreated coal.  $P_L$ , which defines the shape of the Langmuir isotherm, presented values ~3.1 and ~6.7 times higher than for untreated coal. This implies that the decrease in the rate of sorption observed beyond ~500 psi for untreated coal, occurred beyond ~1500 psi and 3000 psi for coals treated for thirty and sixty days respectively. Plotting the Langmuir isotherms beyond 1200 psi, as shown in Figure 4.10, although not of any practical value, illustrates the predicted change in the sorption characteristics as a result of bio-conversion.

Adsorption of  $\text{CO}_2$  on the three coals tested presents a more of a uniform trend compared to adsorption of methane. Since  $\text{CO}_2$  is adsorbed strongly by coal, there was no noticeable change in the sorption capacity at low pressures. However, beyond  $\sim 250$  psi, Figure 4.10 suggests that, unlike untreated coal, additional amount of  $\text{CO}_2$  was being adsorbed. The increase of sorption capacity was more noticeable for coal treated for a longer period of time. The trend is well reflected in the values of the Langmuir constants, where the pressure constants for coal treated for thirty and sixty days was  $\sim 1.6$  and  $\sim 3$  times higher than the values for untreated coal, and volume constants were  $\sim 1.1$  and  $2.1$  times higher.

Ideally, isotherms describing desorption of methane and/or  $\text{CO}_2$  on coals should not

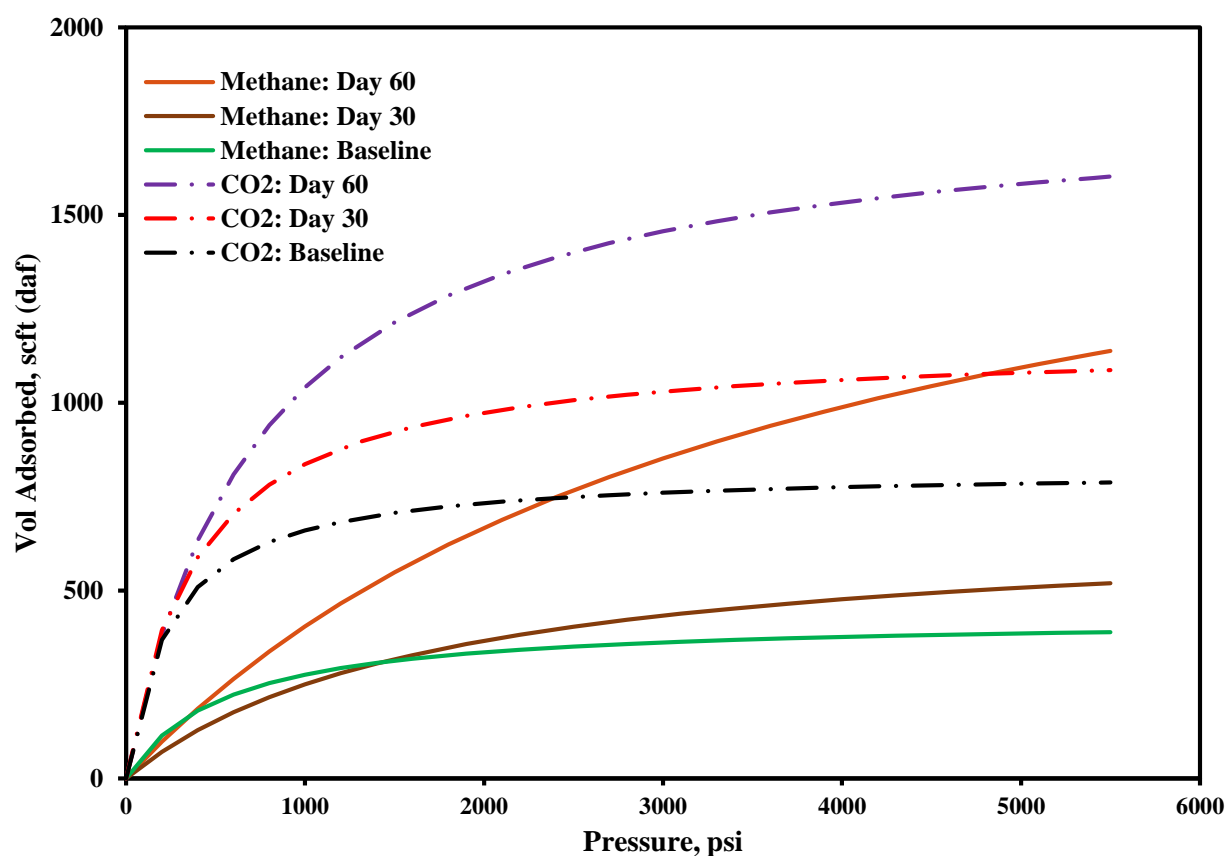


Figure 4.10: Langmuir isotherms for adsorption of methane and  $\text{CO}_2$  on different coals.

deviate from the adsorption isotherms. Ad/de-sorption isotherms for methane on untreated coal, as shown in Figure 4.1, although similar, do exhibit some hysteresis effects. This is not a new finding, and has been reported by several researchers in the past (Greaves et al., 1993; Busch et al., 2003; Ozdemir et al., 2003; Harpalani et al., 2006). Desorption hysteresis on coals may occur due to two reasons: changes in the adsorbent properties/structures, or capillary condensation in the adsorbent micropores (Gregg and King, 1982). Busch et al. (2003) attributed hysteresis to a metastable sorbent-sorbate system that prevents release of gas, to the extent corresponding to the thermodynamically equilibrium value, with decreasing pressure during desorption. Moisture content is also attributed to hysteresis because, as moisture content in the sample decreases, the capacity of the coal to adsorb gas increases (Harpalani et al., 2006).

Compared to desorption hysteresis observed for untreated coal, that for coal treated for thirty and sixty days is staggering, with such trends being un-reported anywhere in the existing literature. The Langmuir pressure and volume constants for adsorption of methane on coal treated for 30 days were  $\sim 7.8$  and  $\sim 2.7$  times the corresponding desorption values respectively. Coal treated for sixty days presented the pressure and volume constants for adsorption to be  $\sim 8.5$  and  $8.2$  times the desorption values respectively. In comparison, the adsorption values for untreated coal were  $\sim 0.98$  and  $1.03$  times the desorption constants. Possible reasons for such desorption behavior is discussed in section 4.4.1.

#### **4.4.2 Surface Area**

As discussed in section 2.9.4, equation 24 can be used to determine the specific surface area available for sorption, which provides an estimate of the pore surface area available. The equation is used to calculate the ratio of the surface areas available for sorption before and after methanogenesis. The ratio for the sorption of the same gas on different coal types requires the

calculation of  $q_m$  for each case. Establishing the Langmuir type isotherms show that the ratio of different  $q_m$ s can be indicated by the ratio of the Langmuir volumes. Table 4.4 illustrates the results of the estimated changes in specific surface area.

**Table 4.4: Estimated changes in surface areas**

<b>Treatment Period (days)</b>	<b>Change in Specific Surface Area (<math>\times</math> Baseline Area, <math>10^{-3} \text{ km}^2\text{kg}^{-1}</math>)</b>	
	<b>CH<sub>4</sub></b>	<b>CO<sub>2</sub></b>
30	1.6	1.4
60	4.5	2.2

The estimation of the surface areas, as shown in Table 4.4, takes in to account the adsorption characteristics of methane and CO<sub>2</sub>. Langmuir parameters obtained from the desorption characteristics provide misleading interpretation of the surface areas available for sorption. This is because, as indicated by the adsorption isotherms, for pressure ranges used in the experimental work, sorption sites for treated coal were continuing to fill, without progressing towards an asymptotic value. Since adsorption of gases was discontinued during the experiment and the process of desorption started, the coal exhibited desorption characteristics similar to the condition where Langmuir parameters indicated lower values of the volume constants. At higher pressures, the isotherm presents itself to be asymptotic, gradually increasing the rate of desorption at lower pressures, typically less than 300 psi. Possible reasons for such behavior are discussed in section 4.4.1.

Given that, for isothermal conditions, the sorption of coal is a function of number of sorption sites available, increase in specific surface area suggests an increase in the number of sites available for sorption. The microbial action is believed to create new pore spaces, or enlarge existing pore space available. Since the microbes need carbon in coal to produce methane, ultimate analysis of the baseline and treated coals were performed. The data illustrated in Table 4.3 suggests that there has been a steady decrease in the carbon content of treated coal. The untreated coal presented itself with ~70% carbon content and, with gradual methanogenesis, the carbon content in coal treated for thirty and sixty days reduced by ~15% and 17% respectively. Such a change is indicative of the increase in pore space of coal due to methanogenesis as represented by the increased surface areas.

#### **4.4.3 Extended Langmuir Isotherm**

The isotherm, as explained by equation 14, and pertinence to this study, has two components: methane and CO<sub>2</sub>. The Extended Langmuir (EL) equation is generally viewed as a correlation, rather than an accurate physical model with theoretical basis. The results of gas production for coal treated for thirty days had ~ 27% undetected gases, in addition to methane and CO<sub>2</sub>. Normalizing such a high fraction of undetected gases into methane and CO<sub>2</sub> fractions would be erroneous. However, data from coal treated for sixty days had ~2% of undetected gases, making it possible to achieve acceptable results for multi-component sorption using methane and CO<sub>2</sub>. The fractions of methane and CO<sub>2</sub> were then normalized to a cumulative value of 100% and the Extended Langmuir isotherm model was used for the coal sample treated for sixty days.

Figure 4.11 above provides the extended Langmuir isotherm, where the normalized free gas composition is 66.2% methane and 33.8% CO<sub>2</sub>, which is representative of the gas produced

after methanogenesis. For CBM production, it is seen that, if  $\text{CO}_2$  is detected during initial production, its percentage increases over the course of production. The problem with  $\text{CO}_2$  is that it reduces the calorific value of the produced gas. Hence, when dealing with high percentages of  $\text{CO}_2$ , it is necessary to apply separation techniques before the produced gas can be brought to pipeline quality. The EL isotherm model, which is capable of providing compositional information over the production period can, therefore, be used to set up the required separation techniques.

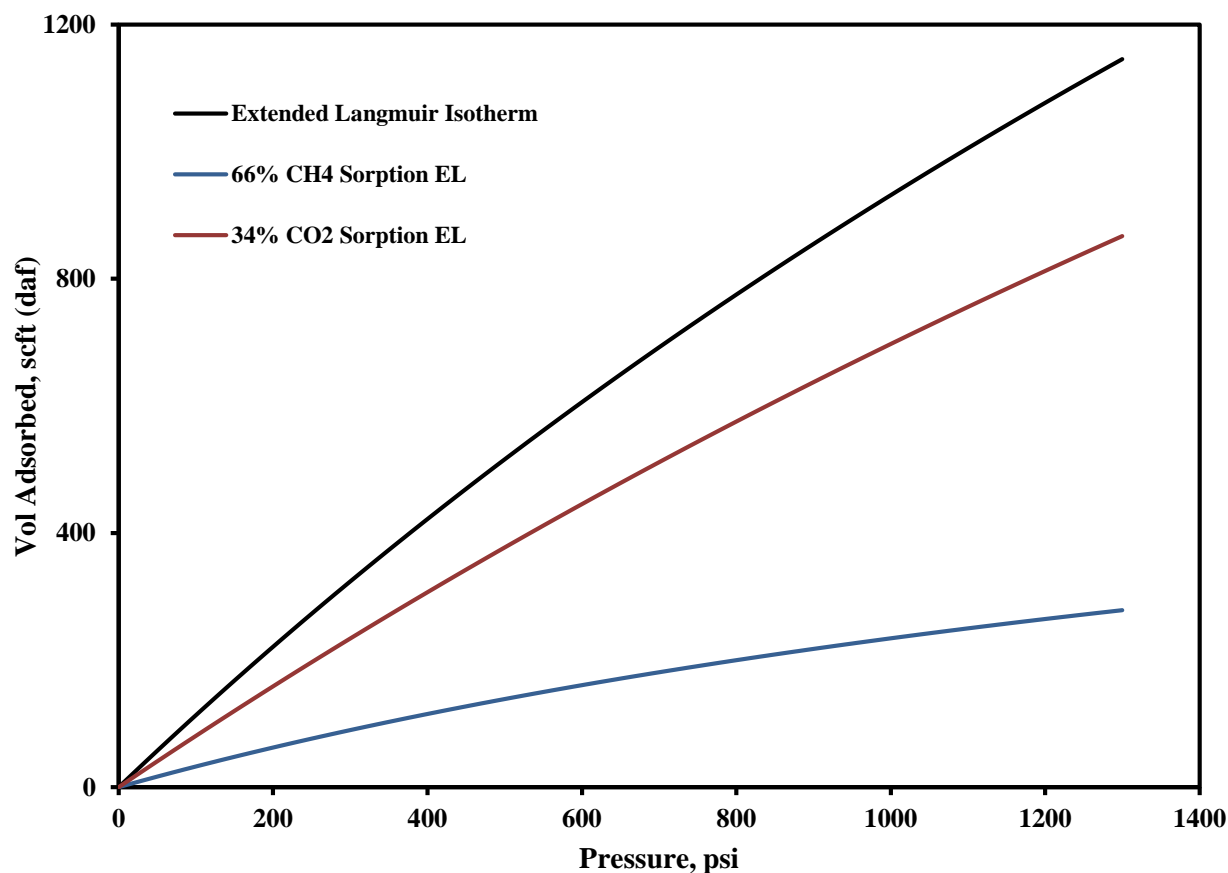


*Figure 4.11: Extended Langmuir isotherm for coal treated for sixty days.*

#### 4.5 Diffusion

As discussed in section 4.3.1, the results indicate a negative correlation between pressure and coefficient of diffusion for both methane and CO<sub>2</sub> for all three coals tested. Such trends are in agreement with the studies by past researchers. Kumar (2007) successfully linked such trends to the Klinkenberg effect and matrix shrinkage phenomenon. In his correlation to the Klinkenberg permeability, where at high pressures, there is crowding of gas molecules in rock fractures making the gas molecules along the fracture surface are practically immobile, the permeability approaches that of liquids. At low pressures, the gas molecules slip along the surface of the fractures, the slippage adding to the permeability of the medium. Hence, with decrease in pressure, there is an apparent increase in permeability. Kumar postulated a similar relationship for diffusion of methane in coal with one difference, where the value of  $D$  flattens out in the high pressure regime. When the gas pressure is high, there is a large number of gas molecules trying to diffuse out of the matrix, resulting in increased inter-molecular resistance and low diffusivity. As the gas continues to desorb from the matrix, there is a reduction in pressure and the number of molecules diffusing out, resulting in lower resistance to its movement and, hence, increased diffusivity.

The variation in the value of  $D$  can, therefore, be assumed to be dual in nature, where its value remains constant at high pressures, retaining a positive value, which may be extremely low. However, once the gas pressure is reduced, the value of  $D$  starts to increase with continued desorption of gas. This was explained mathematically as:

$$D = D_D \quad \text{for } P < P_D \quad (35)$$

where, the gas pressure ( $P$ ) is above the pressure when gas desorption is significant ( $P_D$ ), and

$$D = D_D + b/P_m \quad \text{for } P < P_D \quad (36)$$



when gas desorption becomes significant. The value of “ $b$ ” is expected to be constant for a particular coal type and gas.

The measured values of  $D$  in this study were plotted as a reciprocal of gas pressure, as shown in Figures 4.12 and 4.13 for methane and  $\text{CO}_2$  cycles respectively. One apparent difference between the Klinkenberg permeability plot and the Klinkenberg diffusion plot is that the value of  $D$  approaches a negative value at high/infinite pressure when the measured results are extrapolated, a physical impossibility. For practical and applicability reasons, the experiments in this study were performed only up to 1000 psi, and it was found that, at high pressure, the value of  $D$  flattened out, confirming the dual behavior of the diffusion coefficient.

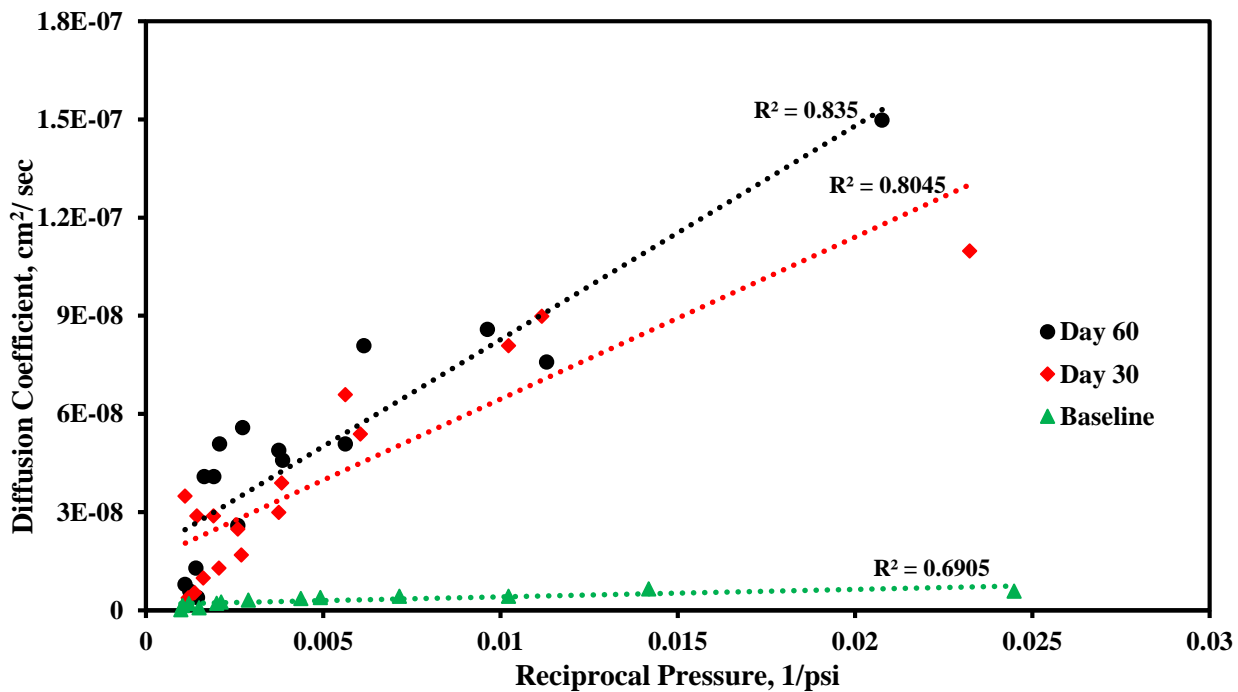


Figure 4.12: Klinkenberg plot showing  $D$  as a function of methane pressure for the three coals tested.

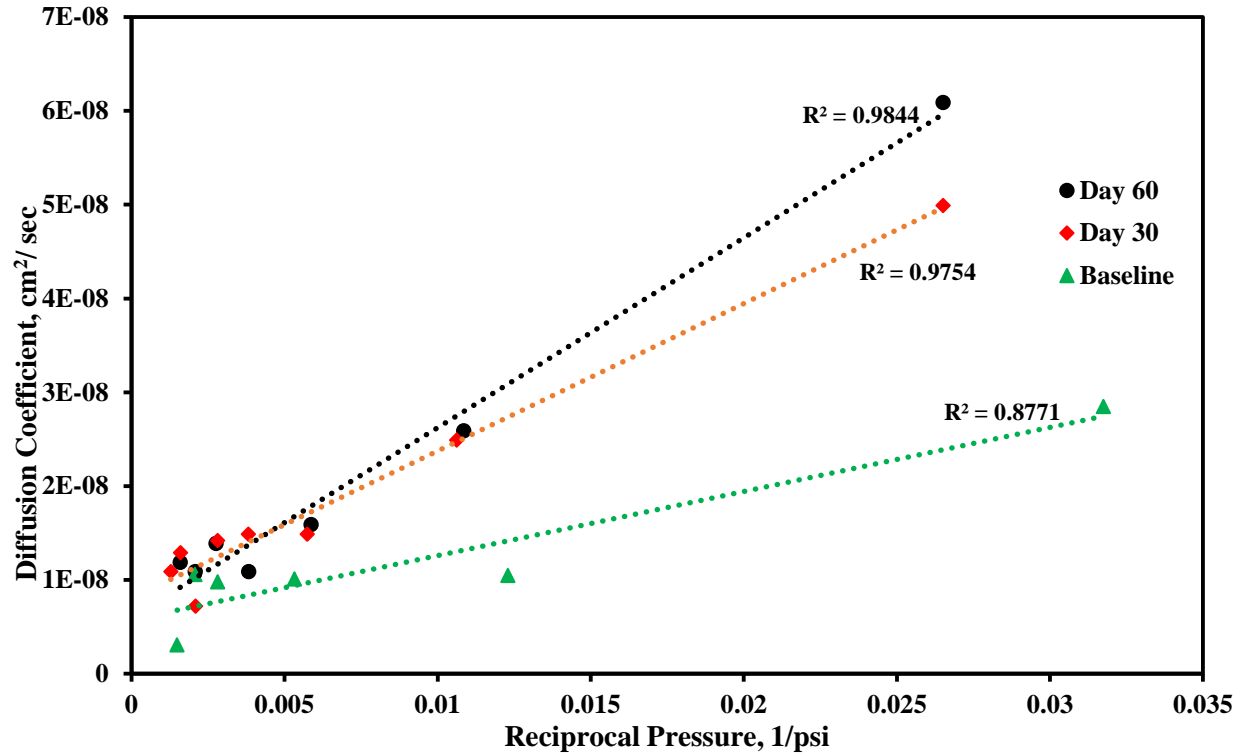


Figure 4.13: Klinkenberg plot showing  $D$  as a function of  $\text{CO}_2$  pressure for three coals tested.

The diffusion coefficients for  $\text{CO}_2$  were found to agree well with the Klinkenberg diffusion hypothesis. Methane diffusion rates, on the other hand, although related positively with the reciprocal pressure, the  $R^2$  value of the regression fit was  $< 0.9$  in all cases. The best fit for both methane and  $\text{CO}_2$  cycles were observed for coal treated for sixty days and the fit got progressively poorer for coal treated for thirty days and untreated coal respectively.

Another explanation, as pointed out by Kumar, for the negative correlation between the diffusion coefficient and pressure, was based on drawing an analogy with the permeability-pressure variation. Typically, there is shrinkage of coal matrix with continued desorption, which has been found to be universally true for all coal types (Harpalani and Chen, 1995). Illinois basin coals have also been shown to exhibit increase in permeability with matrix shrinkage (Zutshi, 2004). For diffusion at the micropore level, as gas pressure decreases, shrinkage of coal matrix

results in decreased space in the micropores, that is, an increase in pore size. As this occurs, movement of methane in the matrix is eased, resulting in an increase in diffusivity. The relationship between pore size distribution and diffusion, reported by researchers in the past (Radovic, 1991) supports this argument since an increase in pore size results in an increase in the value of  $D$ .

The trend in the variation of the value of  $D$  for untreated coal was in agreement with the studies reported by past researchers, where  $\text{CO}_2$  exhibited higher values than methane. The highest diffusion rate for  $\text{CO}_2$  was almost five times higher than that for methane. With continued bio-conversion, there was an increase in the values of  $D$ . For methane at low pressures, the value of  $D$  was almost 18 times higher than for coal treated for thirty days and 25 times higher for coal treated for sixty days at ~50 psi. For pressures below 400 psi, the diffusion coefficient for both treated coals was ~15 to 20 times higher than for untreated coal. The estimated value of  $D$  for  $\text{CO}_2$  was also higher for treated coals than for untreated coal. The change in values of  $D$  was twice that for coal treated for 30 days as well as 60 days, compared to that for untreated coal. Basically, the difference between the two treated coals was very small. The comparison between the values of diffusion coefficient between methane and  $\text{CO}_2$  for treated coal was an aberration from the studies reported in the past. Figures 4.14 (a) and (b), illustrating the values of diffusion coefficient for methane and  $\text{CO}_2$  sorption for untreated coal and coal treated for 60 days respectively, provides a good understanding of the trend in the results.

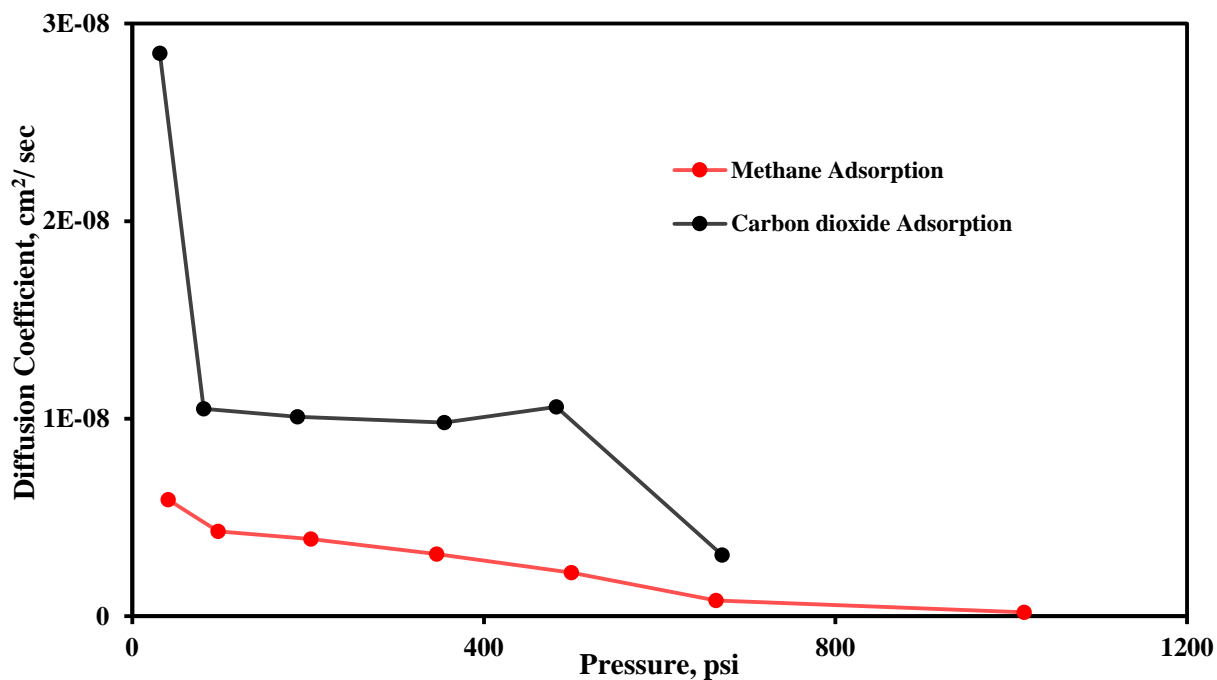


Figure 4.14 (a): Comparison of diffusion coefficient for methane and CO<sub>2</sub> for untreated coal.

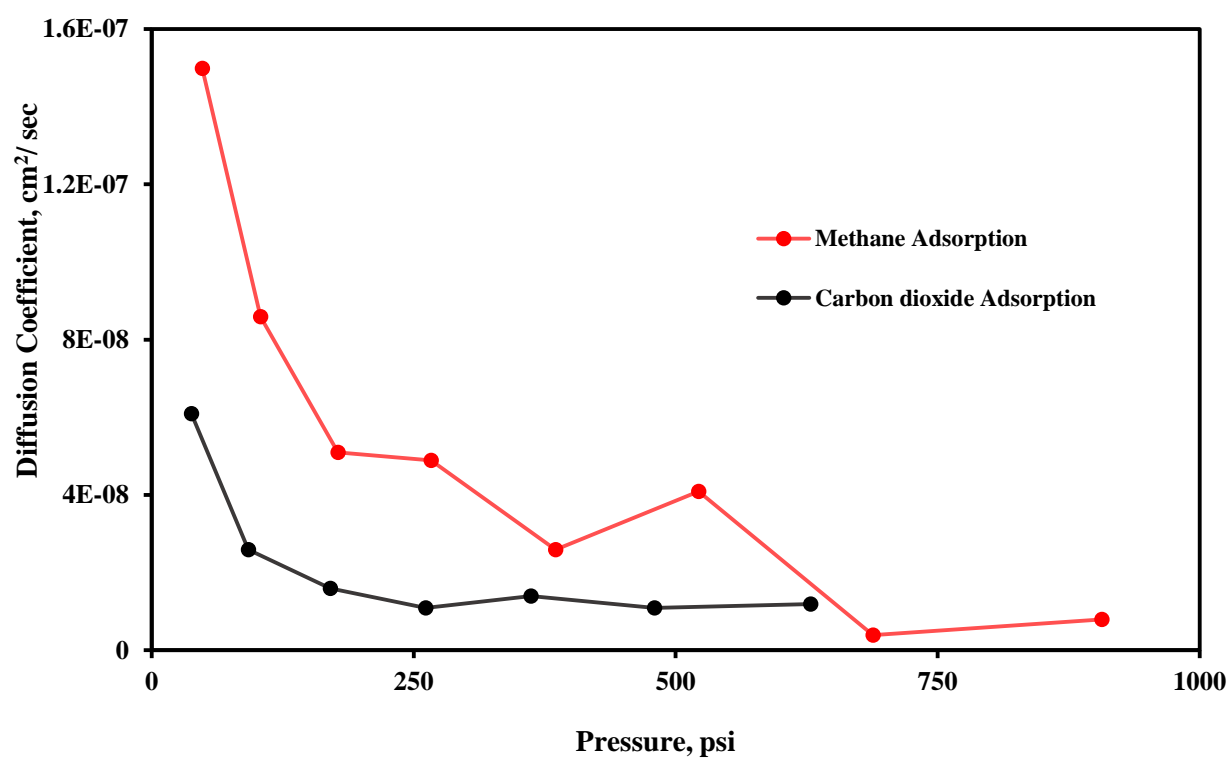


Figure 4.14 (b): Comparison of diffusion coefficient for methane and CO<sub>2</sub> for coal treated for sixty days.

#### 4.5.1 Possible Explanation Using Non-monotonic Size Dependence of Effective Diffusion

##### Constant

##### a. Diffusion

As illustrated in Figure 4-15, for a molecule of assumed spherical radius  $r$ , the Einstein-Stokes equation relating the effective diffusion coefficient is as follows:

$$D_e = \frac{kT}{6\pi\eta r} \quad (37)$$

where,  $D_e$  is the effective diffusivity,  $k$  is the Boltzmann constant,  $T$  is the temperature, and  $\eta$  is the viscosity of the fluid. At constant temperature, the term  $\frac{kT}{6\pi\eta}$  is a constant. The

Einstein-Stokes equation thus becomes:

$$D_e \propto \frac{1}{r} \quad (38)$$



*Figure 4.15: A tube with identical periodic dead ends with entry radius of 'a' and a diffusing particle of radius 'r'. (adapted from Dagdug et al. (2008))*

The above relation suggests that the diffusing particle with a larger diameter will have a slower rate of diffusion. In a coal environment, the molecular diameters of CO<sub>2</sub> and methane are represented by different models. The Lennard-Jones theory estimates methane to have a diameter of 3.751 Å, and CO<sub>2</sub> to have a diameter of 3.615 Å (Kurniawan et al., 2006). The kinetic diameter, which is the geometry optimized diameter of a continually moving set of gas molecules, trackable using computational geometry models of kinetic structure of gases, and is a reflection of the smallest effective dimension of a given molecule, of methane is 3.8 Å and, for CO<sub>2</sub>, it is 3.3 Å (Cui et al, 2004). Given that the methane molecule is larger than CO<sub>2</sub> in, the diffusion characteristics of baseline coal, which is in agreement with the trends of the past studies, is found to comply with the Einstein-Stokes equation.

Dagdug et al. (2008) conducted experiments to determine the diffusion characteristics of spherical particles in a tube with periodic dead ends. The microporous structure of coal can be considered as a tube, from which constricted periodic tubes branch out and terminates as the pore itself. Figure 4-15 depicts such a model representing the pore structure in coals. In the series of experiments performed, it was concluded that the effective diffusion coefficient was inversely related to the size of the diffusing particles, as indicated by the Einstein-Stokes equation. This was found to be true for cases when the radius (size) of the constricted entries/tubes, ‘*a*’, was either much larger or smaller than the radius (size) of the diffusing particles. In essence,

$$D_e \propto \frac{1}{r} \quad \text{for } r \ll a \text{ and } r > a$$

For tube and pore entry diameters of size comparable to the size of the diffusing particles, it was found that values of  $D_e$  noticeably deviate from the Einstein-Stokes relation. The deviation is a non-monotonic function of  $r$ , where particles of larger radii were found to have a higher value of diffusion coefficient. Such deviating behavior was also observed to be a function of the dead-end geometry. When the dead ends have no cavities, i.e., purely cylindrical with long ends, diffusion coefficient was found to comply with equation (38). When cavities are present, the dependence of  $D_e(r)$  was found to be non-monotonic for arbitrary lengths of the connecting channels.

Scientifically, this study establishes that, under certain cases, it is possible for larger particles to diffuse faster compared to smaller particles. This is because a larger particle, methane molecule in our case, cannot enter the dead ends and spends all the time diffusing along the tube axis. The smaller particles, on the other hand, waste time travelling in the dead ends and diffuse along the constricted entries for a fraction of the total observation time. Micropores in coals are classified to be  $< 20 \text{ \AA}$ , with a modal value of  $10 \text{ \AA}$ . With such distribution of pore sizes, it is expected that the pore entries, which are generally even more constricted than the end pores, can be smaller or much larger than the size of gas molecules, and might also be of the same size. Some of the end cavities of the pores might be well developed and some similar to the ends of a long cylindrical tubes. Thus, with reference to the results obtained from the diffusion experiments in this study, it can be concluded that, during the process of bio-conversion, the pore structure of coal changed in such a way that the diffusion paths facilitated longer diffusion times for  $\text{CO}_2$  molecules. Figure 4.14 (b), which compares the values of  $D$  of methane and  $\text{CO}_2$  of coal treated for sixty days provides an indication of such a change.

## **b. Sorption**

The non-monotonic behavior can be used to explain the trends in the sorption behavior of treated coal. As previously discussed, and observed in Figures 4.1 through 4.6, the Langmuir constants for sorption were found to increase, reflecting the availability of larger areas for sorption. In spite of the increasing trend exhibited, for the experimental pressure range, the amount of methane adsorbed by the coal treated for thirty days was considerably lower than the amount sorbed by untreated coal. The coal treated for sixty days presented similar trends for pressure lower than 400 psi. Similar trends were not very noticeable for sorption of CO<sub>2</sub>, which is attributed to the fact that coal has a higher affinity towards CO<sub>2</sub> than for methane. The rate of CO<sub>2</sub> adsorption at lower pressures is much higher than methane, and thus CO<sub>2</sub> covers the monolayer of the sorption sites rather earlier and at a faster pace. This is in agreement with the work completed by previous researchers. Given that methane and CO<sub>2</sub> are adsorbed on the surface of coal, as suggested by the non-monotonic behavior of diffusing particles, it is inferred that methane molecules during early stages of sorption start adsorbing onto the surface of the pore entries and not the pore itself. Given that the porous structure of coal is what provides the enormous surface areas that is available for sorption, the amount of gas sorbed during the initial period of sorption is limited to the entries and, therefore, lower than the amount that would sorb if the methane molecules had unrestricted access to the entire pore geometry. The diffusion characteristics of the untreated coal is indicative of such unrestricted entries.

The theory above is supported by the following hypothesis that microbes, while consuming coal, will have more access to the wider entries that have periodic constricted



entries branching from them. It is believed that consumption of coal, resulting in increased surface area is predominantly from these entries, making sorption on these surfaces easier compared to the surface present in virgin coal. Constricted entries make it difficult for the microbes to avail the pore cavities with large surface areas. The unavailability of such areas is also indicated by the reduced rates of gas generation over time, in spite of the substantial amount of carbon remaining in the sample, as indicated by the ultimate analysis results.

Given that sorption of gases on coal is considered to have mono-layer coverage, sorption would continue as long as there are sufficient sorption sites available. Thus, it is expected that, with increasing pressures, once the surface of the entries are filled with sorbed molecules, gas molecules will eventually diffuse into the pores due to an increase of Brownian collisions. The amount adsorbed would, therefore, continue to increase with pressure, even if the pore entries are filled. The experimental results obtained to date support this hypothesis. For coal treated for sixty days, such behavior was observed at pore pressures  $>400$  psi, below which, only the entries were being filled up, resulting in a smaller volume adsorbed compared to the baseline value. Coal treated for thirty days was just starting to exhibit similar behavior at the highest experimental pressure. Beyond 1500 psi, as suggested by Figure 4.10, coal treated for thirty days is expected to exhibit behavior similar to that treated for sixty days. Finally, this behavior can be the result of the experimental procedure followed when establishing sorption isotherms. The sample is allowed to equilibrate for one day after every pressure step change. Given the nature of data, it is expected that, if given infinite time, the amount of gas sorbed would eventually

increase until equilibrium is attained. The nature of the plots for methane for the three coals tested would then be expected to be similar to that observed for CO<sub>2</sub>.

While hysteresis during desorption has traditionally been related to capillary condensation and change in moisture content of the sample under laboratory conditions, the levels of desorption hysteresis for methane in this study has not been reported in the literature. While the Langmuir sorption theory assumes that each of the sorption site has an equal probability of being occupied by ad/de-sorbing gas, the non-monotonic dependence of  $D_e(r)$  observed adds another factor to the desorption behavior in the experimental results. Given the shape of pore entries, it is possible that, during desorption, the amount of Brownian collisions among desorbed molecules within the pore cavities restricts them from traveling from the pores into the connecting flow path. This might result in preferential desorption of gas molecules sorbed on the walls of the pore entries since this would have a smaller path to travel in order to reach the free state, where the density of the gas is that of the bulk phase density. This would result in smaller amounts to be desorbed at high pressures and the isotherm would continue to be asymptotic even as it approaches lower pressures. With decreasing number of molecules at lower pressures, the Brownian collisions would decline and the desorbing amount would increase. This argument holds for the desorption patterns observed for coal treated for thirty and sixty days.

## **4.6 Potential Impacts of the Observed Trends**

### **a. Sorption**

Sorption capacity of the coals tested was found to increase with continued bio-conversion. For a monolayer coverage of adsorbed gases, increase in sorption capacity is

indicative of increased surface area available for sorption. Data from the calculation of surface area available for sorption is in agreement with such a change. Treating coal seams as a reservoir for these coalbed gases, an increased sorption capacity implies increased reservoir storage capacity for the stored/produced gases. The effects of this can be manifold:

- i) CBM wells, which are depleted or nearing depletion, are normally characterized by rubblized, high permeability coalbeds. Given that there is pre-existing well infrastructure, it might be possible to feed such coal seams with microbial solutions and nutrient amendments, or nutrient amendments alone, to simulate methanogenesis in the local microbial populations. Under optimum conditions, this would enable producing coalbed gases from depleted wells by bio-conversion. Given sufficient time, and the increased sorption capacities of the coal, it might be possible to initiate long-term production of coalbed gases, in excess of the previously documented storage capacities under traditional conditions. Given the nascency of the study, further work is required to establish the techno-economic feasibility of such an operation.
- ii) Microbial gasification can be used to convert coal wastes to methane. Such methods have been studied using laboratory-scale models. The results obtained are positive, suggesting setting up pilot-scale reactors for the same. Although it is unlikely that such reactors will operate under high pressures at pilot/initial stages, higher sorption capacity will facilitate longer periods of gas production given sufficient time for methanogenesis. The results obtained from the EL isotherm, discussed earlier, can be used to set up proper separating facilities at different stages over the production period.

## b. Diffusion

The rates of diffusion, as indicated by the variation in the value of diffusion coefficient, has been found to increase with continued microbial gasification. Baseline coal presented trends similar to those reported by prior researchers, where the values for CO<sub>2</sub> was higher than that for methane. Increase in the value of D resulted in a change in the trend for treated coal, where diffusion rates for methane were higher than that for CO<sub>2</sub>.

- (i) The value of the diffusion coefficients are used as an input parameter, although indirectly, as sorption time ( $\tau$ ), which is the time required by retrieved cores to desorb 63% of the gas in place. The sorption time is an input parameter for production modeling in CBM reservoirs. The sorption time is typically considered a constant parameter and increasing values of diffusion coefficient with declining reservoir pressures is not included in any simulation exercise. Kumar (2007) studied the effect of treating this as a dynamic parameter over the duration of production. Figure 4.15 illustrates the underestimated production values as a result of considering this as a constant. Increasing the values of the diffusion coefficient gradually results in increased production capacities, especially during the late stages/low pressures, all other parameters remaining constant. Although simulation was not carried out as a part of this study, extrapolation of the previous simulated results suggests that there considerable increase in production of methane from CBM wells is possible if the coal is treated with microbial consortia aimed to simulate methanogenesis as a result of improved rates of diffusion.

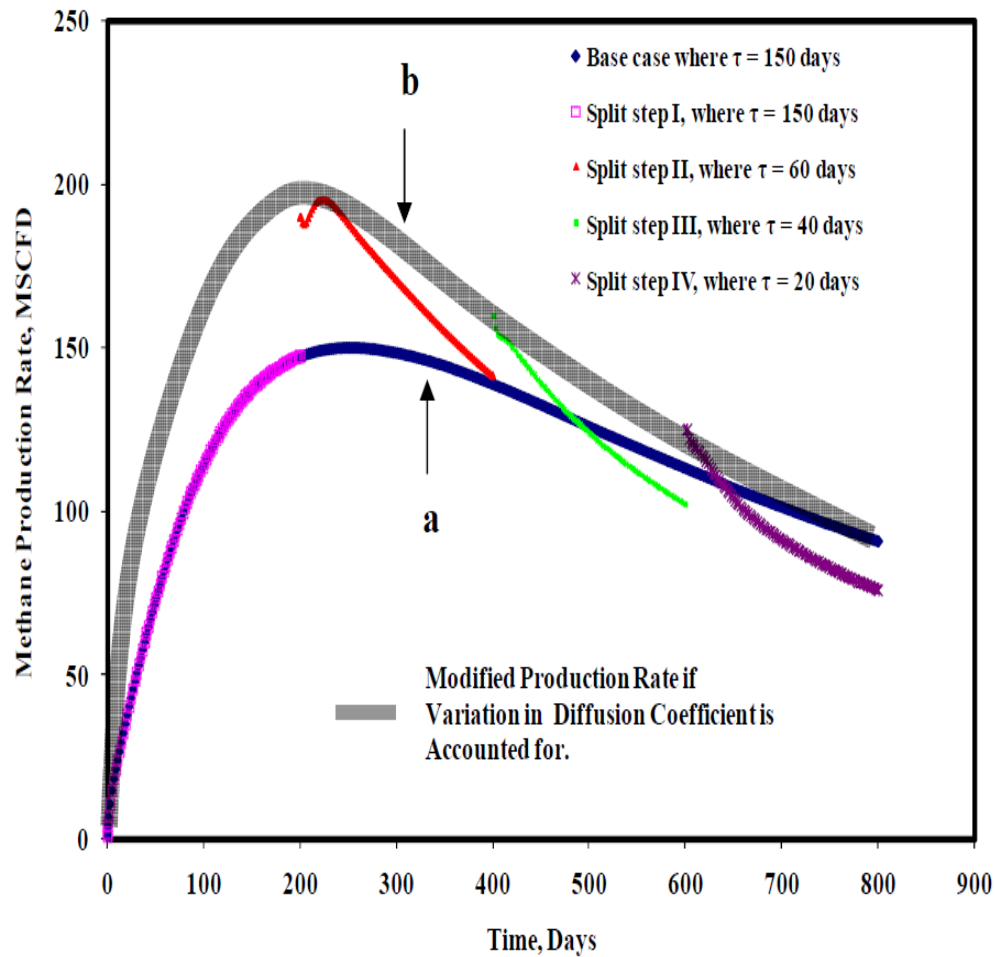


Figure 4.15: Comparison of two cases where, a) normal simulation run for 800 days, and b) where diffusion coefficient variability is taken into account, Kumar (2007)

- ii) Illinois basin has not been prolific in terms of CBM production. Most basins classified similarly have very low values of permeability. However, permeability in the Illinois basin is categorized as average to good. CBM production in the Illinois basin is plagued by very low rates of diffusion. The trends observed in the study point towards the potential of overcoming this bottleneck of low diffusion rates by treating coal with suitable microbial consortia. Methanogenesis would thus result not only in re-charging depleted coal, but also improve the producibility over a period of time.

## 4.7 Summary

In this chapter, trends in the variation of sorption-diffusion properties of methane and CO<sub>2</sub> on coal treated with microbial consortia were established. From the observed results, it is concluded that, due to increased rates of diffusion, there is a definite change in the pore structure of coal. This change was confirmed to be positive by the nature of the isotherms of treated coal, which suggested increased availability of pore surface areas available for sorption. The nature of results also established an additional factor affecting the desorption hysteresis in coals, selective desorption of molecules from sites in the pore entries rather than the sites in the pores cavities. The nature of the diffusion data was also found to be in agreement to the Klinkenberg diffusion model, suggested by Kumar. Finally, possible impacts of such changes on CBM applications have been discussed.

## CHAPTER 5

### CONCLUSIONS AND RECOMMENDATIONS

Based on the results of experimental work and theoretical analyses, the following conclusions are made:

1. Sorption capacity of the coal tested was found to increase with continued bio-conversion. Hence, new surface area is created as a result of bio-conversion. However, at lower pressures, the volume sorbed did not change significantly. This is attributed to the fact that, at lower pressures, sorption of methane is limited to the surface of the pore entries and not the pore cavities, which get filled slowly. It is hypothesized that microbes *consume* carbon more from the entries, thus increasing the surface area along the sides of these entries. A gradual increase in the sorption capacity with increasing pressures for treated coals is indicative of the filling of the pore cavities, which offer larger surface areas to sorption.
2. Desorption of methane from coal surface exhibited significant hysteresis. The hysteresis effect resulted in an asymptotic isotherm at higher pore pressures and significant desorption at lower pressures. It is believed that, at high pressures, increased Brownian collisions within the pore cavities prevent the molecules to diffuse from the pore cavities, allowing them to exist in the free state. This results in preferential desorption from the pore entries, where only a small volume of gas is sorbed. At lower pressures, the gas eventually desorbs from the pore cavities, where large volume of gas is stored.
3. The diffusion coefficient for baseline coal exhibited behavioral trends similar to that reported earlier, where diffusion rate for CO<sub>2</sub> was higher than that for methane. After bio-conversion, the overall rates of diffusion increased and the results contradicted the expected trend, where

diffusion rates of methane were higher than CO<sub>2</sub>. Such behavior is adequately explained by the non-monotonic size dependence of effective diffusion coefficients.

4. The diffusion data obtained from the experiments was fit to the Klinkenberg model, as hypothesized by Kumar (2007). The baseline coal provided relatively poor fit for the model, especially for sorption of methane. Sorption of CO<sub>2</sub> fitted the Klinkenberg model extremely well. The fit of the model became progressively better with increased bio-treatment of coal. This suggests that the model, as hypothesized by Kumar, is applicable more to gases which are sorbed rather strongly on coal surfaces, or on coals which have higher sorption capacities.
5. The study by Zhang et al (2015) was successful in formulating methods to produce methane from coal by simulating methanogenesis using suitable nutrient amendments. From a CBM perspective, wells which are depleted or nearing depletion, can be treated with suitable microbial consortia. Given sufficient time and amendments for the production of biogenic gas, the increased sorption capacities of treated coals are indicative of the potential of long-term production of coalbed gases.
6. Increased rates of diffusion can have a significant impact in basins like Illinois, where low production rates have plagued reservoirs with moderate to good permeability. Extremely low rates of diffusion have proved to be the bottleneck to commercial CBM production. Increase in the value of diffusion coefficient suggest that, at low pressures, the production would increase significantly. Methanogenic treatment in such conditions can thereby result not only in recharging depleted coal seams, but opening up the possibility of having more economically producing reservoirs over a period of time.

Based on experience gained in this study, the following topics of research should be pursued further:



1. The non-monotonic dependence of effective diffusivity to the size of diffusing molecule needs to be studied in more detail. Approaches similar to dynamic light scattering experiments can be conducted to measure the Brownian motion and relate it to the size of the particle by correlating it with the Einstein-Stoke equation. Other approaches, such as, microscopy shape analysis, small angle X-ray scattering and mercury porosimetry, can also be applied.
2. Surface energy levels are an important factor affecting the sorption of gases on coal. Given the chemical treatment of coal to simulate methanogenesis, chemical change is a distinct possibility. Measuring the change in the surface energy levels and associated chemical changes was beyond the scope of this study. Future researchers are encouraged to study these effects.
3. Given that there is evidence of enhancement of diffusion properties of Illinois coal, different approaches to enhance the *in situ* permeability of Illinois coal should be studied in detail. Pressure-dependent-permeability studies can be carried out on coal cores post bio-conversion in order to obtain flow characteristics in the macropore network of coal. Coupling this flow characteristics in micropores, as estimated in this study, would provide a complete picture, providing input parameters to model flow behavior for possible future *in situ* bio-conversion production wells.
4. Given the nascency of the study, most conclusions with regards to the applicability of this study to future potential biogenic CBM wells require extensive techno-economic analysis prior to application of such methods.

## REFERENCES

- Amankwah, K.A.G., and Schwarz, J.A. (1995). A modified approach for estimating pseudo-vapor pressures in the application of the Dubinin-Astakhov equation. *Carbon*, 33(9), pp. 1313-1319.
- Arri L.E. and Yee D. (1992). Enhanced coalbed methane recovery. *Paper SPE 24363 presented at the SPE Rocky Mountain Regional Meeting held at Casper, Wyoming, U.S.A. May 18-21.*
- Ayers, W.B. Jr. (1991). Geologic evaluation of critical production parameters for coalbed methane resources. *Quarterly Review of Methane from Coalseams Technology* 8, No. 2, pp. 27-32.
- Brunauer, S., Emmett, P.H., and Teller, E. (1938). Adsorption of gases in multimolecular layers. *Journal of the American Chemical Society* 60, pp. 309 – 319.
- Busch, A., Gensterblum, Y., and Krooss, B. M. (2003). Investigation of preferential sorption behavior of CO<sub>2</sub> and CH<sub>4</sub> on coal by high pressure adsorption/desorption experiments with gas mixtures. *International Coalbed Methane Symposium*, Tuscaloosa, AL.
- Clarkson C.R. and Bustin R.M. (2000). Binary gas adsorption/desorption isotherms: effect of moisture and coal composition upon carbon dioxide selectivity over methane. *International Journal of Coal Geology*. Vol 42, pp. 241–271.
- Clarkson, C.R. and Bustin, R.M. (1999). The effect of pore structure and gas pressure upon the transport properties of coal: A laboratory and modeling study. 2. Adsorption rate modeling. *Fuel*, 78, pp. 1345-1362.

- Close, J.C., and Mavor, M.J. (1991). Influence of coal composition and rank on fracture development in Fruitland coal gas reservoirs of San Juan Basin. *Coalbed Methane of Western North America, Guidebook for the Rocky Mountain Association of Geologists Fall Conference and Field Trip, Glenwood Springs, Colorado*, pp. 109-121.
- Collins, R.E. (1991). New theory for gas adsorption and transport in coal. *Proceedings of the 1991 Coalbed Methane Symposium*, Tuscaloosa, AL, pp. 425-431.
- Conrad, R. (2005). Quantification of methanogenic pathways using stable carbon isotopic signatures: a review and a proposal. *Organic geochemistry*, Vol. 39, pp. 739-752.
- Craig, H. (1953). The geochemistry of the stable carbon isotopes. *Geochimica et Cosmochimica Acta*, Vol. 3, pp 53-92.
- Crank, J. (1975). Mathematics of diffusion. *London: Oxford University Press*.
- Cui, X., Bustin, R. M., and Dipple, G. (2004). Selective transport of CO<sub>2</sub>, CH<sub>4</sub> and N<sub>2</sub> in coals: insights from modeling of experimental gas adsorption data. *Fuel*, 83, pp. 293-303.
- Dagdug, L., Alexander, M.B., Makhnovskii, Y.A., and Zitserman, V.Y. (2008). Particle size effect on diffusion in tubes with dead ends: Nonmonotonic size dependence of effective diffusion constant. *The Journal of Chemical Physics*, Vol. 129, pp. 184706-1- 184706-5.
- Do, D.D. (2008). Adsorption analysis: Equilibria and kinetics. *Imperial College Press*.
- Dubinin, M.M. (1967). Adsorption in micropores. *Journal of Colloid and Interface Science*, 23, pp. 487-499.

- Dubinin, M.M. (1975). Physical adsorption of gases and vapors in micropores. In D.A. Canhead, J.F. Danielli, M.D. Rosenberg (Eds.). *Progress in surface and membrane science (Vol. 9)*, New York: Academic Press.
- Dutta, P., Bhowmik, S., and Das, S. (2010). Methane and carbon dioxide sorption on a set of coals from India. *International Journal of Coal Geology*, Vol. 85, pp. 289-299.
- Faiz, M. and Hendry, P. (2006). Significance of microbial activity in Australian coal bed methane reservoirs- a review. *Bulletin of Canadian Petroleum Geology*, Vol. 54, No. 3. 261-272.
- Ferry, J.G. (2011). Fundamentals of methanogenic pathways that are key to the biomethanation of complex biomass. *Curr. Opin. Biotech*, Vol. 22, pp. 351-357.
- Formolo, M. (2010). The microbial production of methane and other volatile hydrocarbons. In: Timmis, K.N. (Eds), *Handbook of Hydrocarbon and Lipid Microbiology*, pp 113-126.
- Friend, D.G. (1992). NIST mixture property database 14. *National Institute of Standards and Technology, U.S. Department of Commerce*.
- Games, L.M., and Hayes, J.M. (1978). Methane-producing bacteria: natural fractionations of stable isotopes. *Geochimica et Cosmochimica Acta*, Vol. 42, pp. 1295-1297.
- Gray, I. (1987). Reservoir engineering in coal seams: Part 1. The physical process of gas storage and movement in coal seams. *SPE Reservoir Engineering* 2, 28-34.
- Greaves, K.H., Owen, L.B., and McLennan, J.D. (1993). Multi-component gas adsorption – desorption behavior of coal. Paper 9353, *International Coalbed Methane Symposium*, Tuscaloosa, AL.

- Gregg, S. J. and Sing, K. S. W. (1982). Adsorption surface area and porosity. *London: Academic Press*.
- Harpalani S. and McPherson M.J. (1986). Retention and release of methane in underground coal workings. *International Journal of Mining and Geological Engineering* 4(3).
- Harpalani, S. and Chen, G. (1995). Estimation of changes in fracture porosity of coal with gas emission. *Fuel*, 74, pp. 1491-1498.
- Harpalani, S. (2002). Potential impact of CO<sub>2</sub> injection on permeability of coal. *Proceedings of First International Forum on Geological Sequestration of CO<sub>2</sub> in Deep, Unmineable Coalseams*. Houston. TX.
- Harpalani, S., Prusty, B.K., and Dutta, P. (2006). Methane/CO<sub>2</sub> sorption modeling for coalbed methane production and CO<sub>2</sub> sequestration. *Energy Fuels*. Vol. 20(4), pp. 1591-1599.
- Hunt, J.M. (1979). Petroleum geochemistry and geology. *San Francisco, W.H. Freeman and Co.*, pp. 617.
- Itodo, A.U., Itodo, H.U., Garfar, M.K. (2010). Estimation of specific surface area using Langmuir isotherm method. *Journal of applied science environment management*. Vol. 14 (4) pp 141-145.
- Shinn, J.H. (1984). *Fuel*, Vol. 63. pp. 1187–1196.
- Jenden, P.D., and Kaplan, I. R. (1986). Comparison of microbial gases from the Middle America Trench and Scripps Submarine Canyon: implications for the origin of natural gas. *Applied Geochemistry*, Vol. 1, pp. 631-646.

- Jones, A. H., Bell, G., and Schraufnagel, R. (1988). A review of the physical and mechanical properties of coal with implications for coal-bed methane well completion and production. *Geology and Coal-Bed Methane Resources of the Northern San Juan Basin, Colorado and New Mexico*, Rocky Mountain Association of Geologists, Denver, CO, pp. 169-181.
- Jones, E.J.P., Voytek, M.A., Corum, M.D., Orem, W.H. (2010). Stimulation of methane generation from a non-productive coal by addition of nutrients or a microbial consortium. *Applied and environmental Microbiology* 76, pp. 7013-7022
- Karweil, J. (1969). Aktuelle probleme der geochemie der kohle, in Schenk, P.A., and Havernaar, I., eds. *Advances in organic geochemisty, 1968: Oxford, Pergamon Press*, pp. 59-84.
- King, G.R. (1985). Numerical simulation of the simultaneous flow of methane and water through dual porosity coal seams during the degasification process. *Ph.D. Dissertation, Pennsylvania State University*.
- Kolesar, J.E., Ertekin, T., and Obut, S.T. (1990a). The unsteady-state nature of sorption and diffusion phenomena in the micropore structured of coal: part 1—theory and mathematical formulation. *SPE Form, Eval.* 5, pp. 81–88.
- Kolesar, J.E., Ertekin, T., and Obut, S.T. (1990b). The unsteady-state nature of sorption and diffusion phenomena in the micropore structured of coal: part 2—solution. *SPE Form, Eval.* 5, pp. 89–97.
- Kotarba, M. 1988. Geochemical criteria for the origin of natural gases accumulated in the Upper Carboniferous coal-seam-bearing formations in Walbrzych coal basin (in Polish with English summary). *Stanislaw Staszio Academy of Mining and Metallurgy Scientific Bulletin* 1199, pp. 119.

- Krooss, B.M., Van Bergen, F., Gensterblum, Y., Siemons, N., Pagnier, H.J.M., and David, P. (2002). High-pressure methane and carbon dioxide adsorption on dry and moisture-equilibrated Pennsylvanian coals. *International Journal of Coal Geology*, 51(2), 69-92.
- Kumar, A. (2007). Methane diffusion characteristics of Illinois coals. *Thesis, Department of Mining and Mineral Engineering, SIU Carbondale*.
- Kurniawan, Y., Bhatia, S.K., and Rudolph, V. (2006). Simulation of binary mixture adsorption of methane and CO<sub>2</sub> at supercritical conditions in carbons. *AIChE J.*, 52(3), pp. 957—967.
- Lin, W. (2010). Gas sorption and the consequent volumetric and permeability change of coal. *PhD Dissertation, Department of Energy Resources Engineering, Stanford University*.
- Marshak, S. (2012). Essentials of geology, 3<sup>rd</sup> Ed. Norton, W. W. & Company, Inc.
- Mavor M.J., Gunter W.D., and Robinson J.R. (2004). Alberta multiwell micro-pilot testing for CBM properties, enhanced methane recovery and CO<sub>2</sub> storage potential. *Paper SPE 90256 presented at SPE Annual Technical Conference and Exhibition held at Huston, TX U.S.A. on 26-29 September*.
- Mavor, M. J., Owen, L. B., and Pratt, T. J. (1990). Measurement and evaluation of coal sorption isotherm data. *Proceedings of SPE 65th Annual Technical Conference and Exhibition, SPE 20728. New Orleans, LA*
- Mehta, S.D. (1982). An improved potential theory method for predicting the adsorption equilibria of gas mixtures. *MS Thesis, Pennsylvania State University*.
- Moore, T.A. (2012). Coalbed methane: A review. *International Journal of Coal Geology* 101. pp 36-81.

- Opara, A. (2012). Biochemically enhanced methane production from coal. *PhD Dissertation, Environmental Engineering, University of Utah.*
- Ozdemir, E., Morsi, B.I., and Schroeder, K. (2004). CO<sub>2</sub> adsorption capacity of Argonne premium coals. *Fuel*, 83(7-8), pp. 1085–1094.
- Radovic, L. (1991). Adsorption and transport in coalbed reservoirs. *Proceedings of the Gas Research Institute Workshop, Chicago, IL.*
- Rice, D.D.(1993). Composition and origins of coalbed gas. *In: Law, B.E., Rice D.D (Eds), Hydrocarbons from Coal. : AAPG Studies in geology, 38. American Association of Petroleum Geologists, Tulsa, Oklahoma, pp. 159-184*
- Rightmire, C. T., Eddy, G. E., and Kirr, J. N. (1984). Coalbed methane resource of the United States, Oklahoma. *The American Association of Petroleum Geologists*, 17, pp. 387.
- Rogers, R. E. (1994). Coalbed methane: Principles and practices. *New Jersey: Prentice Hall Inc.*
- Ruckenstein, E., Vaidyanathan, A. S., and Youngquist, G. R. (1971). Sorption by solids with bidisperse pore structure. *Chemical Engineering Science*, 26, pp. 1305-1318.
- Ruppert, L.F., Kirschbaum, M.A., Warwick, P.D., Flores, R.M., Affolter, R.H. and Hatch, J.R. (2007). The US Geological Survey's national coal resource assessment: the results. *International Journal of Coal Geology*, Vol. 50, pp. 247-274
- Ruthven, D.M. (1984). Principles of adsorption and adsorption processes. *Wiley, New York.*
- Sawyer, W.K., Zuber, M.D., Kuuskraa, V.A., and Horner, D.M. (1987). A field derived inflow performance relationship for coalbed gas wells in the black warrior basin. *Proceeding of the 1987 International Coalbed Methane Symposium, Tuscaloosa, Alabama, pp. 207-215*



- Scott, A.R. (1995). Limitations and benefits of microbially enhanced coalbed methane. *Intergas '95 The University of Alabama Tuscaloosa, Alabama USA*, pp. 423-432
- Simmons, A.T. (1897). Physiography for advanced students. *Macmillan and Co. Ltd*
- Smith, D. M. (1982). Methane diffusion and desorption in coal. *Ph.D. Dissertation, University of New Mexico*.
- Smith, D.M. and Williams, F.L. (1984). Diffusional effects in the recovery of methane from coalbeds. *SPEJ*, 24, pp. 529-535.
- Smith, J.T., and Ehrenberg, S.N., (1989). Correlation of carbon dioxide abundance with temperature in clastic hydrocarbon reservoirs: relationship to inorganic chemical equilibrium. *Marine and Petroleum Geology*, Vol. 6, pp. 129-135.
- Smith, J.W., Gould, K.W., Hart, G.H., and Rigby, D. 1985. Isotopic studies of Australian natural and coal seam gas. *Bulletin of Australasian Institute of Mining and Metallurgy*, Vol. 290, pp. 43-51.
- Spearing, A. J. S. (2014). Personal communication, SIU Carbondale.
- Stach, E., Mackowsky, M.-Th., Teichmuller, M., Taylor, G.H., Chandra, D., and Teichmuller, R. (1982). Stach's textbook of coal petrology. *Berlin, Gebruder Borntraeger*. 535.
- Strapoć, D. (2007). Coalbed gas origin and distribution in the southeastern Illinois basin. *PhD Dissertation, Department of Geological Sciences, Indiana University*
- Sudibandriyo, M., Pan, Z., Fitzgerald, J.E., Robinson, R.L., and Gasem, K.A.M. (2003). Adsorption of methane, nitrogen, carbon dioxide, and their binary mixtures on dry activated carbon at 318.2 K and pressures up to 13.6 MPa. *Langmuir*, 19, pp. 5323-5331.

- Talu, O., Li J., and Myers, A.L. (1995). Activity coefficients of adsorbed mixtures. *Adsorption* 1, pp. 103 – 112.
- Thauer, R.K. (1998). Biochemistry of methanogenesis: A tribute to Marjory Stephenson. *Microbiology*, Vol. 144, pp. 2377-2406.
- Thimons, E.D. and Kissel, F.N. (1973). Diffusion of methane through coal. *Fuel*, 52, pp. 274-280.
- Thorstenson, D.C. and Pollock, D.W. (1989). Gas transport in unsaturated porous media: The adequacy of Fick's law. *Reviews of Geophysics*, 27, pp. 61-78.
- Ting, F.T.C. (1977). Origin and spacing of cleats in coal beds. *J. Pressure Vessel Technol. Trans, ASME* 99, pp. 624–626.
- Tissot, B.P., and Welte, D.H. (1984). *Petroleum Formation and Occurrence*, 2<sup>nd</sup> Ed. Springer-Verlag Berlin Heidelberg GmBH.
- US EIA. (2012). <http://www.eia.gov/coal/production/quarterly/pdf/t1p01p1.pdf>
- Valentine, D.L., Chidthaisong, A., Rice, A., Reeburgh, W.S. and Tyler, S.C. 2004. Carbon and hydrogen isotope fractionation by moderately thermophilic methanogens. *Geochimica et Cosmochima Acta*, Vol. 68, pp. 1571-1590.
- Van Krevelen, D.W. (1993). Coal. *Elsevier Scientific Publishing Company, NY*.
- Vandecasteele, J.-P. (2008). Microbiology of methane and of C1 compounds. In petroleum microbiology: concepts, environmental implications, industrial applications. *Vandecasteele, J.-P., Ed.; Editions Technip: Paris, France, pp. 79-172*.
- Ward C.R. (1984). Coal geology and coal technology. *Blackwell Scientific Press*.

- Warren, J. E. and Root, P. J. (1963). The behavior of naturally fractured reservoirs. *Society of Petroleum Engineers Journal*, pp. 245-255.
- Whitehurst, D. D. (1978). A primer on the chemistry and constitution of coal. *ACS Symposium Series No. 77, Organic Chemistry of Coal*, pp. 1-35.
- Whiticar, M.J. (1996). Stable isotope geochemistry of coals, humic kerogens and related natural gases. *International Journal of Coal Geology*, Vol. 32, pp. 191-215.
- Worm, P., Muller, N., Plugge, C.M., Stams, A.J.M., and Schink, B. (2010). Syntrophy in methanogenic degradation in endosymbiotic methanogenic archaea. *Hackstein, J.H.P., Ed.; Springer: Berlin, Germany*, pp. 143-162.
- Yang R.T. (1987). Gas separation by adsorption processes. *Butterworths Publishers*.
- Zhang, J., Liang, Y., Pandey, R., and Harpalani, S. (2015). Characterizing microbial communities dedicated for conversion of coal to methane. *International Journal of Coal Geology*. Paper accepted.
- Zhao, X. (1991). An experimental study of methane diffusion in coal using transient approach. *Ph. D. Dissertation, The University of Arizona*.
- Zinder, S.H. (1993). Physiological ecology of methanogens. *In: Ferry, J.G. (Eds). Methanogenesis. New York: Chapman and Hall*, pp. 126-206.
- Zutshi, A., and Harpalani, S. (2004). Matrix swelling with CO<sub>2</sub> injection in a CBM reservoir and its impact on permeability of coal. Paper 0425, *International Coalbed Methane Symposium*, Tuscaloosa, AL.

## VITA

Graduate School  
Southern Illinois University

Rohit Pandey

rohit.mining1990@gmail.com

Bengal Engineering and Science University, Shibpur, India  
Bachelor of Engineering, Mining Engineering, May 2012

Thesis Title:

Changes in Properties of Coal as a Result of Continued Bioconversion

Major Professor: Satya Harpalani

Publications:

- Zhang, J., Liang, Y., Yau, P. M., Pandey, R., & Harpalani, S. (2015). A metaproteomic approach for identifying proteins in anaerobic bioreactors converting coal to methane. *International Journal of Coal Geology*, Vol. 146, pp. 91-103.
- Zhang, J., Liang, Y., Pandey, R., & Harpalani, S. (2015). Characterizing microbial communities dedicated for conversion of coal to methane in situ and ex situ. *International Journal of Coal Geology*, Vol. 146, pp. 145-154.
- Zhang, J., Liang, Y., Yau, P. M., Pandey, R., & Harpalani, S. (2015). Bioconversion of coal waste to methane – Study of microbial community conversion pathway and property of the residual coal. The 40<sup>th</sup> International Technical Conference on Clean Coal and Fuel Systems, Paper presented.
- Park, S., Zhang, J., Liang, Y., Pandey, R., & Harpalani, S. (2015). Optimization and techno-economic analysis of the microbial conversion of coal to methane. The 40<sup>th</sup> International Technical Conference on Clean Coal and Fuel Systems, Paper accepted.